UNIVERSITÀ DEGLI STUDI DI TRIESTE

XXVIII CICLO DEL DOTTORATO DI RICERCA IN BIOMEDICINA MOLECOLARE

NOVEL METABOLIC ROLES OF UNACYLATED GHRELIN: FROM PATHOPHYSIOLOGY TO DISEASE MODELS TREATMENT

Settore scientifico-disciplinare: MED/09

DOTTORANDO
GIANLUCA GORTAN CAPPELLARI

COORDINATORE
PROF. GUIDALBERTO MANFIOLETTI

SUPERVISORE DI TESI
PROF. ROCCO BARAZZONI

ANNO ACCADEMICO 2014 / 2015

Contents

1 Synopsis

Ghrelin is a gastric hormone circulating in acylated (AG) and unacylated (UnAG) forms. AG represents ~10% of total plasma ghrelin, has an appetite-stimulating effect and is the only form for which a receptor has been identified. UnAG has no orexigenic effects, and its circulating levels are positively associated with insulin sensitivity in metabolic syndrome patients. Skeletal muscle oxidative stress and inflammation are key negative modulators of tissue and whole-body insulin action, and UnAG was recently reported to reduce oxidative stress in non-muscle cells in-vitro. Its potential direct involvement in the regulation of muscle intermediate metabolism in vivo and its clinical impact remain however largely unknown.

In the current studies, we first investigated potential associations between plasma AG, UnAG and HOMA insulin resistance index in the general population. In 719 individuals from the North-East-Italy MoMa epidemiological study, TG and UnAG but not AG were negatively associated with HOMA after adjusting for gender and body mass both at baseline and at 5-year follow-up (n=350), and changes in TG and UnAG but not AG were negatively associated with changes in HOMA independently of potential confounders.

We next tested the hypothesis that UnAG increases insulin sensitivity by modulating oxidative stress, inflammation and insulin action in skeletal muscle tissue. In healthy 12-week-old male rats, 4-day UnAG administration consistently reduced muscle mitochondrial ROS production and improved muscle redox state, reduced NF-κB activation and inflammatory cytokines, activated insulin signalling mediators involved in glucose utilization and protein anabolism (AKT, GSK, p70S6k). UnAG also concomitantly increased muscle glucose uptake and selectively favoured the utilization of glucose-derived substrates for mitochondrial ATP synthesis. Analogous findings were observed in transgenic mice with systemic UnAG overexpression, and in UnAG-treated myotubes in vitro, thereby supporting

a potential direct hormone effect. Importantly, these findings were not observed with AG administration nor in liver samples, thus further indicating independent and tissue specific UnAG actions.

Autophagy, the removal of dysfunctional organelles, is an emerging protective mechanism in both cardiac and skeletal muscle. We therefore also hypothyzed that UnAG could reduce ROS production by inducing muscle autophagy. In cardiomyocytes UnAG reduced ROS production in association with increased dysfunctional mitochondria removal and in UnAG but not AG treated myotubes silencing of autophagy promoter ATG5 restored ROS generation.

We next investigated the potential clinical relevance of UnAG actions in disease models characterized by muscle oxidative stress, inflammation and insulin resistance. In high-fat diet (HFD)-induced obese and diabetic mice, chronic UnAG overexpression prevented hyperglycaemia and whole-body insulin resistance, as well as muscle oxidative stress, inflammation and altered insulin signalling. In rodent chronic kidney disease induced by 5/6 nephrectomy, protein-energy wasting, enhanced skeletal muscle ROS production, increased tissue inflammation and impaired insulin signalling were also completely normalized by UnAG treatment. Importantly, these findings were associated with a recovery of gastrocnemius muscle mass.

Our combined findings suggest that excess ghrelin acylation with parallel limitation of circulating UnAG may have unfavourable metabolic and clinical consequences. Factors involved in the modulation of ghrelin acylation in vivo are however poorly defined, and nutritional regulation of this process as well as the potential role of lipid substrates remains unknown. We therefore further investigated the impact of free fatty acids (FFA) on ghrelin acylation by assessing the associations between plasma FFA, AG and UnAG in 850 individuals from the MoMa cohort. FFA were positively associated with AG and AG/TG and

negatively with TG also after adjustment for HOMA and metabolic confounders. The potential causal role of FFA in the regulation of plasma ghrelin profile was also assessed by i.v. infusion of lipid emulsions in rodents. Under these conditions, acute plasma FFA elevation increased AG and AG/TG with no impact on TG.

While a specific receptor for UnAG needs to be identified, our combined findings consistently point towards a novel independent role of UnAG as a regulator of muscle metabolic pathways maintaining energy status and tissue anabolism. Underlying mechanism appear to involve the modulation of mitochondrial function with reduced ROS generation, which could be mediated at least in part by autophagy induction. Data from disease models also suggests that modulation of ghrelin acylation to enhance UnAG availability is a potential novel target in the treatment of metabolic derangements in disease states characterized by metabolic and nutritional complications.

2 Introduction

2.1 Ghrelin - Cell biology

Ghrelin is a gastric hormone, first identified in 1996 by Kojima et al. in rat stomach [1]. In the previous years, several small synthetic molecules had been discovered to induce growth hormone (GH) release by acting at hypothamical level independently from GH releasing hormone pathways [2] and were therefore named growth hormone secretagogues (GHS) [3,4]. While a specific receptor for GHS (GHSR) had been identified in 1996 [5], its endogenous ligand was unknown. Kojima et al. demonstrated that a novel hormone was able to simulate GH secretion through GHSR [1] and named it “ghrelin” after the Proto-Indo-European word root (“ghre”) meaning “grow” [6]. Almost contemporarily, Tommassetto and others identified the same hormone for its regulatory role in gastrointestinal motility and named it motilin-related peptide [7].

2.1.1 Transcriptional regulation

The gene coding for ghrelin peptide, GHRL, spans 5 kb on chromosome 3p 25-36 in humans. Four exons encoding a precursor 117 aa protein, preproghrelin were initially identified [8], while 2 further exons were discovered later [9]. Preproghrelin, encoded by exons 1-4, includes 28 aa ghrelin and the 66 aa C-terminal peptide of preproghrelin, termed C-ghrelin. In turn C-ghrelin contains another bioactive 23 aa peptide, obestatin (Figure 1). Both ghrelin and C-ghrelin are released from preproghrelin by cleavage of a signal peptide and of the resulting proghrelin. Studies on the more recently identified exons 0 and -1 have shown that ghrelin locus splicing regulation may also produce gene-derived peptides independently of preproghrelin, suggesting an important physiological role for the modulation of GHRL-derived peptides expression [9]. Moreover, ghrelin sequence is highly conserved in mammals with only two different amino acids between human (GSSFLSP EHQ

RVQ QRKESKK PPAKLQPR) and rat/mouse (GSSFLSP EHQ **KA**Q QRKESKK PPAKLQPR) forms, also denoting a potential important biological role for this peptide [6].

Interestingly, genomic variation of the ghrelin gene has been associated with obesity development in humans. Two polymorphisms have been reported in humans: Leu72Met and Arg51Gln [10-12]. Individuals presenting Leu72Met allele have been shown to be protected against fat accumulation and associated metabolic comorbidities [13]. The Arg51Gln polymorphism changes the processing site of ghrelin within its precursor protein, preventing normal ghrelin editing. Importantly, its prevalence was shown to be 6.3% in obese subject, while it was not detectable among non obese individuals, showing a clear link with obesity development [12].

2.1.2 Post-translational modifications

Importantly, the hormone described by Kojima et al. as an endogenous ligand for GHSR is an acylated peptide. The ghrelin peptide, in fact, undergoes post-translational modifications, the main being acylation on S3 by the membrane bound enzyme ghrelin-O-acyl-transferase (GOAT) [14] (Figure 1). This enzyme, highly conserved across species, has a tissue expression profile similar to ghrelin, with highest expression in stomach, pancreas and intestine and ghrelin acylation is completely prevented in GOAT knock-out mice [15-17]. While fatty acids derived from acetic (C2) to tetradecanoic acid (C14:0) are all possible ligands, octanoic acid (C8:0) is the principal fatty acid involved in this reaction, and decanoic (C10:0) and likely decenoic (C10:1) acids have also been reported as optimal ligands [16,18-20]. In human stomach and plasma samples both octanoyl-Ser3-ghrelin and decanoyl-Ser3-ghrelin forms have been detected also lacking the C-terminal amino acid Arg28. In vitro experiments did not show different effects between these identified acylated forms on receptor binding and GH secretion activity [19].

In vitro studies have also shown that the ghrelin peptide is an excellent substrate for protein kinase C at Ser18. Ghrelin phosphorylation induces protein structural changes which affect both acylation and membrane binding in vitro [21], but its potential importance in vivo is currently unclear.

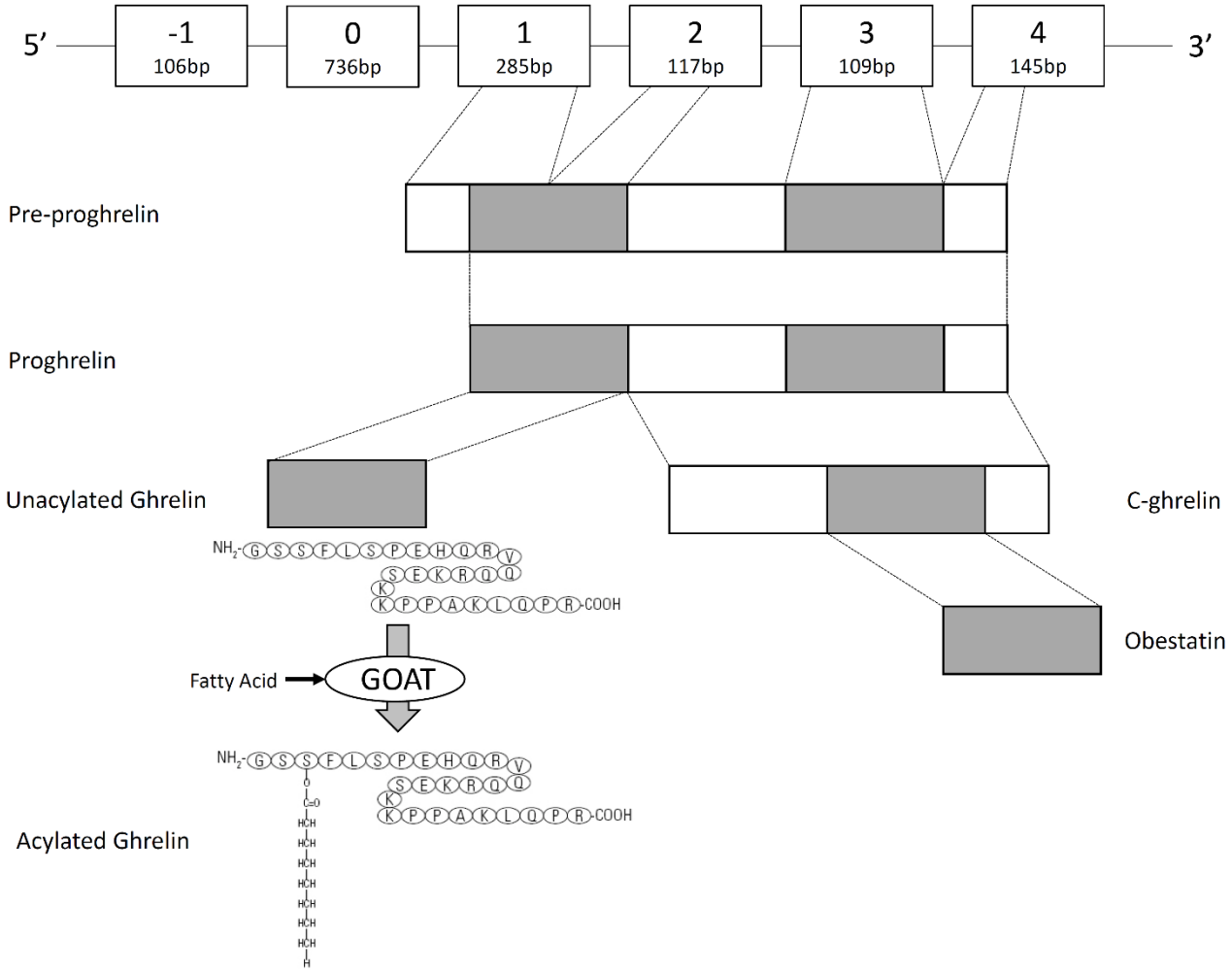

Figure 1. Diagram showing ghrelin gene splicing products and ghrelin's post translational modifications. Adapted from Liu et al. 2011 and Sato et al. 2012 [22,23].

2.1.3 Tissue expression, mechanisms of secretion and circulating forms

Ghrelin is mainly secreted by endocrine cells (P/D1 in humans and X/A-like in rats) located in the gastric fundus, and gastrectomy reduces ghrelin plasma concentrations by 65% [24], but its expression has also been described in duodenum, jejuna, ileum, colon and at lower concentrations in the pancreas, adipose tissue, kidneys, testes, placenta, hypophysis and

nucleus arcuatus in the hypothalamus, an important region for appetite regulation [25-34]. Ghrelin mRNA has also been identified in several cell lines including TT cells from medullary carcinoma of the thyroid, ECC10 cells from gastric carcinoid, HL-1 cardiomyocytes and kidney-derived NRK-49F cell line [30,35,36].

Ghrelin release from the stomach has been reported to involve sympathetic nerves [37] and recent evidence shows that ghrelin secretion in gastric endocrine cells is mediated by a series of G-protein coupled receptors (GPCRs), allowing for its release to be integrated in a network of modulatory signals. Release stimulation is in fact generally mediated by all Gs-coupled GPCRs including the β1-adrenergic receptor, the GIP receptor, the secretin receptor (SCTR), the sensory neuropeptide receptor CGRP, and the melanocortin 4 receptor, while inhibition is modulated by Gq and/or Gi coupled receptors including the somatostatin receptors (SSTRs), the lactate receptor (GPR81) and receptors for short chain (FFAR2) and long chain fatty acids (FFAR4) [38].

Both acylated (AG) and unacylated (UnAG) ghrelin forms are detectable in human and animal plasma. Interestingly, most circulating ghrelin is unacylated, whereas the acylated hormone is generally considered to only account for approximately 10% [14,39-41], with possible variations depending on the detection technique used. Mizutani et al. have shown that, while unacylated ghrelin is localized in both gastric open-type cells and closed-type round cells, the acylated form is present only in the latter [42,43]. Both cell types are able to release hormone forms, with enhanced unacylated but not acylated ghrelin secretion at lower gastric pH [43], suggesting a potentially different physiological roles for the two forms.

Moreover, circulating ghrelin is subject to de-acylation and cleavage, with a half-life of respectively 240 min in humans and 30 min in rats. Ghrelin inactivation is mediated by different enzymatic systems across species, allowing for the above reported different half-life of acyl-ghrelin: while butyrylcholinesterase is reportedly the main responsible system for

ghrelin inactivation in humans, carboxylesterases are the predominant enzymes involved in ghrelin des-octanoylation in rodents [44].

Ghrelin acylation also impacts on its transport across compartments, in particular across the blood brain barrier (BBB). While octanoylated ghrelin crosses the mouse BBB mainly from brain to blood, passage for the unacylated peptide was observed only in the opposite direction [45]. Interestingly, later studies showed that whole body energy balance impacts on ghrelin transport at BBB level, with obese mice showing reduced permeability compared to lean animals. Moreover, triglyceride co-administration increased ghrelin transport [46], suggesting a role for nutrients in modulating ghrelin action at central level.

2.1.4 Ghrelin release modulation and feedback regulation

Regulation of ghrelin secretion is still partly unknown but it is well established that ghrelin mRNA and plasma concentrations are increased during fasting [47,48] and in humans circulating ghrelin is characterized by a peak just before meals, suggesting a potential role in meal initiation [49,50]. On the contrary, ghrelin expression and plasma concentrations are decreased by food intake [50,51] and in relation to food composition, with maximum inhibitory effect observed after carbohydrate ingestion, compared to proteins and lipids [52,53].

In the long term, plasma ghrelin levels are related to body weight and composition, with lower levels in obese patients and higher concentration in anorexia and in negative energy balance conditions including cachexia [6,54,55]. Moreover, among selected obese individuals, lower ghrelin levels was related to a decrease in UnAG with no change in AG levels compared to non-obese [56]. The same study also showed that AG levels in obese individuals which did not meet the diagnostic criteria for metabolic syndrome were comparable to both lean and obese subjects with the metabolic syndrome [56].

Regarding the modulation of acylation, ingested fatty acids are directly used for AG acylation and GOAT activation is reported to be modulated by ingestion and availability of medium chain fatty acids and triglycerides [6,57,58]. GOAT is also potently inhibited by octanoylated ghrelin end-products, suggesting the existence of a negative feedback regulation in AG synthesis [16]. Moreover, recent evidence shows that GOAT expression levels decrease during prolonged fasting, leading to an increase in UnAG rather than AG in that condition. Interestingly, GOAT-null mice, while producing no AG, present a marked increase in UnAG levels in association with lower body weight and fat mass, and opposite effects are observed in transgenic mice overexpressing GOAT [16,57]. This body of evidence strongly supports the hypothesis that the GOAT-ghrelin system acts as a nutrient sensor providing information on the presence of nutrients, potentially leading to the optimization of nutrient partitioning and growth signals [57-59].

2.1.5 Ghrelin receptor (GHSR)

Acylated ghrelin's receptor is a G-protein coupled receptor produced in two isoforms by alternative splicing of an mRNA transcript of a single gene, located on chromosome 3 q26-27 [6]. Transcript 1a encodes the functional protein by excising an intron, which is instead retained in 1b. The latter isoform is not functional as AG receptor but its expression may prevent the activity of the form 1a by heterodimerization [60]. AG binding sequence has been identified in the first 4 residues at the N- terminus of ghrelin, which include the octanoylation site in Ser3 [61], and its interaction with GHSR leads to a Gq-mediated activation of phospholipase C and subsequent production of inositol 3 phosphate and diacylglycerol. In turn, this leads to Ca^{2+} release from the sarcoplasmic reticulum and ultimately to GH secretion.

GHSR1a is highly expressed in the pituitary and hypothalamus but also at lower levels in other brain areas including hippocampus, ventral tegmental area, nucleus tractus solitarius

and substantia nigra. Interestingly, also numerous peripheral tissues express GHSR including intestine, pancreas, heart, lung, kidney and adipose tissue [62-66]. Evidence by several authors is consistent in failing to detect GHSR1a expression in both skeletal muscle and liver [62,67-71]. Interestingly the expression of both ghrelin and GHS-R1b has been reported also in tissues not expressing the active receptor form, including liver [62,70], suggesting that ghrelin may produce tissue-specific effects by activating different pathways potentially through modulation by other GHSR splice variants and their interactions [62,72].

Although some reports suggest that UnAG shares some non-endocrine functions with AG such as cellular proliferation regulation and adipogenesis [73], no receptor for UnAG has been currently identified [59]. Evidence suggesting a potential interaction of UnAG with GHSR sub-types or other receptors, including CRF type two receptors [67,73,74] has not been confirmed.

2.2 Ghrelin effects on energy metabolism, body mass and composition

Since its discovery, ghrelin has been progressively characterized as a hormone involved in energy balance homeostasis as well as in GH secretion. Its functions span from central regulation of feeding to the modulation of whole body and tissue-specific metabolism [59]. With regard to ghrelin acylation, AG has long been considered the active form of the hormone for its interaction with GHSR and for its impact on GH secretion and on appetite stimulation, while UnAG was regarded as a degradation product without biological activities. As a consequence, until recent years most studies were focused on AG, or did not differentiate the two forms [75].

2.2.1 Food intake and energy balance

Ghrelin has a modulatory role in the regulation of energy homeostasis including appetite stimulation, with its acylated form being by far the most active [76]. Both peripheral and central treatment with AG increase food intake and body weight in experimental models [77-79]. In

agreement with the described low permeability of BBB to AG in the blood-to-brain direction [45], one study reports that ghrelin signalling from the stomach to the central nervous system (CNS) is principally mediated by afferent vagal nerve, and ghrelin-induced stimulation of appetite and GH secretion are prevented by blocking vagal fibres [34]. This point remains controversial since other studies show that vagal afferents are not necessary for AG effects on appetite stimulation and ghrelin analogues are effective also after gastrectomy and related vagotomy [80-82]. Importantly, effects of AG in appetite stimulation are preserved in GH-deficient rats, showing its independence from GH release [77].

At CNS level AG-induced effect on appetite stimulation is mediated by hypothalamic neuropeptide Y (NPY) secretion but also by interaction with other known appetite regulators at this level, including AgRP, orexin, endocannabinoids and leptin [6,77,83,84]. NPY-producing cells largely express ghrelin receptors, and ghrelin i.v. administration in mice largely stimulates hypothalamic activity in the same neurons [85,86]. Further studies have shown that ghrelin-induced effects on appetite regulation through NPY/AgRP neurons are dependent on variations in mitochondrial reactive oxygen species generation, and that this mechanism involves the increase of mild uncoupling activity by enhancing uncoupling protein-2 (UCP2) expression [87].

Nucelus caudatus and mesolimbic centres are also involved in long term energy homeostasis regulation by ghrelin [49] and effects on appetite possibly involve hedonic appetite regulation pathways [88]. In agreement, using functional magnetic resonance imaging, Davis et al. have shown that ghrelin administration increases activity in food-reward brain regions in humans [89].

UnAG effects on energy metabolism are largely unknown. While some authors report that in rodent models peripheral UnAG treatment decreases food intake in association with slower gastric transit [90], others do not confirm this effect but describe an inhibitory effect of

UnAG on AG-induced increase in food intake when both forms are administered simultaneously [91]. This effect appears to be independent of GHSR1a modulation and at least in part mediated by UnAG-induced release of nesfatin-1, an inhibitor of NPY. Central administration of UnAG, on the contrary, is reportedly also orexigenic [92], indicating that further investigation on UnAG effects and receptor interaction is needed.

2.2.2 Whole body glucose homeostasis

Ghrelin also causes several direct effects on systemic and tissue metabolism, independently of food intake. At whole body level, ghrelin has an important impact on glucose homeostasis. Not long after ghrelin's discovery, Broglio et al. reported that AG increases blood glucose levels and reduces insulin secretion [93]. Later studies showed that AG reduces glucose stimulated insulin secretion, rather than fasting insulin levels [94]. Consistently GHSR null mice have lower fasting glycaemia compared to control [95]. Underlying mechanisms were later investigated, showing that AG inhibits insulin release at pancreatic level by acting on voltage-dependent K channels (Kv) in β-cells. In fact, AG interaction with GHSR activates Kv channels through the receptor coupled G-protein α_i, thus preventing Ca^{2+} signalling and limiting insulin exocytosis [96]. Further studies unveiled a more complex regulatory mechanism, showing that the interaction between GHSR and somatostatin receptor in β-cells was able to shift G-protein activation from type α_i to α_q, thereby stimulating instead of inhibiting insulin release [97]. Interestingly, ghrelin modulates glucose homeostasis also by action on CNS, in parallel with appetite stimulation. Selective restoration of GHSR expression in the brainstem of GHSR null mice, in fact also recovered fasting blood glucose levels [98].

Ghrelin also impacts on insulin sensitivity. In humans, total circulating ghrelin levels are positively associated with insulin sensitivity both in the general population [99] and in insulin-resistant diseases, including chronic renal disease [100] and obesity [101]. In addition,

epidemiological data clearly shows that total plasma ghrelin is also inversely associated to the risk of developing type 2 diabetes and to several cardiovascular risk factors [99].

With regard to ghrelin forms, in 2004 Broglio et al. reported that UnAG coadministration with AG in humans counteracted the decrease in insulin levels induced by AG alone [102]. Later evidence showed that, at variance with AG, UnAG potently rises insulin release in glucose-stimulated conditions in rats [103], suggesting a potential independent role for UnAG in regulating glucose and lipid metabolism. Studies performed in a cohort of 45 metabolic syndrome patients clearly showed different associations of ghrelin forms with insulin resistance. AG ghrelin levels were, in fact, positively correlated with insulin resistance (HOMA index), while UnAG levels were markedly inversely correlated with the same parameter [56]. These results, combined with observations that despite a positive modulatory effect on insulin release in vitro [104,105], acute administration of UnAG does not impact basal or stimulated insulin secretion in β-cells in humans [106], strongly suggests that UnAG may have a regulatory role on insulin action at tissue level. Ghrelin is, in fact, known to have several important modulatory effects on insulin-sensitive tissues including adipose tissue, liver and especially skeletal muscle. Moreover, AG metabolic effects are emerging to be tissue specific, as supported by several studies showing the complexity of ghrelin signalling transduction in relation to the different expression of receptor forms and their interactions among tissues [107-110]. The role of UnAG in tissue insulin action and metabolism is largely unknown.

2.2.3 Liver

Ghrelin modulates hepatic gluconeogenesis and therefore glucose release from the liver. AG and UnAG were shown to have differential effects on glucose production in cultured hepatocytes, with AG stimulating gluconeogenesis and UnAG suppressing it [111]. The same effects were not replied with the GHSR1a agonist hexarelin, in agreement with reports of no

expression of GHSR in hepatocytes [111] and hexarelin administration in humans does not increase plasma glucose levels [111]. Consistently with experiments in vitro, PGC1α, a gluconeogenesis inducer, is increased in the liver of AG-treated rats [112] and mice studies with radiolabeled glucose showed that AG partially antagonizes insulin-induced suppression of gluconeogenesis [107]. Moreover, AG reduces insulin signalling in rodents, and this effect is not associated with changes in mitochondrial function [108,112].

The same authors showed that sustained AG treatment also causes modulation of liver lipid metabolism by inducing a pro-lipogenic gene expression pattern, increasing tissue triglyceride content and reducing the activation of stimulator of fatty acid oxidation AMP-activated protein kinase (AMPK) activation [108].

Both antioxidant and anti-inflammatory effects of AG have also been reported in the liver. In in vivo experiments in rodent models of liver injury as well as in in vitro experiments on primary human stellate cells exposed to chemical damage, AG blunted liver pro-oxidant and pro-inflammatory changes and this result was associated with reduced fibrosis [69,113].

AG was also reported to improve liver redox state in association with improved inflammation markers in high fat diet-fed rats [114,115]. Studies in high fat fed rats show that the beneficial impact of AG on liver redox state and inflammation is not paralleled, expect in one study [114], by improved hepatic insulin signalling, but rather by decreased activating phosphorylation at AKT and GSK-3β levels [112,115,116]. This finding is in agreement with in vitro studies in hepatoma cells [116] and is consistent with reports showing that in rodent high-fat feeding liver AKT activation may directly contribute to hepatic lipogenesis, oxidative stress and inflammation [117].

2.2.4 Adipose tissue

Appetite stimulating effects of ghrelin were very soon associated with increased body weight, and particularly of fat mass [79]. Further studies in animal models have shown that ghrelin impacts principally on retroperitoneal fat mass and only to a lesser extent on subcutaneous adipose tissue [118]. In a model of daily peripheral ghrelin administration these effects were found to be independent of appetite-induced increased food intake but instead related to reduced fat utilization [79], and in vitro experiments confirmed that ghrelin inhibits lipolysis in adipocytes [119]. Also, AG administration did not impact on food intake in high fat diet feeding but increased adipose tissue mass and favoured the expression of lipogenesis markers [120]. Consistently, ghrelin- or GHRS-null mice were protected from high fat diet induced obesity [121,122].

Ghrelin promotes adipocyte differentiation [123] and ghrelin's proadipogenic effect are at least in part mediated by peroxisome proliferator-activated receptor γ (PPARγ2), a transcription factor which favours triglyceride synthesis and downregulates lipolysis [124]. Also, mRNA levels of ATP binding cassette G1, a transporter involved in lipid exportation, are reduced in rats after ghrelin treatment [118].

Interestingly, in white adipose tissue, ghrelin enhances the expression of the uncoupling protein (UCP) 2, a protein involved in the regulation of mitochondrial reactive oxygen species (ROS) generation, and in UCP-2 null mice, ghrelin enhances its lipogenic effects, suggesting a possible feedback regulation mechanisms involving mitochondrial function [125].

UnAG impact on adipose tissue has been less investigated. While in vitro reports suggest that it may induce at least in part superimposable effects to those produced by AG on adipogenesis upregulation and lipolysis inhibition [119,126], in vivo studies in rodents show that UnAG peripheral administration may reduce fat mass [127]. Although further studies are needed on the potential role of UnAG on adipose tissue regulation, reported evidence

suggests that UnAG is an active hormone with modulatory functions in the complex context of lipid homeostasis.

2.2.5 Skeletal muscle

In muscle cells, ghrelin induces similar effects on cell differentiation to those observed in adipocytes, independently of acylation. AG and UnAG equally increase differentiation and fusion of C2C12 myoblasts [71], reduce skeletal muscle atrophy and enhance muscle repair by downregulating apoptosis, and these effects appear to be modulated by GHSR1a independent mechanisms, as this receptor is reportedly not expressed in myotubes [128-130]. However, not all effects are shared by ghrelin forms in skeletal muscle. In fact, UnAG but not AG reportedly facilitates the recruitment of muscle stem cells for tissue repair after ischemic damage [131].

Skeletal muscle metabolism is characterized by a cluster of interlinked metabolic functional pathways, including mitochondrial function, redox state regulation, inflammation and insulin signalling and action. Increased muscle ROS production and inflammation are linked at the level of IκB/NF-κB activation, and may cause insulin resistance by inhibition of insulin signalling downstream of insulin receptor [132-135]. Interestingly, ghrelin has been reported to be an important modulator of these factors at several levels.

2.2.5.1 Mitochondrial function

Mitochondrial respiration may be modulated by several mechanisms including UCPs, which selectively reduce mitochondrial ROS generation by inducing mild uncoupling [136,137]. Interestingly, ghrelin has been also reported to increase UCP-2 expression not only in NPY/AgRP neurons as described, but also in white adipose tissue and in brain cells after traumatic brain injury, in association with increased mitochondria stabilization and reduced pro-apoptotic caspase-3 expression [125,138].

In skeletal muscle, both UCP2 mRNA and protein levels are increased after 4-day AG treatment at non orexigenic doses in healthy rats, and this finding is importantly associated with enhanced mitochondrial enzyme activities [108]. Moreover, the same AG treatment improved altered mitochondrial oxidative capacity and transcription of mitochondrial regulatory genes in uremic rats [139], and was associated with preserved muscle triglyceride accumulation in high fat diet-fed rodents [112]. While these findings highly support mitochondria as a target for GHSR-independent AG activities in skeletal muscle, no data is currently available on UnAG effects.

2.2.5.2 Redox state

In addition, a role for ghrelin in blunting oxidative stress is supported by several studies at whole body level and in several tissues. In obese patients ghrelin levels negatively correlate with systemic oxidative stress marker 8-epi-prostaglandin $F_{2\alpha}$ (8-epi-PGF2α) [140] and in normobaric hypoxia, ghrelin administration attenuates hypoxia-induced increase in plasma levels of malondialdehyde (MDA), another marker of oxidative stress [141]. At tissue level, the same study also showed reduced MDA levels in the brain of ghrelin-treated hypoxic rats compared to non-treated, with no difference in the activities of antioxidant systems [141]. Moreover, evidence supporting ghrelin as a negative modulator for oxidative stress has been reported also in other tissues. Beside previously described antioxidant effects in the liver, in experimental models of ischemic or alendronate-induced gastric injury, intravenous ghrelin treatment lowered tissue damage in association with lower ROS production [142,143]. Also, reperfusion with ghrelin in a rat model of cardiac cachexia decreased myocardial lipid peroxidation [144].

Underlying mechanisms may involve a negative modulation in ROS generation. AG effect on ROS production by inducing mild uncoupling in mitochondria has already been described. Ex-vivo ghrelin incubation of aortic rings has been reported to produce attenuation in

superoxide generation by NADPH oxidase [145]. Interestingly, UnAG but not AG reduced NADPH oxidase activation markers in endothelial progenitor cells (EPC) both in individuals with type 2 diabetes and in a mouse model of obesity, with improved EPC cell function [146].

Other authors observed that AG increases antioxidant mechanisms. AG reportedly enhances the activities of antioxydant enzyms superoxide dismutase (SOD), catalase and glutathione peroxidase (GPx) in preadipocytes, ovarian cells and kidney [147-149]. In vitro studies have shown that AG also increases the bioavailability of nitric oxide (NO) [150], a well-known superoxide scavenger [151]. Very recent reports suggest that UnAG may also increase antioxidant systems activities. Incubation with UnAG of human retinal microvascular endothelial cells, in fact, increased SOD-2 and catalase expression in association with lower apoptosis, in a mechanisms madiated by sirtuin-1 activation [152].

While both the hypotheses that ghrelin lowers ROS generation and that it increases tissue antioxidant mechanisms are supported by studies in different tissues, the topic is still debated. In fact, some evidence shows that ghrelin may induce lower ROS generation without parallel modifications in antioxidant systems [141] and the mechanisms underlying the interaction between the two systems in ghrelin stimulation conditions are not known.

Very few data are available on ghrelin effects on skeletal muscle oxidative stress. AG potential role in skeletal muscle redox state modulation has been investigated in a rodent model of diet-induced obesity. In one-month high fat diet-fed rats, sustained 4-days AG treatment did not modify obesity-induced increase in muscle GPx or glutathione oxidation status [153]. Interestingly, recent reports by Togliatto et al. have shown that increased skeletal muscle ROS imbalance in a mouse model of limb ischemia was counteracted by UnAG but not AG treatment via an increase in SOD-2 expression. Moreover, this effect led to enhanced miR-221/222 expression with improved muscle regeneration [131].

2.2.5.3 *Inflammation*

AG has been reported to lower inflammation in different experimental settings [154]. GHSR is expressed in both human T lymphocytes and monocytes, and in these cells ghrelin inhibits the expression of the pro-inflammatory cytokines IL-1β, IL-6 e TNF-α [155]. In endothelial cells incubated with H_2O_2, an in vitro model of oxidative injury, as well as in rats and healthy humans treated with i.v. endotoxin administration, an in-vivo model of sepsis, AG blunts inflammatory cytokine release and fever [156-158]. Importantly, ghrelin levels are increased in septic dogs [159] and ghrelin is among the first increasing hormones responding to endotoxic shock in humans [157], further supporting its anti-inflammatory role. Moreover, AG-induced reduction of pro-inflammatory cytokines is paralleled by increased levels of the anti-inflammatory cytokine IL-10 in several cell types [160,161].

This consistent evidence on the systemic and tissue anti-inflammatory effects of ghrelin has suggested its potential use as a therapeutic agent in clinical settings characterized by high inflammation. Clinical trials have so far shown that ghrelin treatment suppresses airway neutrophil-dominant inflammation in patients with chronic respiratory infection [162] and that postoperative ghrelin administration in patients with oesophageal cancer inhibited inflammatory mediators and ameliorated their clinical course [163].

The role of ghrelin in skeletal muscle inflammation is largely to be investigated. However, sustained administration of AG markedly lowered tissue NF-κB nuclear translocation and tissue TNFα expression in a rodent model of diet-induced obesity, independently from changes in redox state [153].

Interestingly, AG effects in lowering inflammation are also associated with improved redox state in different models [142,143], strongly suggesting an interplay between ROS production or scavenging and inflammation modulation. Since in skeletal muscle high TNFα levels may

reduce mitochondrial function [164], AG might improve mitochondrial function with a mechanism at least in part involving the reduction of TNF-α levels.

With the exception of one report, stating that UnAG does not share with AG anti-inflammatory effects in endothelial cells in vitro [158], the role of the unacylated form of the hormone on inflammation is currently unknown.

2.2.5.4 Tissue insulin signalling and action

Available data globally suggests that AG enhances mitochondrial function, improves redox state and inflammation. In several models and experimental settings, it has been shown that these effects, alone or combined, are associated with increased tissue insulin sensitivity and action [133-135], suggesting that AG may potentially improve insulin sensitivity at least partly through these pathways.

In several tissues AG has in fact been reported to activate protein kinase B (AKT), a main mediator of insulin signalling pathway (Figure 2), in association with various effects. These include the improvement of engrafted mesenchymal stem cells functional survival in an in vitro model of ischemic heart [165], the alleviation of early brain injury in a rat model of subarachnoid haemorrhage [166], the promotion of intestinal epithelial cell proliferation in vitro [167], the protection of cultured pulmonary artery endothelial cells from hypoxic damage [168], the induction of endothelial progenitor cells migration [169], However, it must be noted that these effects are to be considered tissue specific, since previously described evidence conversely shows that AG lowers AKT activation in the liver. Moreover, in HL-1 cardiac cells and neonatal rat cardiomyocytes, AG does not modify AKT activation [170].

Acute AG infusion in humans [171,172] or experimental models [107] has provided conflicting results in term of systemic or muscle insulin sensitivity changes, with reports of enhanced [107], unchanged [172] or reduced [171] insulin action. However, when sustained administration

studies are performed, AG administration at non-orexigenic doses has been consistently reported to improve systemic or muscle insulin sensitivity in experimental models [112,155]. In lean rats, 4-day AG treatment enhances activating phosphorilation of insulin signalling mediators at pAKT^{S473} and pGSK-3β^{S9} levels, in association with increased transcript levels of GLUT-4, a transporter involved in glucose uptake that is in turn stimulated by AKT activation [112,173]. Consistently, incubation of C2C12 differentiated myoblasts with AG also resultes in increased GLUT4 translocation and enhanced glucose uptake [67].

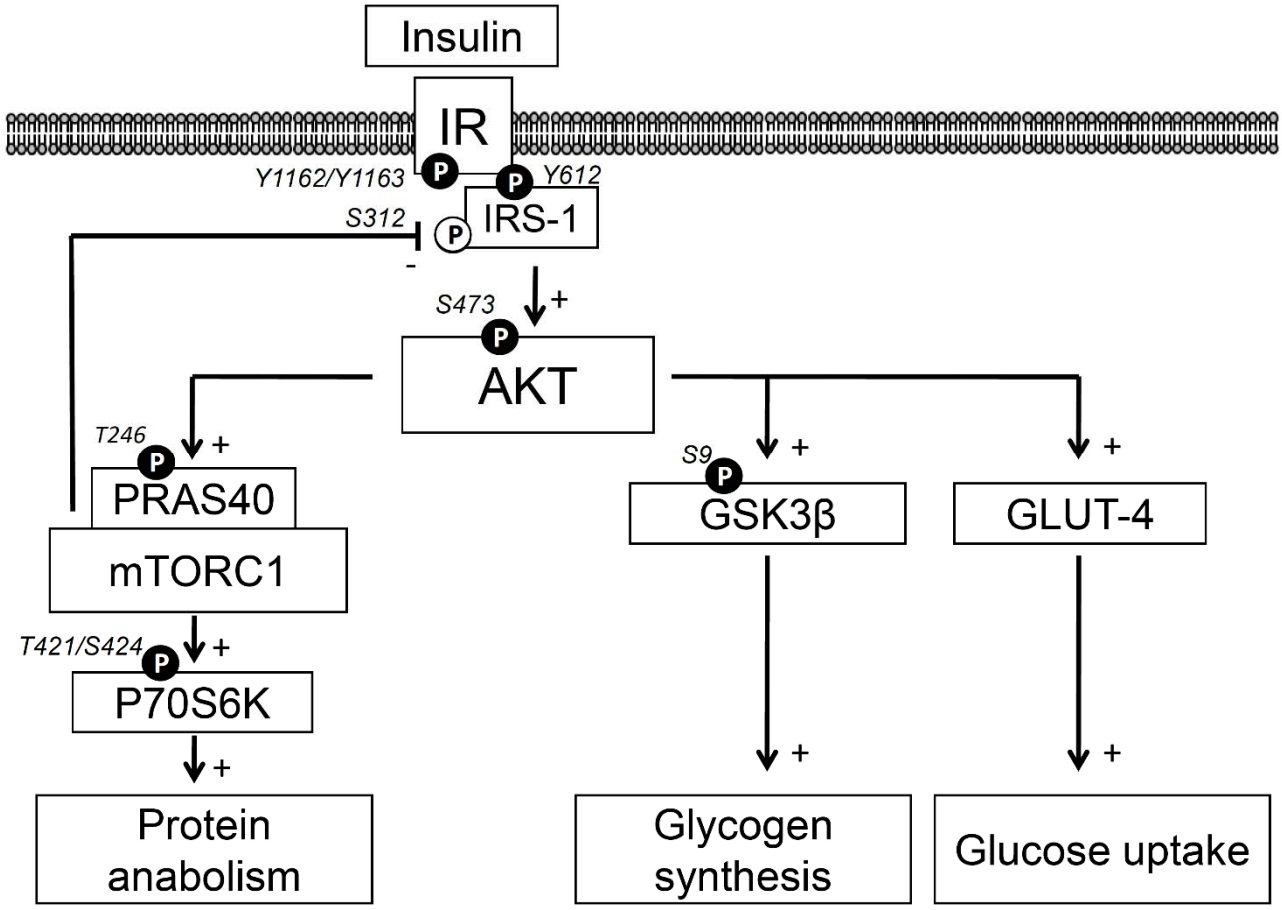

Figure 2. Diagram illustrating the principal insulin signalling pathway mediators and their biological effects in skeletal muscle [174,175]. Main regulatory phosphorylation sites are also reported.

Activation by AG of skeletal muscle insulin signalling at AKT level has also been reported in a rat model of chronic kidney disease, but these findings could have been at least in part

dependent on the increased food intake observed in that study, in which a high hormone dose was chosen [139]. On the contrary, studies in high fat diet-induced obesity and insulin resistance models failed to show significant increases in muscle insulin signalling activation at AKT and GSK-3β levels [153].

UnAG effects on insulin signalling are currently largely unknown. Interestingly, one study by Lear et al. showed that in HL-1 cardiac cells and in primary cultures of neonatal rat cardiomyocytes, while both ghrelin forms do not activate AKT, UnAG but not AG increases insulin-induced GLUT4 activation [170].

2.3 Ghrelin effects on autophagy

Autophagy is an intracellular selective auto-degradation process first observed by Ashford and Porter in 1962 [176]. Further studies have characterized this mechanism by which the cell may remove unnecessary or dysfunctional cellular components, including misfolded or aggregated proteins, endoplasmatic reticulum, peroxisomes and mitochondria, thus contributing to balancing energy sources, especially at critical times in development as well as in response to nutrient stress [177]. In fact, autophagy has a role in the degradation of unneeded proteins, contributing to amino acid recycling for essential proteins synthesis, but may also eliminate dysfunctional mitochondria, thus removing inefficient energy consumption and also excess ROS generation [178,179]. However, although autophagy may be considered a survival mechanisms, its deregulation may lead to non-apoptotic cell death [180].

Autophagy is triggered by stress signalling pathways, which start the formation of a phagophore by Becilin-1/vacuolar protein sorting 34 (VPS34) at the endoplasmatic reticulum level. The phagophore is then multimerized by interaction with the ATG5-ATG12 autophagy proteins complex, a key player in the autophagy machinery. The growing phagophore may then recruit microtubule-associated protein 1A/1B-light chain 3-II (LC3-II), another key

player derived from proLC3 by ATG4-mediated proteolytic cleavage and ATG3-mediated phosphatidylethanolamine conjugation. Following steps consist in selected targets capture, fusion with the lysosome and, finally, proteolytic degradation (Figure 3). Mechanism of target identification are currently unclear but interaction between phagophore LC3-II and adaptor molecules on the target is likely [177].

In 2012 Słupecka et al. showed that enteral AG administration was able to favour small intestine mucosa renewal in new-born piglets in association with enhanced autophagy [181], demonstrating for the first time a link between ghrelin and autophagy. These findings were followed by other studies in different tissues, experimental models and conditions, and mostly confirmed ghrelin as an autophagy inducer.

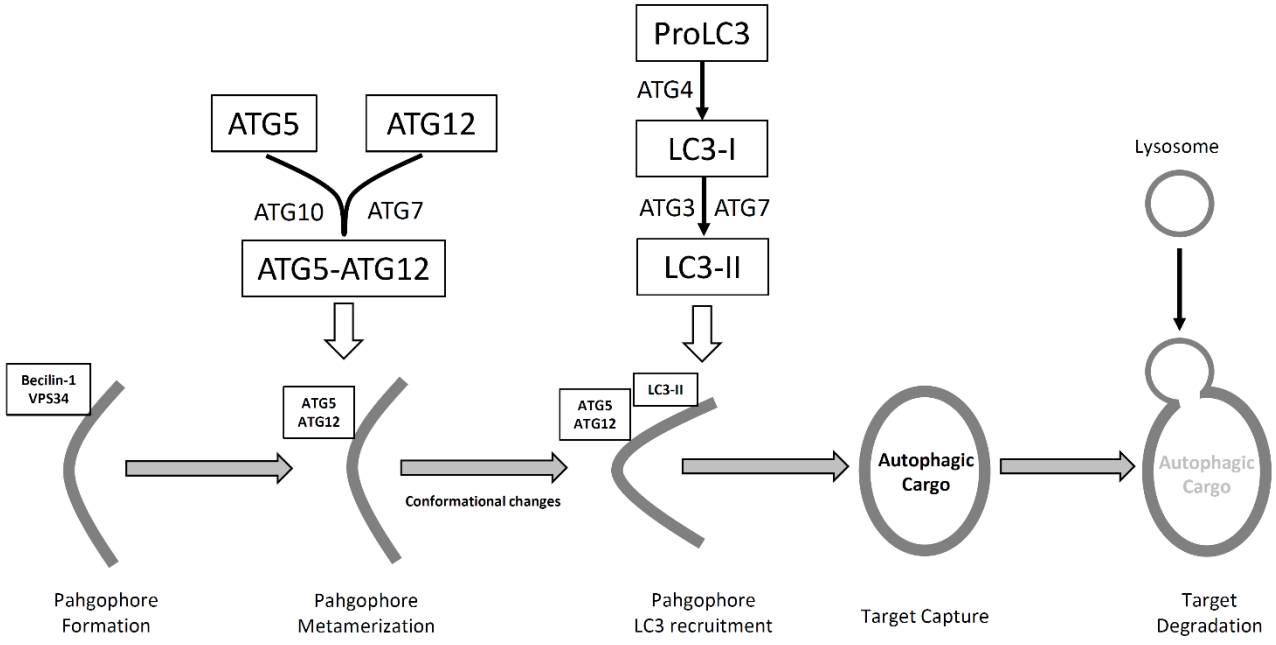

Figure 3. Main passages involved in autophagy machinery [177,182]. After phagophore formation via Becilin-1/VPS34, and its metamerization by binding with the ATG5-ATG12 protein complex, conformational changes occur, favouring binding with processed LC3, subsequent activation and target capture, lysosomial fusion and target degradation. ATG: Autophagy protein, LC3: microtubule-associated protein 1A/1B-light chain 3, VPS34: vacuolar protein sorting 34.

In colon adenocarcinoma and ovarian epithelial carcinoma cells, AG induces autophagy via mTOR signalling pathways, causing reduced cell proliferation and ultimately apoptosis [183,184]. Moreover, both ghrelin forms reduce TNF-α-induced autophagy in human visceral adipocytes [185] and in both hepatocytes in vitro and in a model of high fat diet-induced obesity, AG treatment reduces lipotoxicity via autophagy induction [186]. In full agreement with data suggesting a role of ghrelin in autophagy stimulation, autophagic flux was found to be reduced in the livers of ghrelin deficient mice [187].

Conversely, it must be noted that fewer reports instead reported that ghrelin treatment in vitro and in vivo and reduces autophagy, in association with attenuated CCl_2-induced liver fibrosis, improves liver dysfunction in acute hepatitis and blunts doxorubicin-induced cardiotoxicity [188-190].

Interestingly, experiments in an in vitro model of cardiac hypoxic injury showed that AG stimulated autophagy with parallel reduction of ROS generation [191]. In skeletal muscle cells, both AG and UG enhanced autophagy markers including LC3II to LC3I ratio and ATG5-ATG12 complex levels, while blunting apoptosis. Moreover, in a mouse model of gene-induced insulin resistance, UnAG was also able to improve muscle insulin signalling and GLUT4 activation in association with increased autophagy [192]. These data show that ghrelin effects on autophagy are likely independent of hormone acylation, therefore suggesting the involvement of a signalling pathway not related to GHSR1a [129]. Moreover, they suggest that the impact of ghrelin forms on ROS generation and insulin signalling may at least in part be mediated through upregulation of autophagy.

2.4 Ghrelin and obesity-induced insulin resistance

2.4.1 Obesity and obesity related metabolic complications

Obesity is an emerging important health risk factor. More than 1.1 billion adults and 10% of children are classified as overweight or obese and at least 2.8 million adults die each year

from obesity-related complications [193,194]. World Health Organization has classified obesity among chronic diseases for its life-lasting effects and for its strict association with increased morbidity and mortality. Excess weight, with relative increase in fat mass, is in fact related to the developement complications at cardiovascular and tissue levels including insulin-resistant diabetes, liver diseases, hypertension and cancer [194].

Several authors have shown that in subjects aged <65 years, the relative death risk steadily increases with body mass index (BMI) [195,196]. Importantly, weight and fat mass gain is strictly associated with the development of metabolic complications, including insulin resistance, and atherogenic dyslipidaemia [197,198]. Consistently, bariatric surgical approaches, when successful in achieving a durable reduction of body weight, also improve metabolic comorbidities [193].

With regard to molecular mechanisms, excess dietary lipid intake is associated with metabolic complications that include oxidative stress, inflammation and insulin resistance at both systemic and tissue level [199-201] and these factors are an emerging cluster of causally linked metabolic alterations [132,199,200,202] that may further cause mitochondrial dysfunction and tissue lipid accumulation [112,201]. The onset of these changes in insulin-sensitive tissues, and particularly in skeletal muscle and liver, may lead to impaired glucose metabolism, increased protein catabolism and tissue lipid accumulation, with enhanced morbidity and mortality [194,203].

2.4.1.1 Type 2 diabetes and insulin resistance

The association between obesity and type 2 diabetes has been known for decades, and the term “diabesity” was introduced by Sims in the seventies [204,205]. In 1998 Stevens et al. reported that 90% of individuals developing type 2 diabetes have a BMI>23 [206]. Following studies have shown that among obese patients the risk of diabetes development is further

increased by familiarity, abdominal fat distribution and time from obesity onset, with a higher risk for obese children to develop diabetes in the adulthood [194].

Type 2 diabetes is a metabolic disease characterized by high blood glucose levels in association with insulin resistance and relative insulin deficiency [207] leading to impaired insulin-stimulated glucose utilization in skeletal muscle and impaired gluconeogenesis inhibition in the liver. These alterations are also associated with the progressive impairment of β-cell compensation of insulin resistance by enhanced insulin secretion [208].

Type 2 diabetes diagnosis in humans is actually based on meeting one of the following criteria [209]:

1) blood glycated haemoglobin (A1C) levels ≥6.5%

2)fasting plasma glucose levels ≥ 126 mg/dL (7.0 mmol/L)

3) plasma glucose level ≥ 200 mg/dL (11.1 mmol/L) at two hours after administration of a 75g anhydrous glucose dissolved in water bolus

4) random plasma glucose level ≥ 200 mg/dL (11.1 mmol/L) in a patient with classical symptoms related to hypoglycaemic or hypoglycaemic crisis

Systemic insulin resistance may be directly quantified by euglycemic hyperinsulinemic clamp, the gold standard technique [210]. While not performed in humans, insulin tolerance test (ITT) [211] is still widely used and accepted in standardized animal models. In clinical practice, several indexes calculated from plasma glucose and insulin levels may be used, and the most widely accepted is the Homeostasis Model Assessment (HOMA) [212]. Insulin resistance assessment is important in clinical practice since increased insulin resistance is a strong predictor for type 2 diabetes, cardiovascular diseases and mortality also in the absence of hyperglycaemia alone [213,214].

2.4.1.2 Metabolic Syndrome

Metabolic syndrome is a term dating back to 1950s and used to describe associations of risk factors with diabetes. While the association between obesity and diabetes was reported in the literature since 1921 [215], progressively other factors were included. Today, while several definitions have been proposed by different expert groups, most include among diagnostic criteria increased central adiposity, dyslipidaemia in terms of high plasma triglycerides or low HDL levels, hypertension and hyperglycaemia [216,217] (Table 1).

Table 1. Metabolic Syndrome Criteria as proposed by different expert groups as summarized by Okafor [217].

Clinical measure		WHO (1998)[14]	EGIR (1999)	NCEP-ATP III[14] (2001)	AACE (2003)	1DF (2005)[15]	AHA
Insulin resistance		IGT, IFG, Type 2 DM or Insulin resistance *	Plasma insulin ≥75th percentile *	None †	IGT or IFG §	None	None
Body weight	M	WHR>0.90	WC ≥94 cm	WC ≥102 cm	BMI ≥ 25 kg/m^2	Increased WC (population specific)	WC ≥102 cm
	F	WHR >0.85 and/or BMI >30 kg/m^2	WC ≥80 cm	WC ≥ 88 cm			WC ≥ 88 cm
Lipid		TG ≥150 mg/dl (1.7 mmol/l)	TG ≥150 mg/dl (1.7 mmol/l)	TG ≥150 mg/dl (1.7 mmol/l)	TG ≥150 mg/dl (1.7 mmol/l)	TG ≥150 mg/dl (1.7 mmol/l)	TG ≥150 mg/dl (1.7 mmol/l)
	M	and/or HDL-C <35 mg/dl (0.9 mmol/l)	And/or HDL-C <39 mg/dl (1.0 mmol/l)	HDL-C <40 mg/dl (1.03 mmol/l)	And HDL-C <40 mg/dl (1.03 mmol/l)	HDL-C <40 mg/dl (1.03 mmol/l)	HDL-C <40 mg/dl (1.03 mmol/l)
	F	HDL-C <39 mg/dl (1.0 mmol/l)	HDL-C <39 mg/dl (1.0 mmol/l)	HDL-C <50 mg/dl (1.3 mmol/l)	HDL-C <50 mg/dl (1.29 mmol/l)	HDL-C <50 mg/dl (1.3 mmol/l)	HDL-C <50 mg/dl (1.3 mmol/l)
Blood pressure (mmHg)		≥ 140/90	≥ 140/90	≥ 130/85	≥ 130/85	≥ 130/85	≥ 130/85
Glucose		IGT, IFG or Type 2 DM	IGT or IFG (but not diabetes)	>110 mg/dl [6.1 mmol/l] (including DM)	IGT or IFG (but not DM)	≥ 100 mg/dl (5.6 mmol/l) [includes DM]	≥ 100 mg/dl (5.6 mmol/l)
Others		Micro-albuminuria			Other features of insulin resistance		

M: Males, F: Females, IGT: Impaired glucose tolerance, IFG: Impaired fasting glycemia, WC: Waist circumference, WHR: Waist hip ratio, DM: Diabetes mellitus, HDL-C: High-density lipoprotein cholesterol. *Plus any 2 of the following, †but any 3 of the following, §plus any of the following based on clinical judgment

Interestingly, all these alterations are obesity-associated comorbidities, and define a constellation of interconnected risk factors for increased cardiovascular risk [216,218-220]. While the underlying mechanisms linking these factors are largely unknown, a central role for obesity and insulin resistance in metabolic syndrome is recognized by most authors [216].

Available data from epidemiological studies shows that 30% middle-aged individuals in developed countries currently meets metabolic syndrome diagnostic criteria, while the prevalence increases to 60% in subjects in their 70s [194,221], with similar values recorded for both genders [222]. While differences may be observed in different ethnic groups, the actual prevalence in the Italian population is reportedly 23% in both genders [222].

2.4.2 Ghrelin in obesity-induced insulin resistance

Despite the fact that ghrelin was at first characterized for its effects on GH secretion, above described polymorphism studies in ghrl gene have also established a link between ghrelin, obesity and obesity-correlated comorbidities development [12,13]. Moreover, effects of ghrelin on appetite stimulation and therefore on body weight and fat mass increase were soon identified [59]. Also, patients with Prader-Willy Syndrome (PWS), a complex genetic disease characterized by hypomentia, hormonal impairments and early obesity development, present high levels of circulating AG but not UnAG both in fasting and in postprandial conditions [223-226]. These findings soon led to the hypothesis that ghrelin agonists could be potentially used as anti-obesity drugs. Some studies further supported this hypothesis showing that engineered mice lacking GHSR expression, as well as mice with inducted expression of an inactive form of GHSR, did not develop obesity under high fat diet treatment [121,122,227]. However, enthusiasm for treating obesity by counteracting ghrelin-mediated effects on appetite was replaced by scepticisms as data from other studies showed that decreased ghrelin action does not always result in hypophagia and loss of body mass [228,229], and that ablation of ghrelin cells in adult mice does not decrease response to HFD [230].

However, observations suggesting that ghrelin could regulate glucose homeostasis and energy metabolism also independently of food intake, led to further investigations of its potential role in obesity and obesity-related co-morbidities. The first evidence linking ghrelin with human obesity and insulin resistance was reported soon after the discovery of the

hormone. In 2001 Tschöp et al. clearly showed that plasma ghrelin levels were decreased in obese humans [55] and a few years later McLaughlin et al. showed that among obese individuals, ghrelin levels were lower in insulin-resistant subjects [101]. This finding was further investigated in studies in selected patients with the metabolic syndrome which demonstrated that obesity-associated reduction in total plasma ghrelin levels was related to a decrease of the unacylated form, while absolute AG levels were not modified compared to non-obese [56]. The same study also showed that in metabolic syndrome patients, while AG levels were positively associated with insulin resistance, waist circumpherence and BMI, UnAG levels strongly negatively correlated with HOMA [56]. While further studies are required due to cohort numerosity and selection, these results for the first time demonstrated that insulin resistance was related with changes in circulating ghrelin profile, and in particular provided the proof of principle that increased insulin sensitivity is associated with higher UnAG levels.

At tissue level ghrelin has shown to produce a pattern of tissue specific effects in obese models. In rats fed with high fat diet (HFD) (60% of calories from fat) diet for 4 weeks, 4 day sustained AG administration improved liver oxidative stress and inflammation [115] and similar results were obtained also by other authors after 8 weeks HFD and AG treatment throughout the whole period [114]. These findings were not paralleled, expect in one study [114], by improved hepatic insulin signalling, but rather associated with decreased activating phosphorylation at AKT and GSK-3β levels [112,115,116]. Decreased hepatic insulin sensitivity in obese rats is also reportedly associated with a decrease in liver expression of insulin receptor substrate 1 (IRS-1), an important mediator and modulator of insulin signalling transmission from insulin receptor to AKT [231]. Interestingly, this finding was reversed by UnAG administration [232]. Collectively, these observations are consistent with reports showing that liver AKT activation may directly contribute to hepatic lipogenesis, oxidative stress and inflammation in rodent models of obesity [117]. Mechanisms involved in AG modulation of liver metabolism in diet-induced obesity are unknown, but a recent report has shown that in fat-induced obese

rodents, and in in vitro hepatocytes incubated with saturated fatty acids, AG treatment reduced lipotoxicity via autophagy induction [186].

With regard to adipose tissue, Perez-Tilve et al. have shown that chronic central AG administration in HFD-fed rats, while not increasing food intake, was however associated with enhanced lipogenesis and increased body fat mass, indicating that AG modulation of adiposity is independent of orexigenic effects [120].

In skeletal muscle, sustained 4-day AG treatment was associated with the prevention of tissue triglyceride content after 4 weeks of HFD [112]. Moreover, although in a similar study by the same group no effect on obesity-induced increase in muscle oxidized glutathione was observed, sustained administration of AG markedly lowered tissue NF-κB nuclear translocation and tissue TNFα expression [153]. This finding was not however associated with significant increases in muscle insulin signalling activation at AKT and GSK-3β levels compared to non-treated obese rats [153].

Despite reported UnAG association with insulin sensitivity in humans, currently almost no data is available on UnAG impact on mitochondrial function, redox state, inflammation and insulin signalling in insulin sensitive tissues.

Taken together, the current findings, while indicating that AG may potentially cause beneficial whole body and tissue-specific metabolic effects in fat-induced obesity, also provide a strong rationale for further investigation of ghrelin forms effects in this setting.

2.5 Ghrelin in chronic kidney disease-related wasting

2.5.1 Chronic kidney disease

Chronic kidney disease (CKD) is a general definition which includes heterogeneous disorders affecting the structure and function of the kidney [233]. Accordingly, its diagnosis in humans is based on the presence of kidney damage irrespectively of clinical diagnosis,

defined as glomerular filtration rate (GFR) <60 mL/min per 1.73 m^2 for 3 months or more [234]. Since GFR is the best overall index of kidney function, CKD is classified in five stages according to GFR [233]:

1. Stage 1: GFR >90 mL/min per 1.73 m²
2. Stage 2: GFR 60-89 mL/min per 1.73 m²
3. Stage 1: GFR 30-59 mL/min per 1.73 m²
4. Stage 1: GFR 15-29 mL/min per 1.73 m²
5. Stage 1: GFR <15 mL/min per 1.73 m²

Other important markers modified by CKD and used in disease evaluation both in humans and in animal models include proteinuria, blood and urine creatinine and plasma urea levels [233,235].

Importantly, metabolic derangements are typically developed in CKD patients, with protein-energy wasting affecting 18 to 75% of adults with end stage renal disease [236,237], in association with a substantial increase in morbidity and mortality [236,238]. However, also early subclinical stages of CKD may be associated with metabolic alterations, and in experimental models these effects have been observed only two weeks after 5/6 nephrectomy [239,240]. Animal models of CKD are therefore frequently used in nutritional research as clinically relevant models of wasting diseases [241].

2.5.2 Nutritional and metabolic alterations in CKD

Muscle wasting and consequent lean body mass decrease are a major problem in CKD, and are associated with increased morbidity and mortality [242,243]. CKD-related muscle loss is mediated by a complex network of nutritional and metabolic alterations. Although calorie intake is often reduced in CKD patients, contributing to a negative energy balance [244], emerging evidence supports a major role in this context for a cluster of metabolic alterations

including chronic systemic inflammation, mitochondrial dysfunction and oxidative stress, that may in turn lead to insulin resistance [132,199,200,202,245].

Systemic inflammation plays a key role in the pathogenesis of wasting. Both onset and progression of wasting syndromes are characterized by a pro-inflammatory cytokine pattern, with upregulation of tumour necrosis factor-α (TNF-α) and decrease of anti-inflammatory IL-10 levels [246] and TNF-α is known to enhance skeletal muscle protein catabolism by parallel inhibition of protein synthesis and stimulation of protein degradation. Moreover, TNF-α further increases tissue cytokine expression, causing amplification of the inflammatory response by inducing nuclear translocation and binding activity of transcriptional factor NF-κB [247].

While uremic toxins, recurrent infections and haemodialysis treatment may play a key role in triggering pro-inflammatory responses in CKD [246], these same factors may also lead to increased oxidative stress [248,249], thus further contributing to amplify inflammation at both whole body [250] and peripheral tissue levels through free radical-mediated NF-κB activation [251].

While several studies in animal models show that pro-inflammatory cytokines as well as oxidative stress may contribute to mitochondrial function impairment [164,201], recent evidence indicates that inflammation may favour mitochondrial dysfunction by inducing respiratory chain leakage and production of reactive oxygen species [252]. Muscle mass maintenance is strictly related to mitochondrial function, as confirmed by studies showing that PGC1α, a major stimulator of mitochondrial biogenesis, inhibits atrophy-inducing genes transcription [253]. In agreement with the above observations, reduced skeletal muscle oxidative capacity has been observed in CKD patients on conservative treatment, supporting the hypothesis that mitochondrial dysfunction may potentially contribute to protein-energy wasting in these patients [254].

Inflammation and oxidative stress have also been reported to cause insulin resistance in skeletal muscle [200,202,255], and this metabolic derangement is also characteristic of several chronic diseases including CKD [256,257]. Insulin resistance is associated with decreased muscle anabolism and high protein catabolism in experimental uraemia, in excellent agreement with results from studies in non-diabetic haemodialysis patients [258,259]. Moreover, further studies showed that insulin acutely increases mitochondrial function in terms of ATP production in healthy but not in insulin-resistant type 2 diabetic human skeletal muscle [260], suggesting that insulin resistance may also directly impair mitochondrial function. Collectively, these data provide evidence supporting the hypothesis that insulin resistance may potentially contribute to the vicious cycle linking muscle wasting and mitochondrial dysfunction, thus leading to reduced function and increased morbidity and mortality.

2.5.3 Ghrelin in CKD

Immediately after the first reports of ghrelin as a modulator of energy balance appeared, a potential role for this hormone in wasting conditions, including uraemia was hypothyzed. However, although ghrelin increases appetite and body mass increase, unexpectedly both clinical and experimental studies showed that plasma ghrelin levels were increased in end-stage renal disease (ESRD) compared to control subjects [261-263]. Moreover, plasma ghrelin levels have been reported to be specifically increased in patients with protein energy wasting and CKD [262].

This alteration may indeed be at least in part related to impaired renal ghrelin degradation and excretion [264], although inverse correlations between plasma ghrelin levels and nutritional markers appear to be preserved also in this setting [261]. Moreover, Yoshimoto et. al report that plasma creatinine levels are associated with total ghrelin but not with AG, thereby suggesting that renal function may have an important impact on UnAG levels [263,265].

Taken together, the paradoxical association between high ghrelin levels and muscle wasting observed in CKD, has led some authors to suggest the existence of a “ghrelin resistance” mechanism in this condition [245]. Consistently with this hypothesis, Bossola et al have shown that among CKD patients, plasma ghrelin levels are higher in those presenting anorexia than in individuals with preserved appetite [266], and similar findings have been described by other authors for UnAG [267]. Consequently, increasing ghrelin levels to overcome hormonal resistance could be regarded as a potential therapeutical approach.

In both rodent models and patients, administration of ghrelin or GHS-R agonists was shown to induce significant increases in food intake and body weight, in association with muscle mass and strength retention [268,269]. In a rat model of prolonged subcutaneous treatment, this effect was reported to be sustained with no decline of orexigenic effects and no relevant side-effects, suggesting a possible long-term beneficial role for ghrelin in CKD patients [270].

Interestingly, recent studies in clinical or experimental wasting, including CKD, have shown that the metabolic effects of ghrelin are not limited to appetite stimulation. In non-obese, non-diabetic haemodialysis patients, preserved insulin sensitivity is associated with higher total ghrelin and negatively associated with whole body inflammation [100]. Consistently, prolonged subcutaneous AG administration in nephrectomized rats reduced loss of muscle mass, in associated with an anti-inflammatory impact on circulating cytokines profile [271]. Since inflammation has a key role in the development of CKD-related anorexia and muscle mass loss [246,247], AG-induced lean body mass preservation could be at least in part mediated by blunting uraemia-related pro-inflammatory cytokine pattern. However, studies showing that ghrelin administration protects mice against acute kidney injury suggest that AG may produce beneficial effects in CKD also by direct modulation of renal function [272].

Further experiments in rodent models demonstrated that AG-induced lean mass retention is associated to enhanced muscle PGC1α transcription and to improved mitochondrial

function [139]. In agreement, AG treatment was recently reported to improve CKD associated physical decline in association with recovery of muscle mitochondrial activation [273]. While pair-feeding clearly demonstrated that these effects were independent of changes in food intake, both ghrelin treatment and increased food intake were necessary to enhance muscle insulin signalling and preserve lean mass [139].

Currently no data is available on the potential role of UnAG on tissue metabolism in CKD.

3 Aim of the studies

Although evidence in a selected patient cohort shows that insulin resistance is selectively inversely correlated with UnAG plasma levels, no information is currently available on the associations between ghrelin forms and insulin resistance in cross-sectional and prospective studies of community-based population cohorts.

We therefore at first aimed at measuring plasma ghrelin forms profile and insulin resistance by the validated HOMA index in a 716-individual community-based cohort from the North-East Italy MoMa epidemiological study [274]. We hypothesized that total ghrelin (TG) and UnAG, but not AG, are negatively associated with insulin resistance and that baseline TG and UnAG but not AG are independent predictors of insulin resistance and its time-related changes in individuals undergoing 5-year follow-up evaluation.

We then also aimed at investigating the molecular mechanisms potentially involved in UnAG modulation of insulin sensitivity by assessing potential ghrelin-induced alterations in a cluster of functional pathways known to modulate insulin activity at tissue level, including mitochondrial function, redox state and inflammation. We also investigated UnAG impact on the same parameters in animal models of diseases characterized by impaired insulin sensitivity, such as obesity and chronic kidney disease. No information is, in fact, currently available 1) on the impact of UnAG on skeletal muscle ROS generation, inflammation and insulin action; 2) on whether UnAG prevents altered oxidative stress, inflammation and insulin action in obesity and diabetes; 3) on whether, by acting through these mechanisms, UnAG may potentially induce a beneficial impact on muscle mass preservation in wasting conditions.

We therefore studied lean rats, transgenic mice with systemic UnAG upregulation [128] and 5/6 nephrectomized rats as a model of wasting disease [275] to test the hypothesis that UnAG

1) lowers mitochondrial ROS production and inflammation and enhances insulin action in lean rodent muscle; 2) normalizes high-fat diet (HFD)-induced muscle metabolic alterations, whole-body insulin resistance and hyperglycaemia; 3) improves metabolic alterations and insulin sensitivity while reducing muscle wasting in 5/6 nephrectomized rats. In addition, effects of UnAG were verified in vitro in myotubes, with the aim of mechanistically testing the hypothesis that UnAG activities are at least in part dependent on autophagy activation.

In addition, since factors involved in the modulation of ghrelin acylation in vivo are only partly known and no data is available in humans, we aimed at assessing whether circulating free fatty acids (FFA) contribute to regulate plasma AG and its ratio to total hormone. We therefore measured TG, AG and AG/TG in a community-based population cohort from the MoMa epidemiological study. In additional experiments, we further determined the potential causal role of enhanced plasma fatty acid availability by measuring plasma ghrelin profile following 150-minute intravenous lipid infusion in a rodent model. Long-chain fatty acid (LCFA)-lipid emulsions were employed in rodent experiments since they represent the predominant component of dietary and circulating FFA in humans and rodents [108]. Finally, since appetite-modulating effects have been reported for long-chain n-3 polyunsaturated fatty acids (PUFA) with controversial results under different clinical conditions [57,112,128], lipid emulsions with or without n-3 PUFA enrichment were infused to determine the potential differential impact of n-3 PUFA per se on ghrelin acylation.

4 Materials and Methods

4.1 Study protocols and experimental design

4.1.1 Human studies

Human studies were performed in the setting of the MoMa epidemiological study, a project supported by Friuli-Venezia Giulia Region aimed at investigating the prevalence of metabolic syndrome and related disorders in the municipalities of MOntereale Valcellina and MAniago, Pordenone, Italy [274].

4.1.1.1 Basal measurements and study population

In 2008, 2500 individuals aged 18-69 were randomly selected from population lists (total population: 16276, aged 18-65: 11393) and invited to participate. 1836 (73.4% participation rate, 16,1% of population aged 18-65) volunteers were enrolled and evaluated over the following 3 years [274]. The study was approved by the Pordenone Hospital Ethics Committee (ASS6 Ethical Committee authorization 41121/DS - 30/06/2006), and each subject received extensive oral and written information on study aims and risks before giving written consent to participate. Exclusion criteria for the current investigation were history or clinical or laboratory evidence of chronic disease including liver failure, renal failure (plasma creatinine > 1.5 mg/dl), thyroid disease, cancer. History of alcohol abuse or self-reported alcohol intake above 50 g/day were also exclusion criteria. Smoking status was also assessed and defined as current smoker, non-smoker or ex-smoker after quitting for more than one year. In all study population, TG, AG, and UG were comparable in the three subgroups and this variable was therefore not included in analyses (not shown).

For data and plasma sample collection, participants were admitted to the outpatient General Medicine wards in Montereale Valcellina or Maniago. A blood sample was collected under post-absorptive conditions after a 10-hour overnight fast for measurement of biochemical

parameters for diagnosis of metabolic syndrome. Blood was centrifuged (1000xg, 4°C, 10 min) and plasma aliquoted and frozen.

A detailed medical examination was also performed, and medical history was collected. Blood pressure was measured using a standard mercury sphygmomanometer, and DBP + 1/3 Diff-BP was defined as mean arterial pressure (MAP), with DBP and Diff-BP as diastolic blood pressure and differential blood pressure, respectively. Weight and height were measured and recorded to the nearest 0.1 kg and 0.5 cm, respectively. Body mass index (BMI) was calculated as weight in kilograms divided by height in meters squared. Waist circumference (WC) was measured at the natural indentation between the 10th rib and iliac crest to the nearest 0.5 cm. All variables were measured in duplicate, and the average of two measures was used for patient classification. General characteristics of the whole MoMa population sample have been previously reported [274].

For measurement of plasma ghrelin profile in the current study, individual samples were randomly selected from the lean, overweight and obese population subgroups in proportions of 1:2:2 respectively. Presence of diabetes mellitus, hypertension or dyslipidaemia were defined based on clinical history, medications or, respectively, by fasting plasma glucose > 126 mg/dl, systolic or diastolic blood pressure > 140 or 90 mmHg, plasma triglycerides > 150 mg/dl or plasma HDL cholesterol < 35 mg/dl in males and 40 mg/dl in females.

4.1.1.2 Follow-Up recall

The follow-up study was aimed at assessing changes in hormonal and metabolic profiles in a subgroup of individuals with or without metabolic syndrome. The follow-up group was selected by randomly inviting 200 individuals with and 200 without metabolic syndrome for a 5-year evaluation. 350 individuals (184 with and 166 without metabolic syndrome) responded positively and participated in this study. Anamnesis, measurements and samples were collected as in the 2008-2010 campaigns.

4.1.2 Studies in Animal Models

4.1.2.1 Exogenous UnAG administration in healthy rats

Experiments were approved by the Animal Studies Committee at Trieste University. Twenty 12-week-old male Wistar rats were purchased from Harlan-Italy (San Pietro-al-Natisone, Udine, Italy) and housed for two weeks in individual cages with a 12-h light–dark cycle at the University Animal Facility, with ad-libitum access to water and standard chow (Harlan Teklad2018, 14.2 kJ/g). Rats were then randomly assigned to 4-day, twice-daily 200µg-subcutaneous injections of UnAG (*n*=10, Bachem, Bubendorf, CH) or vehicle (Ct*, n*=10, NaCl 0,9% w/v). UnAG dose was based on previous studies in which equimolar AG modulated the same parameters at non-orexigenic doses [108]. Body weight and food intake were monitored daily; after the last injection food was removed for three hours followed by anaesthesia (Tiobutabarbital 100 mg/kg, Tiletamine/Zolazepam (1:1) 40 mg/kg IP). Gastrocnemius and extensor digitorum longus (EDL) muscles were then surgically isolated and blood collected in EDTA tubes by heart puncture. Liver explant followed. Tissue samples for ex-vivo analyses were placed in ice-chilled saline and immediately processed, while the remaining material was snap frozen in liquid nitrogen and kept at -80°C for further analysis. Blood was centrifuged (1000xg, 4°C, 10 min) and plasma aliquoted and frozen.

4.1.2.2 High fat diet-induced insulin resistance in transgenic mice with UnAG overexpression

Generation and characteristics of transgenic mice overexpressing UnAG (Tg Myh6/Ghrl) were previously described [128]. Selective ghrelin overproduction in the heart, characterized by negligible acylating activity, results in 40-fold increment in circulating UnAG without AG modification. 14 Tg Myh6/Ghrl and 14 matched wild-type male mice underwent 16-week standard or HFD feeding (10% or 60% calories from fat; Research Diets, New Brunswick, NJ), and were then processed as described above. Insulin tolerance tests (ITT) were performed at 15 weeks of treatment by intraperitoneal insulin injection (Humulin-R, Lilly,

Indianapolis, IN; 3 nmol/kg) after 4-h fasting. Blood glucose was measured from tail blood (AccuCheck Active, Roche, Basel, CH) immediately prior to injection and at 20, 40, 60, 80 min. Tissue and plasma samples were collected and treated as above.

4.1.2.3 Exogenous UnAG administration in uremic rats

Experimental protocol and surgery technique were approved by the Italian Health Ministry Animal Experimentation Authority (DM 274/2013-B 07/11/2013). Forty 12-week-old male Wistar rats (Harlan-Italy) were randomly assigned to 5/6 nephrectomy (n=30) or Sham operation (n=10). Surgery was performed using a single-step laparotomic approach, in order to reduce animal stress and complications. Procedures were performed in surgical sterility and anaesthesia (Premedication: dexemetomodin (0,025- 0,05 mg/kg IP, anaesthesia: Zoletil (20-25 mg/kg IP,). After xifo-pubic cutaneous incision and median laparotomy, left colon and part of the small bowel were mobilized and exteriorized in saline pre-wetted pads. Retro-peritoneum was opened and, after clamping the renal artery, inferior and superior poles were cut. Haemostasis was assured by application of haemostatic absorbable sponge (Spongostan, Johnson & Johnson, New Brunswick, NJ) and packing after temporal repositioning of the remnant kidney. After unclamping, the right kidney was also isolated with the same procedure and completely removed after ligature of vessels and ureter. After accurate haemostasis check, packing was removed and the posterior peritoneum continuity reconstructed. The abdominal wall was reconstructed by mass-layer single absorbable stitch technique. Skin was closed by single stitches (Figure 4). Sham operated animals underwent the same treatment until kidney surgical isolation. During recovery rats were clinically monitored and treated twice a day for 3-6 days with saline solution (0.4ml/kg/die) and analgesic medication (Tramadol 5mg/kg) s.c. as necessary. While no infective complication was recorded, 20% of rats removed by chewing two or more cutaneous stiches, requiring twice-daily medications.

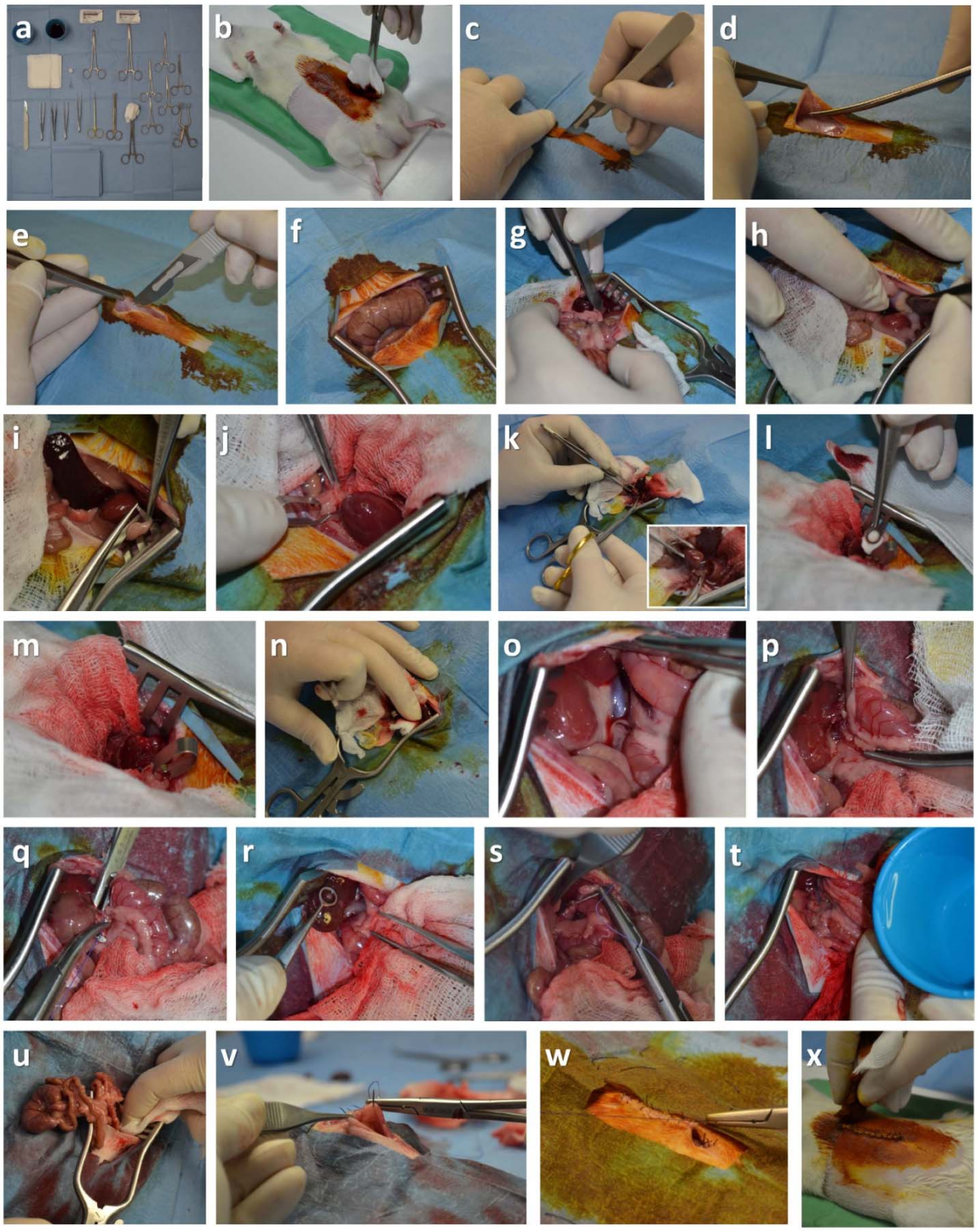

Figure 4. Single step 5/6 nephrectomy laparotomic surgical technique. (a,b): preparation of surgical instruments and of the sterile field, positioning of the rat on a heated pad followed by skin asepsis with iodopovidone; (c,d): cutaneous incision and subcutaneous layer dissection; (e,f): laparotomy by incision of the linea alba, divaricator positioning and viscera exposure; (g,h): mobilization of gross and small bowel and exteriorization in protective pre-wetted dressings, exposure of the left kidney; (i): isolation and mobilization by

blunt dissection of the kidney, identification of the renal artery, vein and of the ureter with preservation of the adrenal gland; (j): temporary positioning of a micro vascular clamp on the renal artery; (k): resection of upper and lower poles in mobilized kidney; (l-n): kidney repositioning followed by placement of absorbable haemostatic sponge on resection surfaces, haemostatic packing and declamping; (o,p): exposure of right kidney and blunt dissection to isolate renal artery and vein; (q,r): ligature of renal artery and vein followed by kidney explant with adrenal gland preservation; (s): packing removal, haemostasis check and reconstruction of posterior peritoneum on both sides; (t,u): peritoneal washing and further accurate haemostasis check; (v): single stitch, single layer closure of the abdominal wall; (w,x): asepsis of the subcutaneous layer with iodopovidone and closure of the cutaneous layer by single stitches followed by final medication.

After 10 days from surgery all animals were free of any complication or treatment. 36 days after surgery nephrectomized rats were randomly assigned to a 4-day, twice-daily s.c. saline (Nx, n=10), AG (Nx-AG, n=10) or UnAG (Nx-UnAG, n=10) injection scheme (200 µg/injection). Sham operated animals were also treated with saline. Throughout the whole study, rats were housed in individual cages as described for the other studies above. Anaesthesia, tissue and blood collecting and processing were also performed as described.

4.1.2.4 Lipid infusion study

The experimental protocol for rat lipid infusion studies was approved by the Committee for Animal Studies at Trieste University. 28 12-week-old male Wistar rats were purchased from Harlan-Italy and housed as above. Intravenous infusion studies were performed as previously described [199]. Starting 3 days before the experiments, 4 h tail-restraint periods were performed each day by pulling the tail through a tail-sized hole in the cage and securing it to a horizontal Plexiglass support. Animals had free access to water and standard rat chow. To minimize potential stress responses and eliminate any differential response among groups, identical restraining training and study protocols were applied to all animal groups. No significant changes in blood glucose, a relevant stress marker, were observed following the 4 h adaptation periods (data not shown). On the morning of the infusion day, catheters were placed percutaneously into one tail vein and one tail artery under local lidocaine

anaesthesia [199], and the tail was then secured as described above. Food was withdrawn after catheter placement and animals were kept in this position for 4 h before the infusions were started. Immediately before the start of infusions (T0), 250 µl blood samples were drawn from the artery and stored at -80 °C for basal measurements of insulin and FFA. Rats were randomly assigned to undergo one of the following 150 min infusion protocols: (1) control, NaCl infusion (n=8); (2) lipid emulsion (Intralipid 10%, Fresenius Kabi) at 600 µl/h and heparin (20 U/h; Epsoclar, Biologici Italia, Novate Milanese, Italia) aimed at elevating circulating FFA through a mixture with saturated, monounsaturated and n-6 PUFA long-chain fatty acids (n=8); (3) lipid emulsion (Omegaven 10%, Fresenius Kabi) at 600 µl/h and heparin aimed at elevating circulating FFA through n-3 PUFA-enriched long-chain fatty acids (n=8). Lipid emulsions with or without n-3 PUFA enrichment were infused to determine the potential physiological impact of n-3 PUFA per se on acylated ghrelin in vivo, since differential and partly controversial appetite-modulating effects have been reported for n-3 PUFA in different clinical settings [276-278]. Heparin infusion identical to that in the lipid infusion groups was performed in control group. At 150 min (T150), 250 µl blood samples were again taken and plasma was separated and stored at −80°C.

4.1.3 In vitro experiments

4.1.3.1 Cardiomyocyte experiments

Ventricular myocytes from 1- to 2-day-old Wistar rats were prepared using methods with a 90% purity yield [279]. Briefly, 2mm pieces obtained by ventricles mincing were dissociated in CBFHH (calcium and bicarbonate-free Hanks with HEPES) buffer added with trypsin (2 mg/ml) and of DNase II (20 mg/ml). Digestion process was repeated ten times for 10 min each with slow stirring. Supernatant was collected at the end of each cycle and added with calf serum (10%, v/v) for trypsin neutralization. Finally cells were collected by centrifugation (10 min, 300xg) and resuspended in DMEM added with 5% foetal bovine serum (FBS). After

fibroblasts removal by 2h pre-plating in 100-mm dishes, myoblasts were then plated at low density in DMEM high glucose containing 5% FBS, vitamin B12 (2 mg/ml) and penicillin–streptomycin (100 U ml)[280]. Cells were treated with AG or UnAG (0.1, 0.5, 1μmol/l) for 48 h, collected and processed.

4.1.3.2 Myotube experiments

C2C12 myoblasts (ATCC CRL-1772) were proliferated in myotubes by culture in high-glucose Dulbecco's modified Eagle's medium (DMEM) plus 10% FBS and penicillin–streptomycin (100 U/ml). Differentiation into myotubes was induced by switching to DMEM plus 1% horse serum when cells reached 80% confluence [281]. Myotubes were then incubated for four days with differentiation medium and, after 18h-starvation for synchronization, treated as described for neonatal cardiomyocytes.

In additional experiments we investigated the potential role of autophagy in UnAG effects by performing knockdown of the autophagy mediator ATG5 [282]. ATG5 genomic silencing was obtained by reverse transfection at final 25nmol/L concentration with mouse ATG5 siRNA (M-064838-02-0005; Dharmacon) or with a non-targeting control siRNA #4 (D-001210-04-20; Dharmacon) using Lipofectamine RNAiMAX (Life Technologies). Culture medium was then replaced 24 hours after transfection and, after 36 hours, cells were differentiated treated and processed as above. ATG5 protein level knockdown was verified by western blot.

In vitro model of uraemia was obtained using the classical validated approach of incubation with diluted serum from uremic or control patients[283,284]. Briefly, blood was collected in EDTA tubes from patients immediately prior to dialysis or from matched for age, gender and BMI healthy subjects. Patients and control subjects were recruited in Rovigo and Trieste and their characteristics have been previously published [285]. The study was approved by the local ethics committees, and all participants gave informed consent. Plasma used for in vitro

experiments was pooled and aliquoted to avoid repeated thaws. 48 h before harvesting 10% (vol/vol) plasma was then added to cell culture. Heparin was also added to a final concentration of 3U/ml to avoid potential clotting.

4.2 Materials

All drugs and chemicals for ex-vivo and in vitro experiments, when not differently specified, were purchased from Sigma-Aldrich (St. Louis, MO, USA) of the highest available purity. 0.9% saline was manufactured by Diaco (Trieste, Italy).

4.3 Analytical methods

4.3.1 Plasma measurements, metabolic profile and ghrelin forms

In human studies, plasma glucose, triglycerides, total and high-density lipoprotein (HDL) cholesterol and insulin concentrations were measured using standard methods at the Analysis Laboratory of Pordenone Hospital, Italy. Plasma FFA were determined by enzymatic colorimetric reaction using a commercial kit (NEFA-C; WAKO Pure Chemical Industries, Osaka, Japan). TG (intraassay coefficient of variation 4%; interassay coefficient of variation 7.6%) and AG (intraassay coefficient of variation 4.2%; interassay coefficient of variation 8.4%) were measured using RIA (Linco, St. Charles, MO) [56]. Plasma UnAG was calculated by subtracting AG from TG. Insulin sensitivity was assessed through the validated homeostasis model assessment (HOMA) index [56] using the following formula: HOMA = (FPG * FPI)/22.5, where FPG and FPI are fasting plasma glucose (mmol/L) and fasting plasma insulin (pmol/L), respectively.

In animal studies plasma insulin concentration was measured by ELISA (Ultrasensitive ELISA, DRG, Springfield, NJ). Plasma glucose levels were determined by standard enzymatic colorimetric assays [199,286]. Plasma NEFA levels were measured as for human

samples. Plasma creatinine and urea were determined by commercially available assays (MAk080, MAK006, Sigma-Aldrich).

4.3.2 Ex vivo redox state

4.3.2.1 Mitochondrial H_2O_2 production

H_2O_2 generation in isolated intact mitochondria was assessed using the Amplex Red-HRP method, modified as previously reported [199]. Briefly, fresh tissue samples tissue or pelleted cells were homogenized in buffer H (sucrose 263 mM, EGTA 1 mM, protease inhibitors 0,1%, HEPES 10,5 mM pH= 7,4; 10 ml/g of tissue) and mitochondria isolated by differential centrifugation: after nuclei and debris removal (720xg, 15 min, 4°C), mitochondria were pelleted (10000xg, 15 min, 4°C), resuspended and washed in buffer H. Final mitochondrial pellet was then suspended in Starkov's Respiration Buffer (KH_2PO_4 4 mM, $MgCl_2$ 1 mM, NaCl 14 mM, KCl 125 mM, EGTA 0,02 mM, HEPES 20 mM pH=7.4). The rate of H_2O_2 synthesis was then measured by monitoring the conversion of Amplex Red (Invitrogen, Carlsbad, CA, USA) to resorufin using a microplate fluorimeter (Infinite F200, Tecan Group, Switzerland, excitation wave length: 535 nm, emission: 595 nm, flashes:25, integration time:25 ms) during an incubation of mitochondria at 37°C in different respiratory states and in the presence of different respiratory inhibitors and substrates (Figure 5). In detail, sample were incubated with or without respiratory chain inhibitors (rotenone 10mmol/L, malonate 10mmol/L, antimycin A 1µg/ml) or the uncoupling agent CCCP 5µmol/L. After a first 20 min read to assess sample basal H_2O_2 production with the above compounds, state 4 mitochondrial respiration was induced by addition of respiration substrates. Final concentrations (mmol/l) were: 8 glutamate, 4 malate (GM); 10 succinate (S); 4 glutamate, 2 malate, 10 succinate (GMS); 0.05 palmitoyl-L-carnitine, 2 malate (PCM). After further 20 min state 3 respiration was obtained by addition of ADP 1mmol/l. Integrity of mitochondrial function was checked by verifying for each preparation the effects of CCCP and AA as well as

ADP on H_2O_2 production since changes in mitochondrial activity after addition of these reagents are only possible in the presence of preserved mitochondrial function. Concentrated aliquots of substrates and inhibitors were previously prepared and stored at -80°C. Working dilutions were prepared immediately before use. The rate of H2O2 synthesis was calculated by interpolation of resorufin fluorescence variation over time with a calibration curve from H_2O_2 standards (3 µmol/l–20 nmol/l). Data were normalised by mitochondrial fraction citrate synthase (CS) activity, quantified as referenced [199,287], and expressed as nmol (CS units)$^{-1}$ min^{-1}.

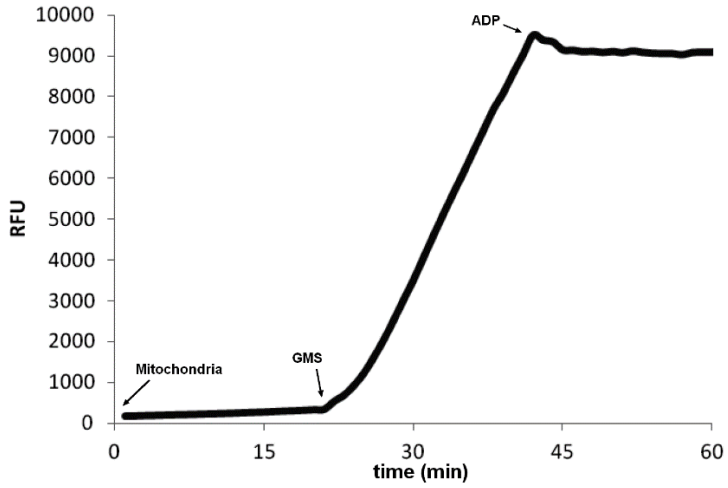

Figure 5. Representative graph showing the effect of the subsequent addition of the respiratory substrate GMS (4 mmol/l glutamate, 2 mmol/l malate, 10 mmol/l succinate) and ADP (1 mmol/l) on H_2O_2 production from mitochondria isolated in skeletal muscle samples using the Amplex Red-HRP method as described.

4.3.2.2 Superoxide anion generation

Cellular superoxide anion production systems in gastrocnemius lateralis muscle homogenate were assayed using the lucigenin chemiluminescent method as described [199]. Lucigenin concentration in the assay was 10 µmol/l to prevent redox cycling. Briefly, freshly isolated tissue was cleaned of connective tissue, homogenised in ice cold Krebs-HEPES buffer (20mM HEPES pH=7.4, 99mM NaCl, 4.7mM KCl, 1.2mM $MgSO_4$, 1mM KH_2PO_4,

1.9mM $CaCl_2$, 25mM $NaHCO_3$, 11mM D-Glucose) with protease inhibitors (Sigma, St. Louis MO, USA), cleansed from debris by centrifugation (240 g, 15 min, 4°C) and the obtained preparation tested in an array-type assay. The impact of subsequent addition of specific inhibitors on specific substrate-stimulated production rates was used to evaluate relative superoxide production from each source (Mitochondria: 5µmol/l CCCP on 10 mmol/l Succinate; NOS: 10mmol/l L-NAME on 10mmol/l L-Arginine; NADPH Oxidase: 200µmol/l Diphenyleneiodonium (DPI) on 1mmol/l NADPH; Xanthine oxidase: 200µmol/l Oxypurinol on 500µmol/l Xanthine) as referenced [199] (Figure 6). In pilot experiments the above concentrations did not alter luminescence in the absence of cellular homogenate.

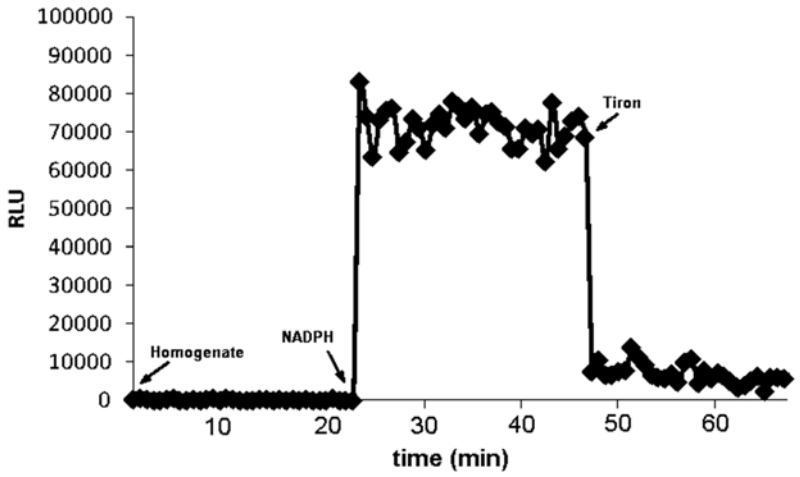

Figure 6. Representative graph showing the effect of the subsequent addition of NADPH (1mmol/l) and of the superoxide scavenger Tiron 10 (mmol/l) on superoxide generation from skeletal muscle homogenate using the lucigenin method as described.

A subsequent reading was then performed with the addition of the superoxide scavenger Tiron (10 mmol/l) to ensure all measurements related to superoxide production. Light emission for all conditions was monitored simultaneously in a microplate luminometer during incubation at 37°C (Sinergy2, BioTek Instruments, Winooski, VT, USA), and the integration of single light-emission measurements was normalised by protein content in the sample

(BCA assay, Pierce, Rockford IL, USA). The impact of a specific inhibitor on substrate-stimulated production values was used to evaluate the relative superoxide production from each source, as referenced.

4.3.3 Glutathione and antioxidant enzyme activities

Total and oxidised glutathione, the major cell ROS buffering system [200] also reflecting overall cell redox state, were determined as referenced [288] on ~50mg of gastrocnemius cleaned and homogenised in ice-cold 5% (wt/vol.) metaphosphoric acid (20ml/g tissue). After clearance (12000xg, 15 min, 4°C), samples were diluted in KPE (EDTA 5 mM, KH_2PO_4 16 mM,K_2HPO_4 81,5 mM, pH=7,5), transferred to a 96-well plate and incubated in reaction buffer (DTNB 0,85 mM, glutathione reductase 10 U/ml, KPE 0,1 M pH 7,4). The conversion of DTNB to TNB which is proportional to the availability of GSH in the sample, was followed on a spectrophotometer after the addition of NADPH 0.8 mM. Measurement of GSSG was performed with the same procedure but after 1h incubation of the diluted sample with 2-vynilpiridin 10% (v/v) and subsequent neutralization by addition of triethanolamine 16.6% (v/v). Reduced glutathione (GSH) was calculated as total minus oxidised fraction (GSSG). Commercial kits were used to measure catalase (Amplex Red Catalase Assay, Invitrogen, Carlsbad, CA) and glutathione peroxidase activities (Abcam, Cambridge, UK) according to manufacturers' instructions.

4.3.4 Protein analyses

4.3.4.1 Multiplex analyses of protein expression (xMAP)

xMAP systems is an immuno-mediated recognition technology which performs discrete assays on the surface of colour coded microspheres [289]. Beads of the same colour are identifiable by a specific fluorescent emission when excited at 635 nm and are univocally coated with antibodies for a single specific analyte. The reporter antibody is instead characterized by fluorescence emission when excited at 535 nm. Dedicated analysers can therefore read

multiplex assay results by reporting the reactions occurring on each individual microsphere, allowing parallel detection of multiple proteins in small samples. Cytokine profile and insulin signalling protein phosphorylation at $IR^{Y1162/Y1163}$, $IRS\text{-}1^{S312}$, AKT^{S473}, $GSK\text{-}3\beta^{S9}$, $PRAS40^{T246}$ and $P70S6K^{T421/S424}$ levels were measured by xMAP technology (Magpix, Luminex Corporation, Austin, TX) using commercial kits, validated by manufacturer for multiplexing profiling (LRC0002M; LHO0001M; LHO0002, Life Technologies, Carlsbad, CA). Frozen aliquots of gastrocnemius muscles were homogenized in a buffer (Tris 10 mM, pH 7.4, NaCl 100 mM, EDTA 1 mM, EGTA 1 mM, NaF 1 mM, $Na_4P_2O_7$ 20 mM, Na_3VO_4 2 mM, Triton X-100 1%, glycerol 10%, SDS 0.1%, deoxycholic acid 0.5%, PMSF 1mM) added with protease inhibitors (P8340, Sigma-Aldrich, St. Louis, MO, USA). Following 20 min centrifugation (13000xg, 4°C), immuno-mediated analyte ibridation to magnetic beads, recognition and reporter quantification was performed as recommended by the manufacturer. Milliplex Analyst software (Millipore, Billerica, MA) was used for interpolating data to standard curve. Cytokine results were expressed as pg/mg of protein as assessed by BCA (BCA assay, Pierce, Rockford IL, USA). Activation of insulin signalling mediators is expressed as phospho protein units/pg protein.

4.3.4.2 Western Blot

Protein expression levels were measured by Western Blot as described [199,286,289]. Frozen tissue samples were homogenized in lysis buffer (50 mmol/l Tris HCl, 0.1 mmol/l EDTA, 0.1 mmol/l EGTA, 0.1% SDS, 0.1% deoxycholate, 1% Igepal) added with protease inhibitors (Sigma) and cleared by centrifugation (14000xg, 10min, 4°C). Protein concentration was determined by the BCA method and equal total protein quantities were tested for each sample. After separation by SDS/PAGE, the resolved proteins were transferred to 0.2 µm nitrocellulose membrane using a semi-dry electrophoretic transfer system (Bio-Rad). Blots were blocked (5% Fat-free milk, 0.05% Tween-20 in PBS pH=7.4) and incubated overnight

with primary antibody. Dilutions used were: anti-MnSuperoxide Dismutase (SOD) and anti-CuZnSOD (Stressgen, Ann Arbor, MI) 1:5000 and 1:1000 respectively; anti-IκB (Cell Signaling, Beverly, MA) 1:500; anti-pIRS-1^{Y612} (Abcam, Cambridge, UK) 1:500; anti-ATG5 (Cell Signaling) 1:2000; anti LC3B (Sigma) 1:1500; anti-b-Actin (Sigma) 1:25000 and anti-GAPDH (Santa Cruz, Dallas, TX) 1:1000. After extensive washing, membranes were incubated (1 h, 20°C) in blocking buffer with the appropriate horseradish peroxidase-conjugated secondary antibody. After further washing, detection was performed by exposure of X-ray films to membranes in the presence of enhanced chemoluminescence reagent (Pierce). Films were analysed using image analysis software (Molecular Analyst, Bio-Rad; ImageJ, NIH) after densitometric scan (GS-700, Bio-Rad). Equal loading was checked by Ponceau-S staining after transfer and GAPDH reprobing.

4.3.4.3 Nuclear factor:DNA binding activity by electrophoretic mobility shift assay (EMSA)

NF-κB binding activity was assessed by non-radioactive EMSA[199] with modifications. Nuclear fraction from muscle samples was obtained by homogenization in a buffered sucrose-salt solution (0.2mM K_2HPO_4, 0.6mM KH_2PO_4, 0.32M Sucrose, 1mM $MgCl_2$, pH=6.8) added with protease inhibitors (Sigma, St. Louis MO, USA), followed by nuclei collection by centrifugation (800xg, 5 min, 4°C). After resuspension in high sucrose buffer (0.2mM K_2HPO_4, 0.6mM KH_2PO_4, 0.32M Sucrose, 1mM $MgCl_2$, pH=6.8), myofibrils and mitochondria were removed by prolonged high speed centrifugation (16000xg, 90 min, 4°C) and nuclei resuspended in PBS pH=7.4. Equal amounts of nuclear protein were loaded for each sample. After incubation with polydeoxyinosinic-deoxycytidylic acid (0.05μg/μl) for non-specific competition and with double-stranded 3′-biotinylated DNA probe representing a known consensus sequence for NF-κB (forward: 5′-AGTTGAGGGGACTTTCCCAGGC-3′-biotin, Eurofins MWG Genomics, Ebersberg, Germany), electrophoretic separation of nuclear extracts was performed in 0.8% agarose gel. Band specificity evaluation and

identification was performed by running a pooled sample pre-incubated for 20 min with excess unlabelled probe (1000x), anti-p65 (Millipore; 2µg) or anti-p105/p50 (Abcam; 2µg) antibody. After transfer and oligomer crosslinking to nylon membrane by UV exposure (UVC500, Hoefer, Holliston MA, USA), membrane was saturated (10mM PBS pH=7.4, 150mM NaCl, 0.5%(w/v) Casein, 0.2%(w/v) SDS) for 1h at 37°C under gentle shaking and washed (10mM PBS pH=7.4, 0.1%(w/v) Tween-20). Biotin recognition was performed using streptavidin–HRP conjugate (Sigma) in detection buffer (10mM PBS pH=7.4, 0.1%(w/v) Casein, 0.1%(w/v) Tween-20) for 30 min. After enhanced chemoluminescence, densitometric analysis was performed on the exposed film. Results were calculated from optical density of NF-κB specific bands.

4.3.5 Tissue Glucose uptake

Measurement of tissue glucose uptake was performed using the ex-vivo non-radioactive 2-deoxyglucose (2-DG) method developed by Yamamoto [290] with modifications. Extensor digitorum longus (EDL) muscle, characterized by a metabolism largely similar to that of gastrocnemius [291], was preferred because of its low thickness and therefore better exchange with the incubation buffer [292]. Two muscle sections were incubated for 30' at 37°C under constant oxygenation with or without insulin (Humulin-R 600pmol/l) [293] in isotonic buffer (NaCl 99 mM, KCl 4,7 mM, $MgSO_4$ 1,2 mM, KH2PO4 1 mM, CaCl2 1,9 mM, $NaHCO_3$ 25 mM, Glucose 11 mM, HEPES 20 mM pH=7,4), added with BSA (1mg/ml) and pyruvate (2mM). After further 20-min incubation when pyruvate was substituted with 2-DG (1mM), samples were snap frozen and kept at -80°C. After mechanical homogenization (Ultra-Turrax T25Basic, Ika, Milano, Italia) in ultrapure water followed by NaOH addition (0.07N), enzymes and endogenous NAD(P)H and NAD(P) were inactivated by 45-min incubation at 85°C. After the addition of equinormal quantities of HCl, samples were cleared from debris by centrifugation (10000xg, 5min) and transferred to 96-well microplates for incubation

(37°C, 60 min) in assay buffer (Triethanolamine hydrochloride 50mM, KCl 50mM, BSA 0.02%(w/v), Diaphorase (0.2U/ml), Resazurin Na salt 10µM) added with (Buffer C) β-NADP (0.1mM) and Glucose-6-phosphate dehydrogenase from L. Mesenteroides (G6PDH, 20U/ml) or (Buffer D) with β-NAD 0.1mM and G6PDH (0.3U/ml). Concentrations of G6P and G6P+2-DG6P were quantified by fluorimetrically measuring (Infinite F200, Tecan, Männedorf, CH) conversion of Resazurin to Resorufin in Buffers C and D, respectively. Values related to 2-DG6P were calculated by subtraction, interpolated on a standard curve of 2-DG6P (1.0-0 mM), and normalized by protein concentration in sample homogenate. Tissue 2-DG6P uptake was expressed in µmol of 2-DG/mg protein/30min.

4.3.6 ATP synthesis and complex-related ATP production

ATP synthesis rate was measured in tissues and cells ex-vivo in freshly isolated mitochondria using a luciferin-luciferase luminometric assay [199]. Mitochondria were isolated by differential centrifugation as described for mitochondrial ROS assay, except that buffers A (50 mM Tris pH 7.2, 100mM KCl, 5mM MgCl2, 1.8mM ATP, lmM EDTA) and B (225mM Sucrose, 44mM KH2PO4, 12,5 mM Mg(CH3COO)2, 6 mM EDTA) were used instead of H and Starkov's solutions. Comparison of citrate synthase measurements in samples before and after membrane disruption was performed to assess integrity of mitochondria isolated by gentle homogenization [294]. Concentrated respiration substrates were previously prepared, aliquoted and frozen at -80°C. ATP synthesis rate was then measured using assay buffer containing luciferin and luciferase (ATP Reagent SL, BioThema) by kinetic assessment of light emission (interval 2 min, integration time 1 sec) using a microplate luminometer (Synergy 2 SL, BioTek) (Figure 7). After signal stabilization and excess substrates addition a first 10-min kinetic read was performed, followed by 100µmol/l ADP addition and 20-min read. Final respiration substrates composition and reaction concentrations (mmol/l) were: 0.25 pyruvate, 0.0125 palmitoyl-L-carnitine, 2.5 α-ketoglutarate, 0.25 malate (PPKM); 0.025 palmitoyl-L-carnitine, 0.5 malate

(PCM); 20 succinate, 0.1 rotenone (SR); 10 glutamate, 5 malate (GM). Luciferase-related ATP decrease rate was calculated from ATP standards to correct measurement slopes. ATP synthesis rate was then calculated by interpolation with the ATP standard curve of sample light emission per minute in the linear phase. The impact of complex-related energy flux on ATP synthesis was measured as the production rate variation induced by the addition, in a subsequent 20-min read in state-3 respiration on excess complex-specific substrate, of a complex-specific inhibitor. For complex I-related ATP synthesis, substrate and inhibitor were GM and rotenone (2µmol/l), while for complex II SR and malonate (1mmol/l). In parallel readings, mitochondrial functionality in each preparation was also tested and confirmed by a >80% and >95% decrease in state 3 ATP synthesis after addition of CCCP 30µM and oligomycin 2µg/µl respectively. Obtained relative production rate measurements were normalized by ATP synthesis rate with the non-specific substrate PPKM, and data presented as the ratio between values obtained for complex I-related over complex II-related production.

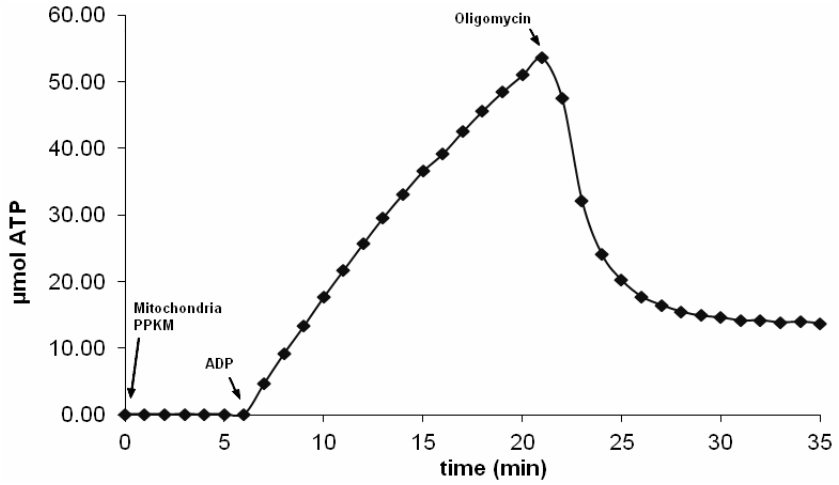

Figure 7. Representative graph showing the effect of the subsequent addition of the respiratory substrate PPKM (0.25 pyruvate, 0.0125 palmitoyl-L-carnitine, 2.5 α-ketoglutarate, 0.25 malate), ADP (100µmol/l) and of the ATP-ase inhibitor Oligomycin (2µg/µl) on ATP synthesis rate in mitochondria isolated in skeletal muscle samples using the luciferin-luciferase method as described.

4.4 Statistical Analysis

4.4.1 Human studies

Data distribution for continuous variables was assessed by Shapiro-Wilk test. For continuous variables, test of statistical similarity between the whole study population and subjects randomly selected for follow-up screening was performed using Student's t test or Mann-Whitney u test as appropriate, while for percentage expressed data by χ-square test. Since several parameters including HOMA, FFA, TG, AG and AG/TG did not present a normal data distribution, associations between variables were evaluated by Spearman correlation and log-transformed values were used for further analyses.

Parameters showing univariate association ($p<0.05$) were included in stepwise multiple linear regression models, in order to assess their impact in the relationship between HOMA, BMI or FFA and ghrelin forms in the presence of potential confounders. Multiple regression analyses were validated by assessing the normality of residuals. Regression coefficients for ghrelin forms, which are low in absolute values due to the different order of magnitude among variables tested, are presented multiplied by a 1000x factor. In quartile analyses differences were tested by ANOVA followed by post-hoc pairwise tests with Bonferroni correction and by trend linear regression analysis. P values <0.05 were considered statistically significant. Analyses were performed with SPSS v.17 software (SPSS Inc., Chicago, IL).

4.4.2 Animal and in vitro studies

Groups were compared using Student t-test or, in case of multiple comparisons, one-way ANOVA followed by appropriate post-hoc tests. Bonferroni correction for multiple comparisons was applied. Paired t-test was used to compare variables before and following lipid infusions in rodent studies. P values <0.05 were considered statistically significant. All analyses were performed using the SPSS v.17 software (SPSS Inc., Chicago, IL).

5 Results

5.1 Total and UnAG but not AG plasma levels are associated with lower insulin resistance development in humans: a 5-year follow-up study

5.1.1 Analysis of basal data

5.1.1.1 Anthropometric and metabolic measurements and plasma ghrelin forms

Anthropometric and metabolic parameters in the whole study population, as well as those of the subgroup undergoing 5-year follow-up evaluation are reported in Table 2. No statistically significant differences between the two groups were observed for any variable.

Table 2 – Study population. Sex, age, body mass index (BMI), waist circumference (WC), plasma glucose and insulin, homeostasis model assessment of insulin resistance (HOMA), plasma total and HDL cholesterol (Chol), plasma triglycerides and mean arterial pressure (MAP), systolic (SBP) and diastolic (DBP) blood pressure; prevalence of diabetes mellitus, hypertension, hyperlipidaemia with percent pharmacological treatment (Tx) at baseline in the whole study cohort and in individuals that subsequently underwent 5-year Follow-Up evaluation. Data are presented as Mean±SD (Range). No statistically significant differences were observed at baseline between the whole cohort undergoing cross-sectional evaluation (All) and the selected subgroup undergoing 5-year follow-up recall.

	All	Subgroup with subsequent follow-up
Gender (M/F)	349/367	168/182
Age (years)	55±9 (22-73)	54±8 (29-72)
BMI (kg/m^2)	28.9±5.41 (17.8-51.1)	28.7±5.1 (17.8-51.1)
WC (cm)	98±13 (65-148)	97±13 (65-140)
Glucose (mmol/l)	5.6±1.4 (3.7-15.3)	5.5±0.9 (3.7-9.8)
Insulin (pmol/l)	77±56 (21-554)	76±55 (21-502)
HOMA	3.2±3.5 (0.4-26.2)	3.0±2.9 (0.6-26.2)
Total-Chol (mmol/l)	5.28±1.09 (2.25-9.41)	5.28±1.03 (2.25-8.77)
HDL-Chol (mmol/l)	1.34±0.36 (0.54-2.97)	1.37±0.39 (0.54-2.97)
Triglycerides (mmol/l)	1.74±0.94 (0.43-7.02)	1.64±1.15 (0.48-6.96)
MAP (mmHg)	102±12 (71-152)	101±11 (72-152)
SBP (mmHg)	140±18 (95-215)	138±18 (95-200)
DBP (mmHg)	83±10 (53-121)	83±10 (55-115)
TG (pg/ml)	776±327 (87-2377)	782±355 (196-2377)
AG (pg/ml)	74±67 (6-436)	77±67 (6-391)
UnAG (pg/ml)	694±313 (11-2318)	703±341 (127-2318)

5.1.1.2 HOMA insulin resistance index is negatively associated with total and unacylated ghrelin independently of gender, BMI, metabolic syndrome and pharmacological treatments

In all subjects, HOMA index was associated positively with BMI, waist circumference, plasma triglycerides and systolic and diastolic blood pressure, while negative associations were observed between BMI and plasma HDL cholesterol (Table 3). HOMA was also associated negatively with plasma TG and UnAG (Table 3), and these associations remained statistically significant after adjusting for sex, BMI, metabolic syndrome parameters and pharmacological treatments in multiple regression analysis (Table 4). In contrast, no statistically significant associations were observed between HOMA and AG (Table 3).

5.1.1.3 BMI is negatively associated with total and unacylated ghrelin independently of gender, metabolic syndrome and pharmacological treatments

Relationships between ghrelin forms and anthropometric parameters were also analysed, in order to further determine potential changes in circulating ghrelin forms with increasing BMI (or waist circumference) and their potential role in BMI-related insulin resistance. In all subjects, BMI was expectedly associated positively with HOMA index and metabolic syndrome parameters (Table 5). Negative correlations were observed between BMI and sex-adjusted plasma TG and UnAG (r= -0.324, -0.320; Table 5), and these associations were also independent of metabolic syndrome parameters and pharmacological treatments for type 2 diabetes, hypertension or hyperlipidaemia in multiple regression analyses (Table 6). Similar associations were also observed for waist circumference (not shown). A weaker (r= - 0.144; Table 4) but statistically significant negative association between BMI and AG was no longer statistically significant after adjusting for sex and in any additional adjustment model in multiple regression analysis (Table 6).

Table 3: Linear regression analysis between baseline HOMA index (HOMA), 5-year follow-up HOMA index (5y HOMA) or changes in HOMA index between baseline and 5-year evaluation (Δ HOMA) and gender (M=male), age (years), body mass index (BMI, kg/m2), waist circumference (WC, cm), plasma glucose (mg/dl), insulin (μU/ml), total and HDL-cholesterol (Chol), mg/dl), triglycerides (mg/dl), systolic (SBP) and diastolic blood pressure (DBP, both mmHg), total ghrelin (TG), acylated ghrelin (AG), calculated unacylated ghrelin (UnAG), presence of diabetes and its treatment (Tx), presence of hypertension and its treatment (Tx), presence of dyslipidaemia and its treatment (Tx).

	HOMA		**5y HOMA**			**Δ HOMA**	
	R	p	R	p		R	p
Gender (M)	0.175	<0.001	0.136	0.013	-	-	-
Age	0.048	0.198	-0.063	0.250	-	-	-
BMI	0.604	<0.001	0.624	<0.001	Δ	0.319	<0.001
WC	0.567	<0.001	0.557	<0.001	Δ	0.179	0.001
Glucose	0.530	<0.001	0.348	<0.001	Δ	0.481	<0.001
Insulin	0.965	<0.001	0.711	<0.001	Δ	0.948	<0.001
Total-Chol	-0.033	0.372	-0.028	0.605	Δ	0.121	0.028
HDL-Chol	-0.328	<0.001	-0.290	<0.001	Δ	-0.032	0.560
Triglycerides	0.401	<0.001	0.392	<0.001	Δ	0.192	<0.001
SBP	0.236	<0.001	0.211	<0.001	Δ	0.029	0.605
DBP	0.308	<0.001	0.270	<0.001	Δ	0.032	0.567
TG	-0.371	<0.001	-0.351	<0.001	Δ	-0.188	0.008
AG	-0.103	0.06	-0.069	0.213	Δ	0.037	0.613
UnAG	-0.377	<0.001	-0.345	<0.001	Δ	-0.206	0.004
Diabetes (Tx)	0.232 (0.117)	<0.001 (0.002)	0.212 (0.143)	<0.001 (0.009)	Δ	0.227 (0.258)	<0.001 (<0.001)
Hypertension (Tx)	0.303 (0.299)	<0.001 (<0.001)	0.207 (0.247)	<0.001 (0.000)	Δ	0.043 (0.102)	0.431 (0.062)
Dyslipidemia (Tx)	0.178 (0.076)	<0.001 (0.041)	0.220 (0.168)	<0.001 (0.002)	Δ	-0.100 (0.098)	0.069 (0.075)

Table 4 –Multiple regression analyses. Multiple regression analyses between total (TG), acylated (AG), unacylated ghrelin (UnAG) and their 5-year changes compared to baseline and HOMA or its 5-year changes compared to baseline (dependent variable) in the whole study population (n = 716) in different statistical adjustment models. B: Unstandardized coefficient (1000x), CI: Confidence interval.

		TG				AG				UnAG			
	Model	B (95%CI) 1000x	F	R^2	**p**	B (95%CI) 1000x	F	R^2	**p**	B (95%CI) 1000x	F	R^2	**p**
HOMA-IR	1	-2.01 (-2.51--1.52)	44.1	0.11	<0.001	-1.08 (-3.57-1.41)	12.1	0.03	0.504	-2.13 (-2.65--1.61)	45.0	0.11	<0.001
	2a	-1.19 (-1.65--0.72)	92.7	0.28	<0.001	-0.24 (-2.43-1.95)	80.5	0.25	0.952	-1.28 (-1.76--0.79)	92.4	0.28	<0.001
	3a	-1.07 (-1.52--0.61)	58.4	0.32	<0.001	-0.92 (-3.05-1.20)	52.9	0.30	0.512	-1.11 (-1.59--0.64)	57.7	0.33	<0.001
	4a	-1.02 (-1.47--0.57)	41.2	0.34	<0.001	-0.71 (-2.82-1.39)	37.7	0.32	0.611	-1.07 (-1.55--0.60)	40.9	0.34	<0.001
5yHOMA	1	-1.34 (-1.90--0.79)	12.9	0.07	<0.001	0.49 (-2.53-3.51)	1.6	0.00	0.794	-1.46 (-2.04--0.88)	14.0	0.07	<0.001
	2a	-0.56 (-1.06--0.06)	50.5	0.31	0.029	1.22 (-1.32-3.76)	47.5	0.30	0.181	-0.65 (-1.17--0.13)	49.9	0.31	0.014
	3a	-0.53 (-1.01--0.05)	32.0	0.36	0.031	0.50 (-1.98-2.99)	30.0	0.35	0.305	-0.60 (-1.10--0.09)	31.4	0.36	0.021
	4a	-0.49 (-0.98--0.01)	21.9	0.36	0.046	0.81 (-1.68-3.30)	20.8	0.35	0.183	-0.56 (-1.07--0.06)	21.5	0.36	0.029
		Δ TG				**Δ AG**				**Δ UnAG**			
	Model	B (95%CI) 1000x	F	R^2	p	B (95%CI) 1000x	F	R^2	p	B (95%CI) 1000x	F	R^2	p
Δ HOMA	2b	-0.55 (-1.01--0.09)	13.2	0.11	0.019	-0.03 (-1.76-1.70)	9.9	0.09	0.973	-0.58 (-1.06--0.11)	13.1	0.11	0.017
	3b	-0.57 (-1.04--0.11)	6.8	0.11	0.016	-0.07 (-1.81-1.68)	5.0	0.08	0.939	-0.60 (-1.08--0.12)	6.7	0.11	0.015
	4b	-0.55 (-1.01--0.08)	4.3	0.11	0.022	-0.10 (-1.84-1.65)	3.4	0.08	0.914	-0.57 (-1.06--0.09)	4.3	0.11	0.021

Data adjustments:
Model 1: gender
Model 2a: Model 1 + BMI
Model 2b: Δ BMI
Model 3a: Model 2a + Triglycerides, HDL cholesterol, Systolic Blood Pressure
Model 3b: Model 2b + Δ Triglycerides, Δ total-cholesterol
Model 4a: Model 3a + Anti-diabetic, -hypertensive, -dyslipidemic Treatment
Model 4b: Model 3b + Anti-diabetic, -hypertensive, -dyslipidemic Treatment

Table 5 - Linear regression analysis between BMI and gender (M=male), age (years), waist circumference (WC, cm), plasma glucose (mg/dl), plasma insulin (μU/ml), plasma total and HDL-cholesterol (Chol), mg/dl), plasma triglycerides (mg/dl), systolic (SBP) and diastolic blood pressure (DBP, both mmHg), plasma total (TG), acylated (AG) and calculated unacylated ghrelin (UnAG) (all plasma ghrelin concentrations: pg/ml). Superimposable results were observed for associations between ghrelin forms and waist circumference (not shown).

	BMI	
	R	p
Gender (M)	0.112	0.003
Age	0.019	0.616
WC	0.850	<0.001
Glucose	0.229	<0.001
Insulin	0.626	<0.001
HOMA-IR	0.604	<0.001
Total-Chol	-0.087	0.019
HDL-Chol	-0.273	<0.001
Triglycerides	0.260	<0.001
SBP	0.260	<0.001
DBP	0.288	<0.001
TG	-0.324	<0.001
AG	-0.151	<0.001
UnAG	-0.308	<0.001

Table 6 –Multiple regression analyses. Multiple regression analyses between total (TG), acylated (AG), unacylated ghrelin (UnAG) and HOMA (dependent variable) in the whole study population (n = 716) in different statistical adjustment models. Superimposable results were observed when waist circumference was used as dependent variable (not shown).

		TG				AG				UnAG			
	Model	β (95%C.I.)	F	R^2	p	β (95%C.I.)	F	R^2	p	β (95%C.I.)	F	R^2	p
BMI	1	-0.004 (-0.006--0.003)	30.2	0.08	<0.001	-0.005 (-0.010-0.000)	4.2	0.01	0.069	-0.004 (-0.006--0.003)	28.1	0.07	<0.001
	2	-0.002 (-0.003--0.001)	81.6	0.25	<0.001	-0.003 (-0.008-0.001)	74.9	0.24	0.116	-0.002 (-0.003--0.001)	80.6	0.25	<0.001
	3	-0.002 (-0.003--0.001)	52.5	0.30	0.001	-0.004 (-0.008-0.001)	50.4	0.30	0.086	-0.002 (-0.003--0.001)	51.9	0.30	0.002
	4	-0.002 (-0.003--0.001)	37.7	0.32	0.001	-0.003 (-0.007-0.001)	36.3	0.32	0.124	-0.002 (-0.003--0.001)	37.3	0.31	0.003

Data adjustments:
Model 1: gender
Model 2: Model 1 + HOMA-IR
Model 3: Model 2 + Triglycerides, HDL cholesterol, Mean Arterial Pressure
Model 4: Model 3 + Anti-diabetic, -hypertensive, -dyslipidemic Treatment

5.1.2 Analysis of 5 years follow-up data

5.1.2.1 Plasma TG and UnAG levels predict 5-year insulin resistance independently of gender, BMI, metabolic syndrome and pharmacological treatments

We also determined potential associations between baseline parameters and 5-year HOMA index. In correlation analyses, basal BMI, waist circumference, plasma triglycerides and systolic and diastolic blood pressure were associated positively with 5-year HOMA (Table 3). 5-year HOMA was also negatively correlated with basal TG and UnAG, while not with basal AG. Plasma TG and UnAG and 5-year HOMA remained negatively associated after adjusting for sex, BMI, plasma triglycerides, blood pressure and pharmacological treatments in multiple regression analyses (Table 4).

5.1.2.2 5-year changes in plasma TG and UnAG levels changes are negatively associated with insulin resistance changes independently of gender and BMI

We next determined potential associations between plasma ghrelin changes and HOMA index changes over the 5-year follow-up period. 5-year changes in plasma TG and UnAG were negatively correlated with changes in HOMA index (Table 3). These associations remained statistically significant after adjusting for sex and 5-year changes in BMI (Table 4). In contrast, no associations were observed between changes in HOMA and changes in AG.

5.2 Effects of UnAG exogenous administration on tissue functional pathways involved in insulin sensitivity modulation in healthy rodents

5.2.1 UnAG reduces skeletal muscle ROS generation and inflammation, enhancing insulin signalling and action

5.2.1.1 Animal characteristics.

Exogenous 4-day UnAG administration did not modify body weight, body weight gain or caloric intake. Plasma glucose, insulin and NEFA concentrations were also comparable among UnAG-treated and Control group (Table 7).

Table 7. Animal characteristics. Animal characteristics after unacylated ghrelin (UnAG) or saline (Ct) 4-day treatment. BW: body weight. Mean±SEM; no significant difference among groups.

	Ct (n=10)	**UnAG** (n=10)
Body Weight (g)	**319.6**±3.6	**324.1**±6.1
Δ BW during 4-day ghrelin treatment (g)	**13.0**±1.4	**11.6**±1.1
Average Caloric intake (kcal/d)	**76.9**±2.3	**73.5**±1.8
Plasma Glucose (mg/dL)	**118.6**±6.0	**120.5**±7.5
Plasma Insulin (µU/ml)	**12.8**±2.1	**14.3**±2.9
Plasma NEFA (mmol/L)	**0.27**±0.06	**0.21**±0.03

5.2.1.2 UnAG lowers skeletal muscle ROS generation

UnAG lowered H_2O_2 and superoxide anion generation rate in gastrocnemius muscle, including a marked decrease in mitochondrial respiration-dependent ROS production (Figure 8A-C). UnAG also reduced superoxide production from nitric oxide synthase (NOS) but not xanthine- or NADPH- oxidase (Figure 8D-F). UnAG-treated rats also had lower muscle oxidized-over-total glutathione, a marker of tissue redox state (Figure 9A-B). Conversely, UnAG did not modify tissue protein levels of SOD isoforms and activities of antioxidant enzymes catalase and glutathione peroxidase (Figure 9C-F).

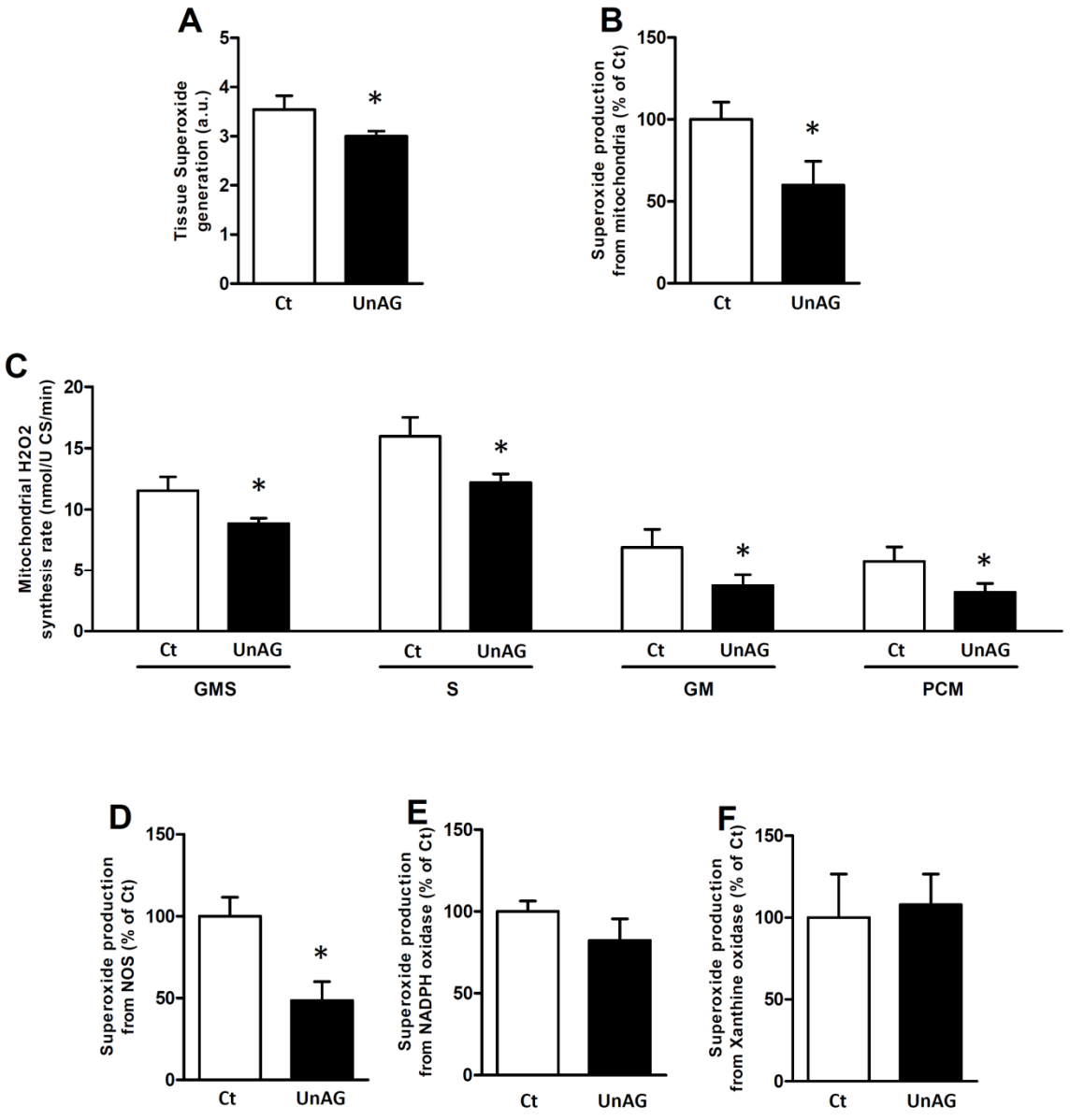

*Figure 8. UnAG and skeletal muscle Reactive Oxygen Species production. Effects of unacylated ghrelin (UnAG, 200μg subcutaneous injection twice per day) vs. saline (Ct) sustained 4-day treatment on overall (A) and specific superoxide production from mitochondrial sources in whole tissue homogenate (B), on H_2O_2 synthesis rate from skeletal muscle-isolated intact mitochondria with different respiratory substrates (C, GMS: Glutamate+Succinate+Malate; S: Succinate; GM: Glutamate+Malate; PCM: Palmitoyl-L-Carnintine+Malate) and on nitric oxide synthase- (D), NADPH oxidase- (E) and xanthine oxidase- (F) derived superoxide generation in skeletal muscle. U CS: units of citrate synthase; a.u.: arbitrary units. *p<0.05 vs. Ct; mean±SEM, n=8-10/group.*

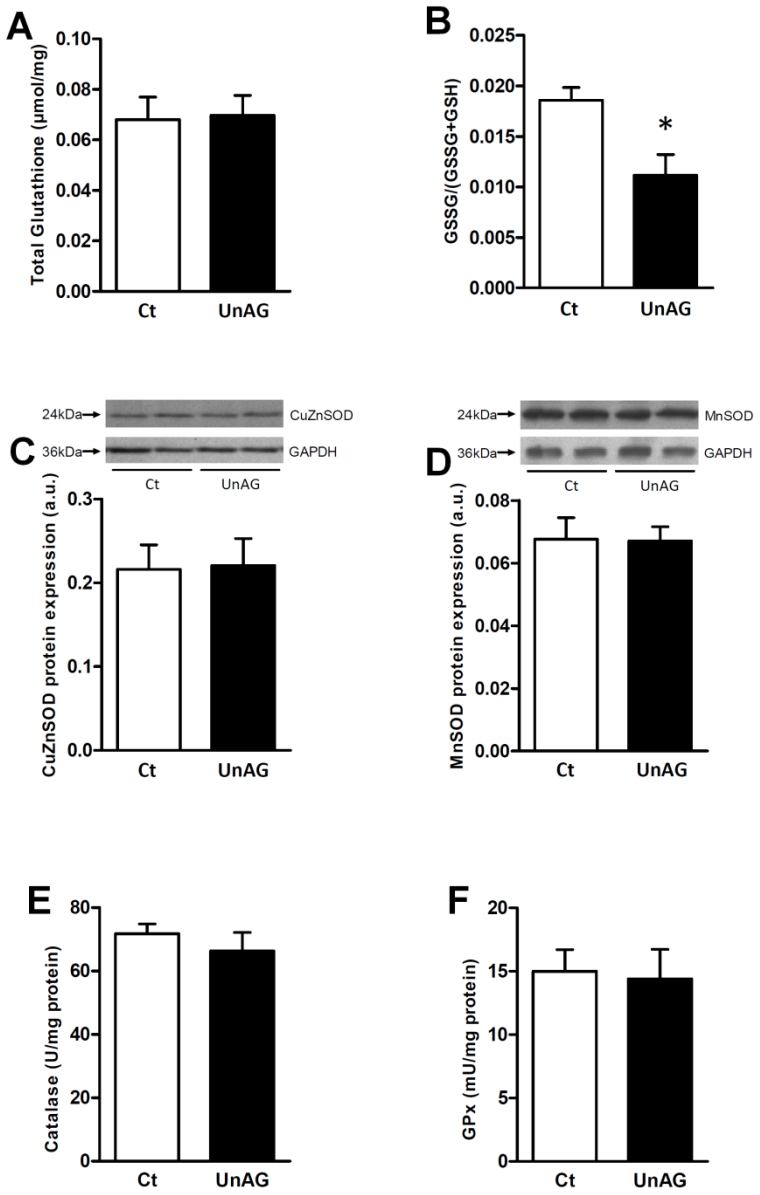

*Figure 9. UnAG and skeletal muscle redox state and antioxidant systems. Effects of unacylated ghrelin (UnAG, 200µg subcutaneous injection twice per day) vs. saline (Ct) sustained 4-day treatment on total (A) and oxidized (GSSG) over total (B, GSH: reduced) tissue glutathione, effects on Cu/ZnSOD (C) and MnSOD (D) protein expression with representative blots, and on catalase (E) and glutathione peroxidase (GPx; F) enzyme activities. a.u.: arbitrary units. *p<0.05 vs. Ct; mean±SEM, n=8-10/group.*

5.2.1.3 UnAG lowers inflammation in skeletal muscle

Rats treated with UnAG had a higher skeletal muscle protein expression of the NF-κB inhibitor IκB compared to saline-treated rats, with parallel reduction of pro-inflammatory NF-κB p65/p50 nuclear binding activity (Figure 10A-B). p50/p50 homodimer binding activity, a transcription activator for anti-inflammatory IL-10 [295], was also increased by UnAG (Figure 10B). Consistently, muscle cytokine pattern presented anti-inflammatory changes after UnAG treatment, with higher IL-10 expression and lower pro-inflammatory IL-1a and TNFα (Figure 10C-G).

5.2.1.4 UnAG enhances skeletal muscle insulin signalling and glucose uptake

UnAG also activated insulin signalling by enhancing the phosphorylation of AKT^{S473}, GSK-$3\beta^{S9}$, $PRAS40^{T246}$ and $P70S6K^{T421/S424}$ (Figure 11A-F), suggesting the activation of both mTORC complexes kinase activity. In agreement with insulin signalling activation, UnAG treated rats also presented higher insulin-stimulated muscle glucose uptake (Figure 11G). These effects were further associated with increased IRS-1^{S312} phosphorylation (Figure 11B), a marker for enhanced insulin signalling depending on mTORC-mediated negative feedback modulation [175]. To investigate IRS-1 activating phosphorylations, we assessed pIRS-1^{Y612} finding no stimulation in UnAG-treated animals (Figure 12), thus further supporting the hypothesis that UnAG-associated activation of insulin signalling occurs downstream of mTORC complexes but not at IR-IRS1 level (Figure 11A-B).

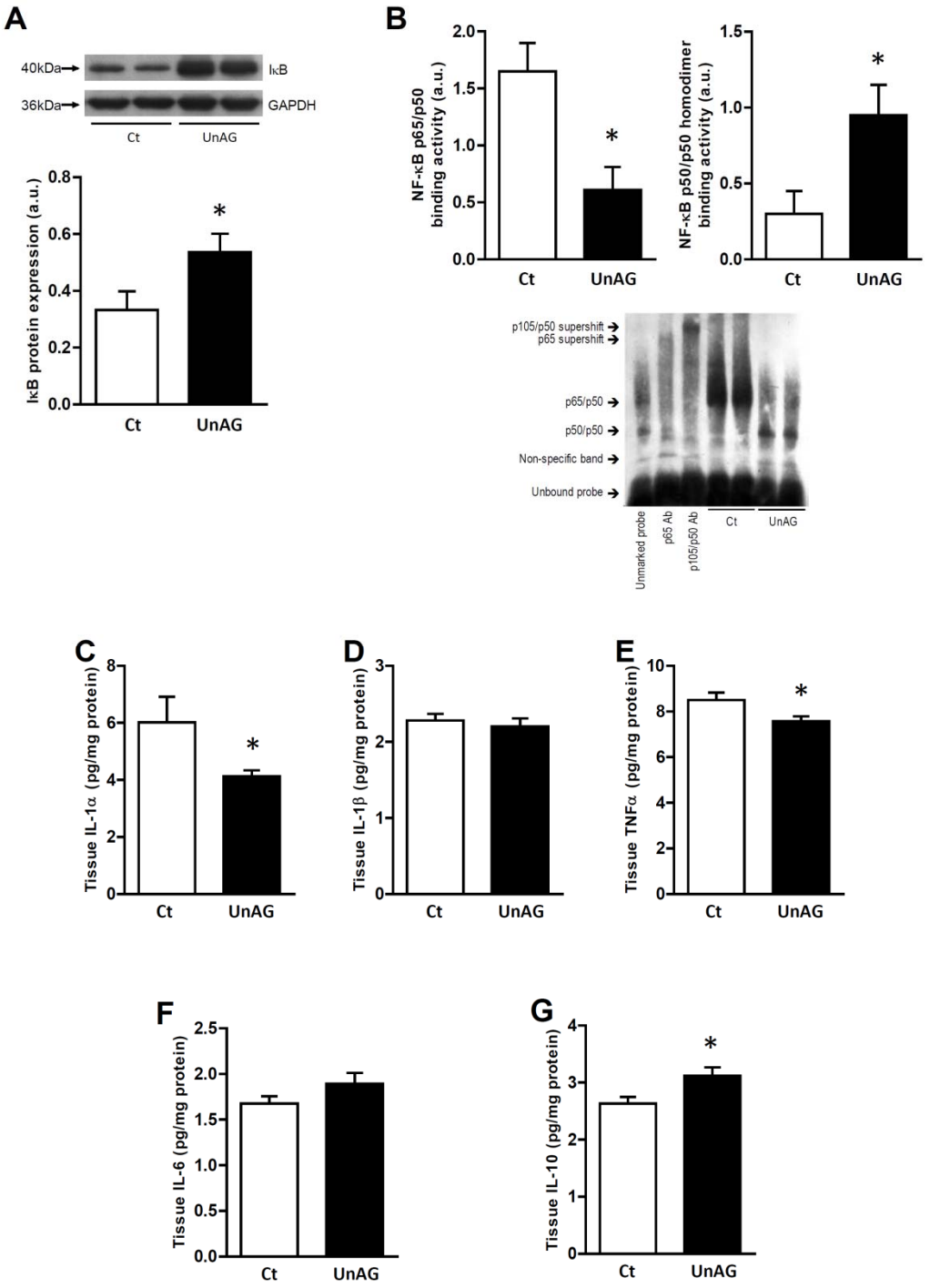

*Figure 10. UnAG and skeletal muscle inflammation. Effects of unacylated ghrelin (UnAG, 200µg subcutaneous injection twice per day) vs. saline (Ct) sustained 4-day treatment on the expression of IκB (A), on NF-κB binding activity (B) with representative blots, and on tissue expression of IL-1α (C), IL-1β (D), TNFα (E), IL-6 (F) and IL-10 (G) measured by xMAP technology in gastrocnemius muscle. a.u.: arbitrary units, Ab: antibody. *p<0.05 vs. Ct; mean±SEM; n=8-10/group.*

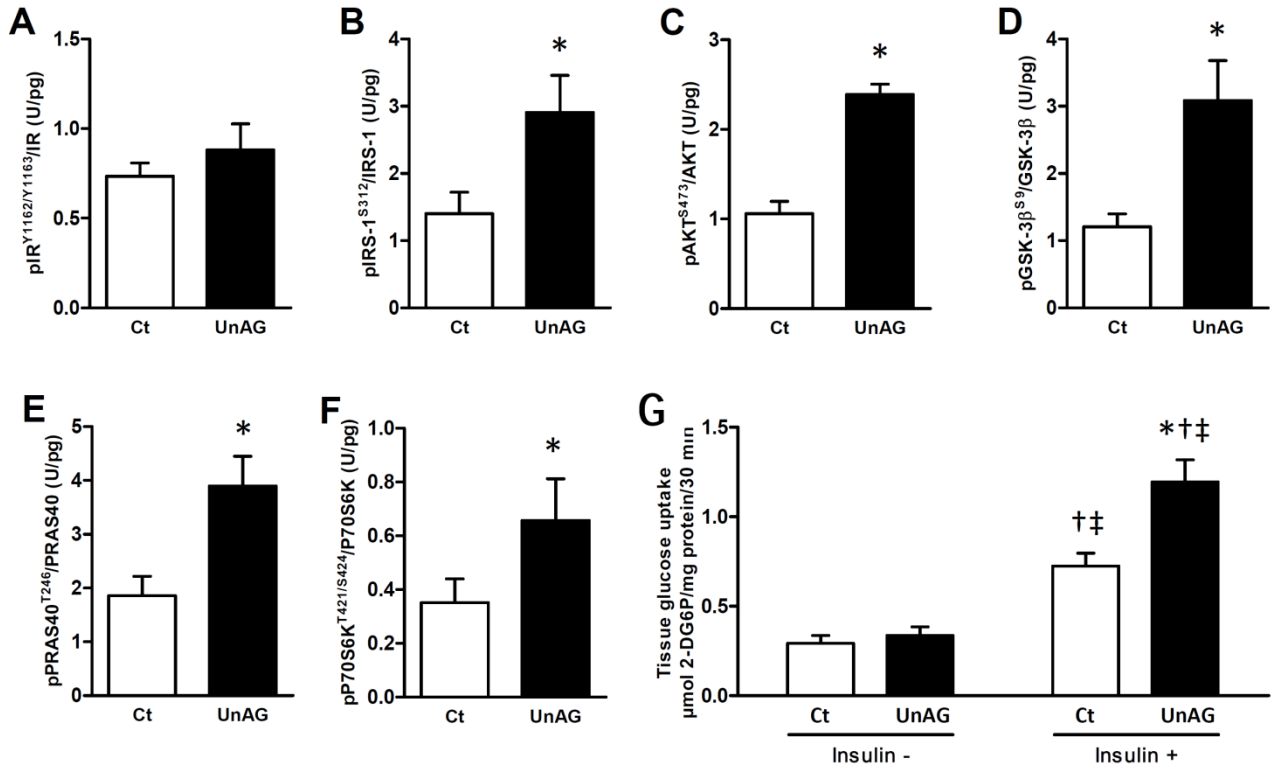

*Figure 11. UnAG and skeletal muscle insulin action. Effects of unacylated ghrelin (UnAG, 200µg subcutaneous injection twice per day) vs. saline (Ct) sustained 4-day treatment on the phosphorylation measured by xMAP technology of insulin receptor (IR$^{Y1162/Y1163}$, A), IRS-1^{S312} (B), AKT^{S473} (C), GSK-3β^{S9} (D), PRAS40^{T246} (E), P70S6K$^{T421/S424}$ (F) and on tissue glucose uptake (G) in gastrocnemius muscle. *p<0.05 vs. Ct; †p<0.05 vs. same treatment Insulin-; ‡p<0.05 vs. other treatment Insulin-; mean±SEM, n=8-10/group.*

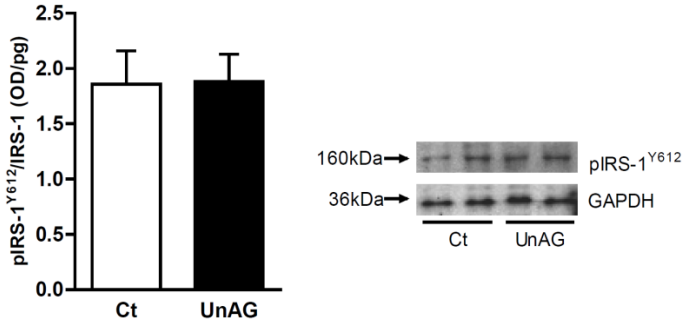

Figure 12. UnAG and IRS-1^{Y612} phosphorylation in skeletal muscle. Effects of unacylated ghrelin (UnAG, 200µg subcutaneous injection twice per day) vs. saline (Ct) sustained 4-day treatment (A, n=8-10/group) on the phosphorylation of IRS-1^{Y612} in gastrocnemius muscle with representative blots. OD: optical density. Mean±SEM.

5.2.2 Effects of UnAG on skeletal muscle ROS generation, inflammation and insulin signalling are tissue specific, at least in part direct and not shared by AG

5.2.2.1 In vivo effects of UnAG are tissue-specific

In liver tissue, UnAG treatment caused a non-statistically significant reduction in mitochondrial superoxide production. As previously shown [112,296], this relatively minor change was not associated with altered redox state, inflammation markers or insulin signalling (Figures 13-15).

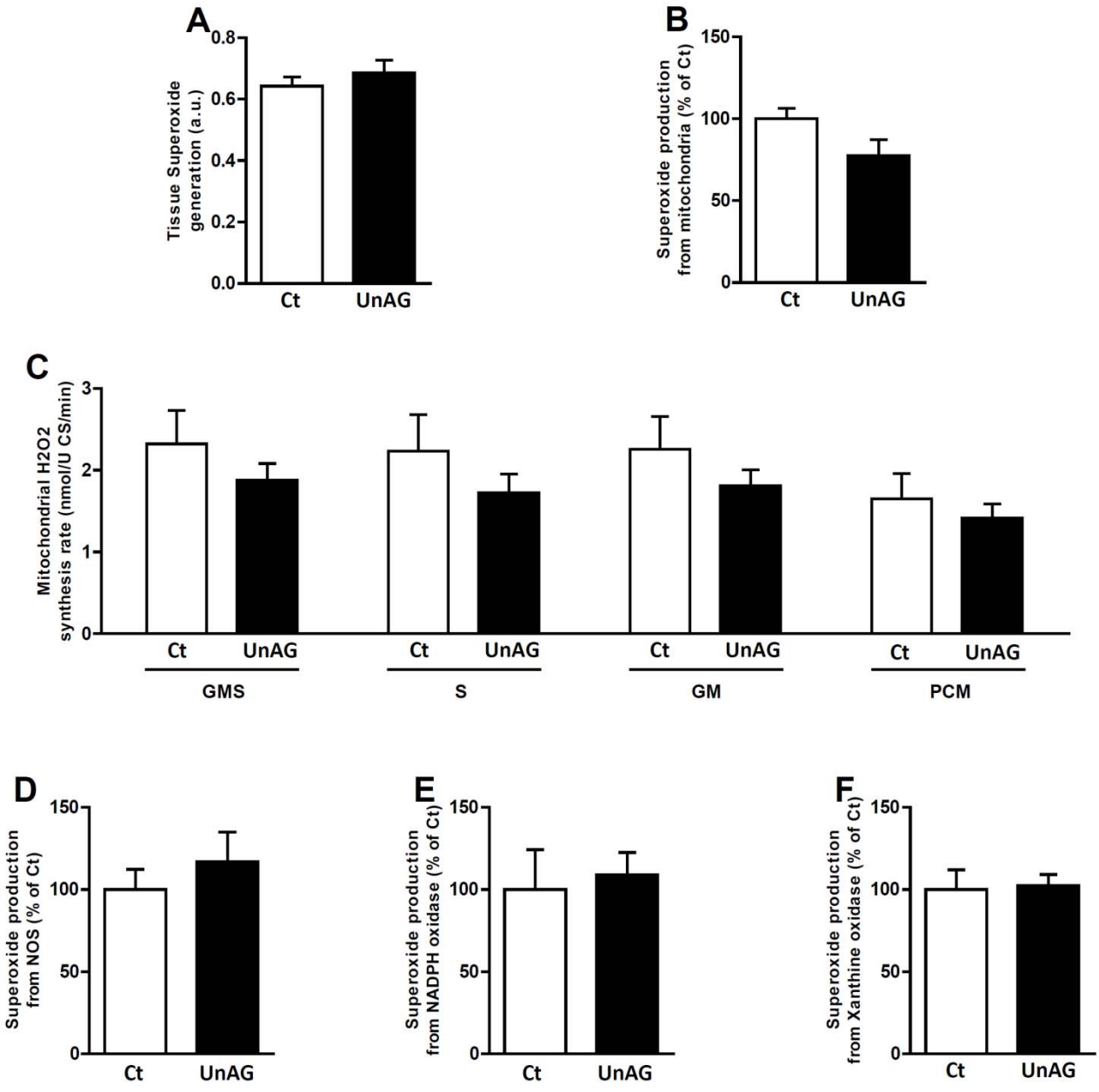

*Figure 13. UnAG and liver Reactive Oxygen Species production. Effects of unacylated ghrelin (UnAG, 200μg subcutaneous injection twice per day) vs. saline (Ct) sustained 4-day treatment on overall (A) and specific superoxide production from mitochondrial sources in whole tissue homogenate (B), on H_2O_2 synthesis rate from liver-isolated intact mitochondria with different respiratory substrates (C, GMS: Glutamate+Succinate+Malate; S: Succinate; GM: Glutamate+Malate; PCM: Palmitoyl-L-Carnintine+Malate) and on nitric oxide synthase- (D), NADPH oxidase- (E) and xanthine oxidase- (F) derived superoxide generation in skeletal muscle. U CS: units of citrate synthase; a.u.: arbitrary units. *p<0.05 vs. Ct; mean±SEM, n=8-10/group.*

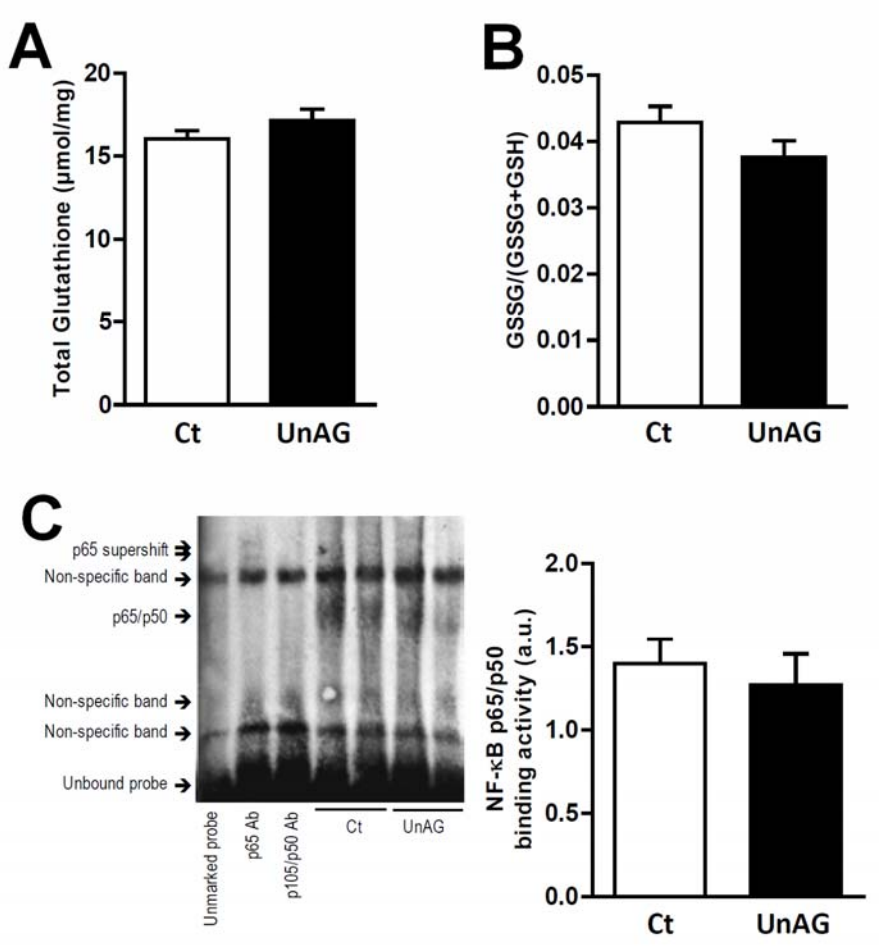

*Figure 14. Figure 1. UnAG and liver redox state and inflammation. Effects of unacylated ghrelin (UnAG, 200μg subcutaneous injection twice per day) vs. saline (Ct) sustained 4-day treatment on total (A) and oxidized (GSSG) over total (B, GSH: reduced) tissue glutathione and on NF-κB binding activity (C) with representative blot. a.u.: arbitrary units, Ab: antibody. *p<0.05 vs. Ct; mean±SEM, n=8-10/group.*

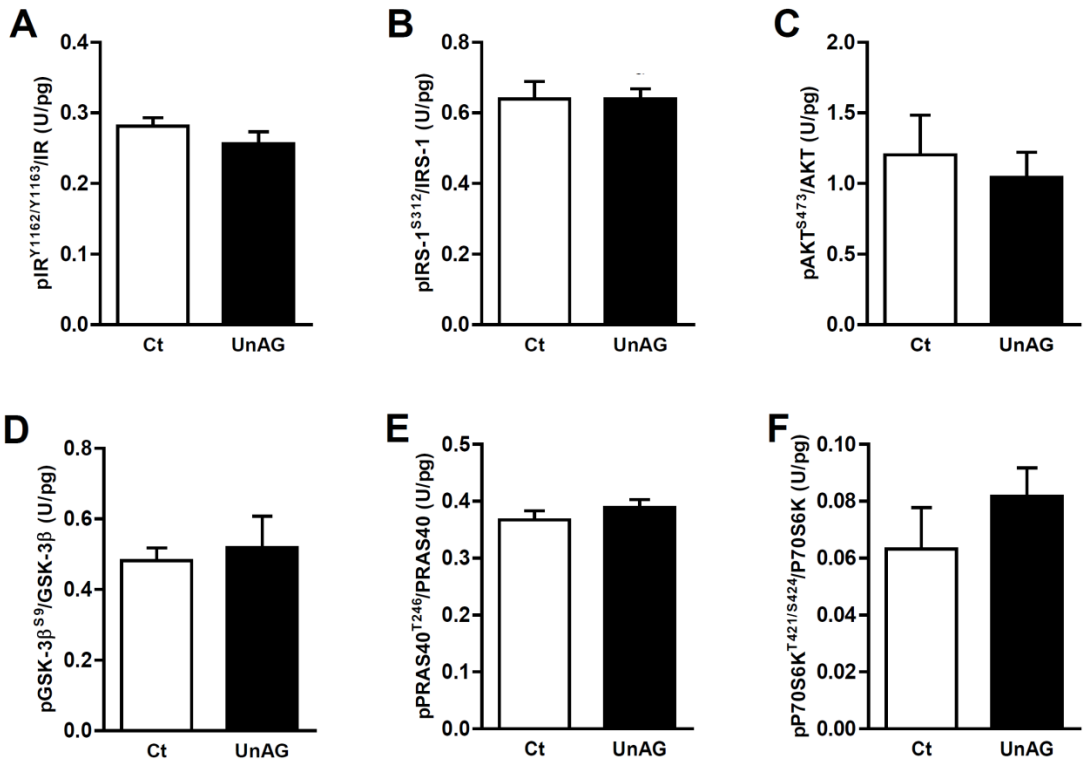

Figure 15. UnAG and liver insulin action. Effects of unacylated ghrelin (UnAG, 200µg subcutaneous injection twice per day) vs. saline (Ct) sustained 4-day treatment on the phosphorylation of insulin receptor (IR)Y1162/Y1163 (A), IRS-1S312 (B), AKTS473 (C), GSK-3βS9 (D), PRAS40T246 (E), P70S6KT421/S424 (F) measured by xMAP technology in rat liver. Mean±SEM, n=8-10/group.

5.2.2.2 UnAG effects on mitochondrial ROS generation and insulin signalling are also observed in cultured C2C12 myotubes

48-hour incubation of C2C12 myotubes with UnAG lowered mitochondrial ROS production with largely dose-dependent effects (Figure 16A). Also consistently with in vivo data, UnAG enhanced activating phosphorylation of insulin signalling proteins dependent on TORC complexes, including AKT^{S473}, GSK-3β^{S9}, PRAS40^{T246} and P70S6K$^{T421/S424}$. Activations of of pIR$^{Y1162/Y1163}$ and pIRS-1^{S312} were also comparable between C2C12 and in-vivo experiments, supporting lack of activation at IR-IRS1 level (Figure 16B-G).

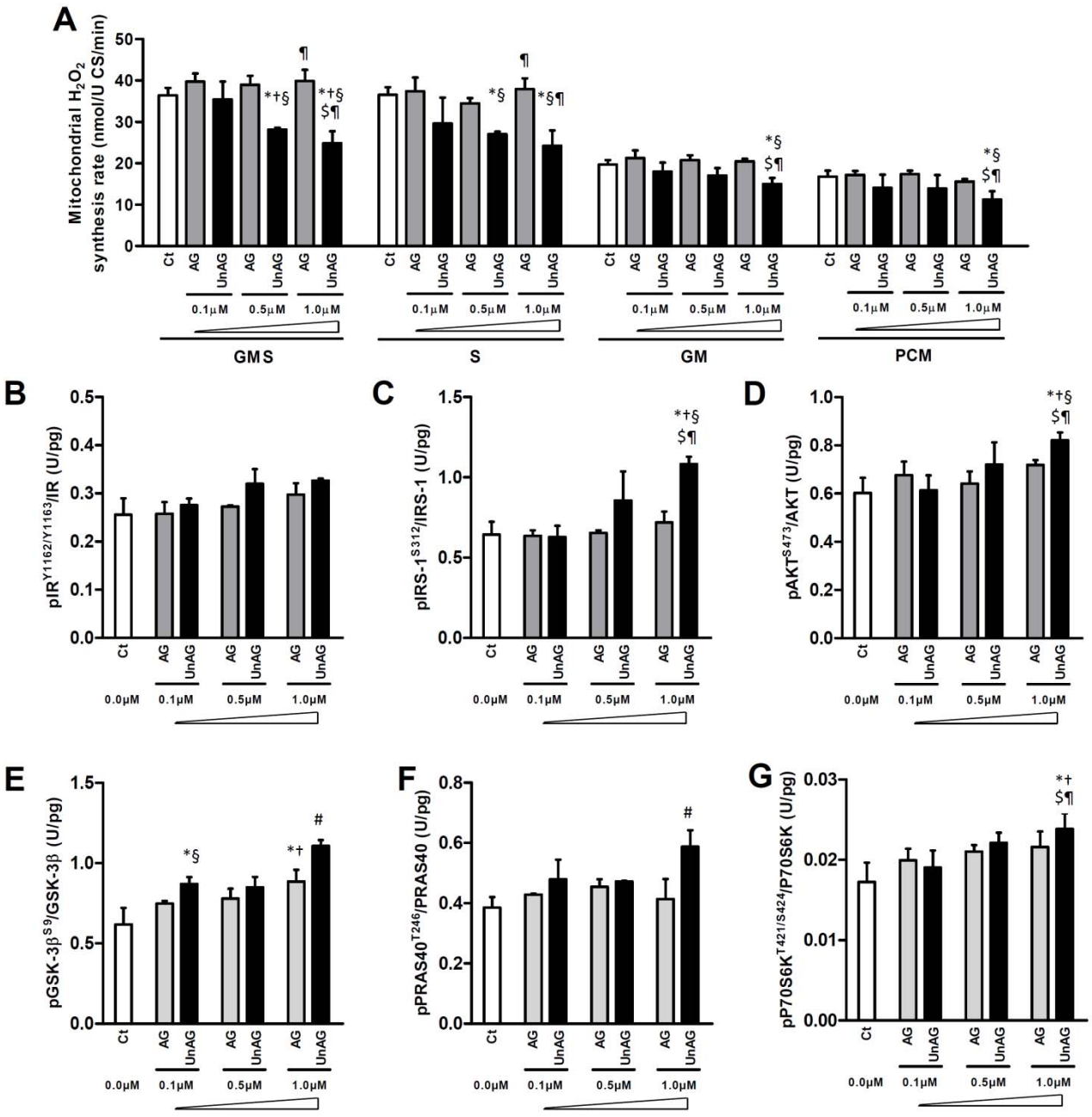

*Figure 16. In vitro impact of UnAG on cultured myotubes. Effects of 48 h incubation with increasing concentrations of acylated (AG) or unacylated ghrelin (UnAG) vs. control (Ct) on isolated mitochondria H2O2 synthesis rate with different respiratory substrates (A, GMS: Glutamate+Succinate+Malate; S: Succinate; GM: Glutamate+Malate; PCM: Palmitoyl-L-Carnintine+Malate) and effects of the above treatments on the phosphorylation of insulin receptor (IR)Y1162/Y1163 (B), IRS-1S312 (C), AKTS473 (D), GSK-3βS9 (E), PRAS40T246 (F), P70S6KT421/S424 (G) measured by xMAP technology in C2C12 myotubes. U CS: units of citrate synthase. *p<0.05 vs. Ct; †p<0.05 vs. same hormone 0.1μM; ‡p<0.05 vs. same hormone 0.5μM; § p<0.05 vs. AG, same concentration; $p<0.05 vs. other hormone 0.5μM; ¶p<0.05 vs. other hormone 0.1μM; #p<0.05 vs. all other groups; mean±SEM, n=3/group.*

5.2.2.3 *UnAG effects in vitro are not shared by AG*

Reportedly, C2C12 myotubes do not express the recognized AG receptor GHSR1a [71]. To further exclude the possibility that UnAG effects result from non-specific activation of additional AG-regulated pathways, we in parallel also performed C2C12 experiments using equimolar AG concentrations. 48-hour AG incubation failed to inhibit ROS generation and to enhance insulin signalling except for less pronounced activation of pGSK-3β^{S9} (Figure 16A-G).

5.2.3 UnAG-induced decrease in mitochondrial ROS generation is not associated with enhanced mitochondrial function

In agreement with previous results [199,297], UnAG-induced changes in redox state, inflammation and insulin signalling were not associated with increased, but with lower or unchanged ATP synthesis rate in vivo and in vitro respectively (Figures 17A and 17C). UnAG treatment modified respiratory chain complex-related ATP production by shifting ATP synthesis towards complex I over complex II both in skeletal muscle in vivo and in myotubes in vitro (Figures 17B and 17D). Differently from UnAG, AG increased ATP production in C2C12 myotubes (Figure 17C). Liver ATP production was not modified by UnAG treatment (Figure 18).

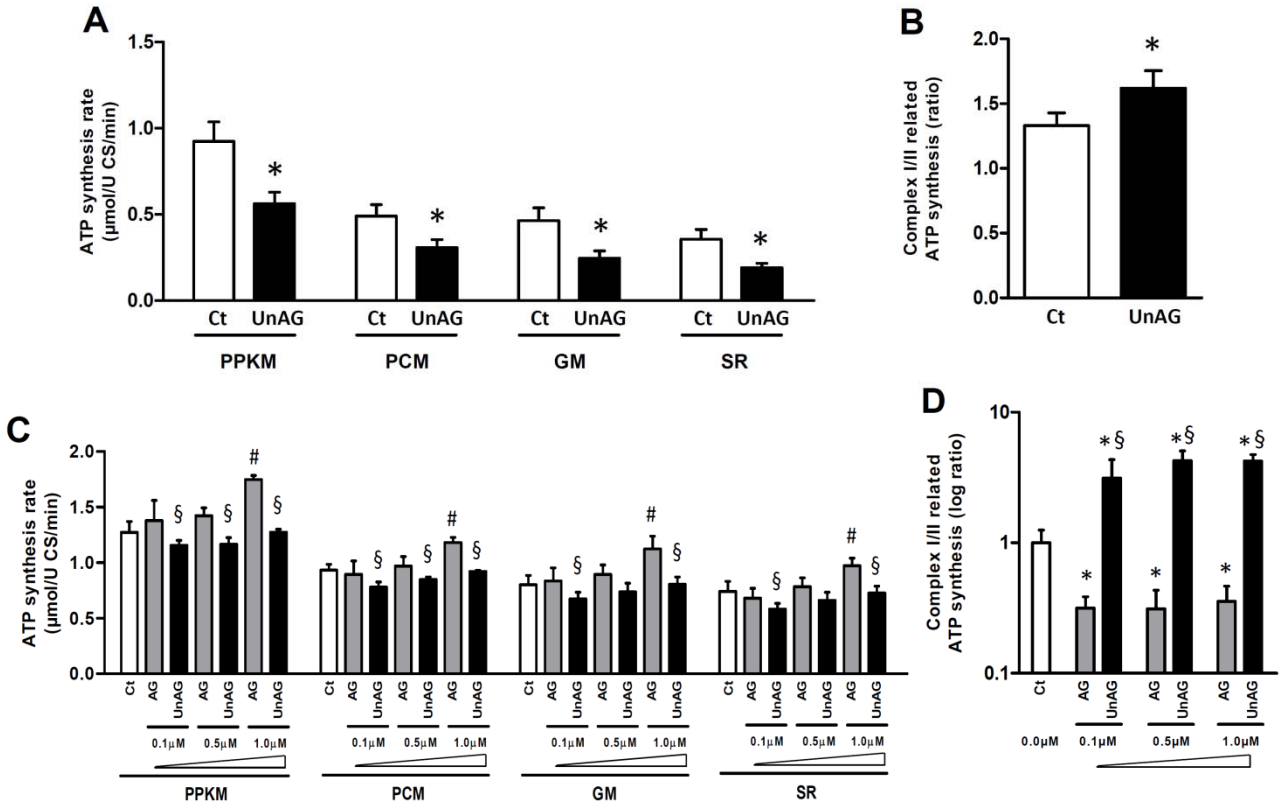

*Figure 17. Impact of UnAG on mitochondrial ATP synthesis. Effects on muscle ATP synthesis rate with different respiratory substrates (PPKM: Pyruvate+Palmitoyl-L-Carnintine+α-Ketoglutarate+Malate; PCM: Palmitoyl-L-Carnintine+Malate; GM: Glutamate+Malate; SR: Succinate+Rotenone) in isolated mitochondria from rat gastrocnemius muscle after unacylated ghrelin (UnAG, 200µg subcutaneous injection twice per day) vs. saline (Ct) sustained 4-day (A, n=8-10/group) treatment, and in C2C12 myotubes after 48 h incubation with increasing concentrations of acylated (AG) or unacylated ghrelin (UnAG) vs. control (Ct) in (C, n=3/treatment). Complex I over complex II related ATP synthesis rate ratio in rat gastrocnemius muscle after sustained treatment (B) and in cultured myotubes (D). *p<0.05 vs. Ct; § p<0.05 vs. AG, same concentration; #p<0.05 vs. all other groups; mean±SEM.*

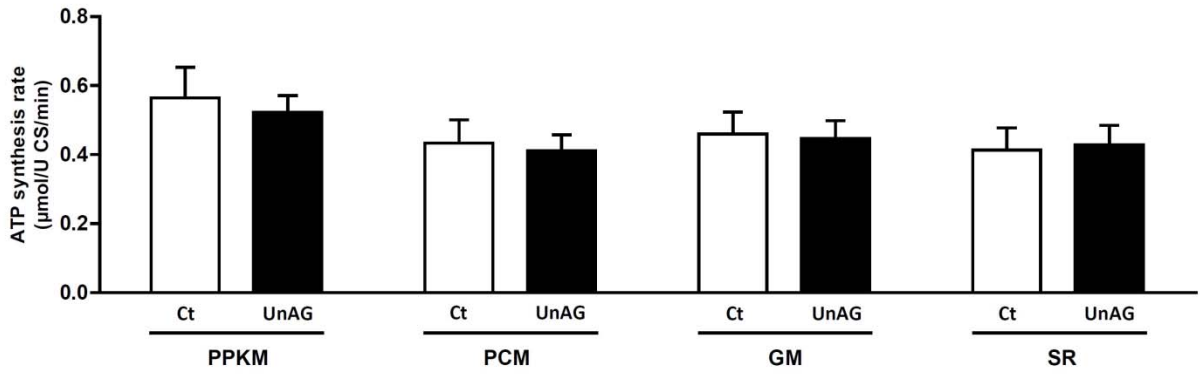

Figure 18. UnAG and liver ATP synthesis. Effects of unacylated ghrelin (UnAG, 200µg subcutaneous injection twice per day) vs. saline (Ct) sustained 4-day treatment on ATP synthesis rate with different respiratory substrates (PPKM: Pyruvate+Palmitoyl-L-Carnintine+α-Ketoglutarate+Malate; PCM: Palmitoyl-L-Carnintine+Malate; GM: Glutamate+Malate; SR: Succinate+Rotenone) in liver isolated mitochondria. Mean±SEM, n=8-10/group.

5.3 HFD-induced obesity and UnAG up-regulation

5.3.1 Animal characteristics

In both lean and obese animals up-regulation of circulating UnAG by myocardial overexpression of the ghrelin gene (Tg Myh6/Ghrl) [128] did not modify body weight or caloric intake. While blood glucose, plasma insulin and NEFA were comparable among control diet fed groups irrespectively of genotype, blood glucose and plasma insulin were conversely higher in HFD-obese wild-type compared to Tg Myh6/Ghrl obese mice, whose glucose and insulin levels were similar to those in lean groups (Table 8).

*Table 8. Animal phenotype. Animal phenotype in transgenic mice (Tg Myh6/Ghrl) with systemic up-regulation of UnAG vs. wild type (Wt) fed 16 wks with Control- or High Fat- Diet. BW: body weight. Mean±SEM; *p<0.05 Wt-HFD vs. other groups.*

	Control Diet		High Fat Diet	
	Ct (n=7)	Tg *Myh6/Ghrl* (n=7)	Wt (n=7)	Tg *Myh6/Ghrl* (n=7)
Body Weight (g)	**31.0**±2.1	**28.7**±2.1	**37.9**±3.0*	**36.6**±1.1*
Average Caloric intake (kcal/d)	**13.5**±0.1	**14.6**±0.6	**17.6**±0.1*	**17.9**±0.5*
Plasma Glucose (mg/dL)	**106.0**±7.3	**98.2**±8.0	**161.9**±30.7*	**102.7**±11.6
Plasma Insulin (µU/ml)	**13.3**±1.8	**14.5**±3.1	**25.1**±2.2*	**16.5**±1.6
Plasma NEFA (mmol/L)	**0.32**±0.06	**0.38**±0.08	**0.27**±0.05	**0.32**±0.10

5.3.2 Systemic circulating UnAG up-regulation is associated with less oxidized redox state, lower inflammation and enhanced skeletal muscle insulin signalling and whole-body insulin sensitivity

In agreement with exogenous UnAG administration experiments, circulating UnAG up-regulation in Tg Myh6/Ghrl was characterized by lower oxidized-to-total glutathione (Figure 19A-B) and by a less pro-inflammatory tissue cytokine profile at skeletal muscle level (Figure 19C-G). Consistent with exogenously-treated animals, changes in redox state and inflammation were paralleled by enhanced phosphorylation of AKT^{S473}, GSK-$3\beta^{S9}$, $PRAS40^{T246}$ and $P70S6K^{T421/S424}$ (Figure 20A-F), with no changes at $IRS\text{-}1^{Y612}$ level (Figure 20G). These effects were associated with higher whole-body insulin sensitivity as measured by area-under-the-curve (AUC) for ITT-induced blood glucose changes (Figure 21).

5.3.3 Systemic circulating UnAG up-regulation prevents obesity-associated hyperglycaemia, whole-body insulin resistance and skeletal muscle oxidative stress, inflammation and impaired AKT phosphorylation

Obese wild-type mice were hyperglycaemic and insulin resistant (Figure 21A-C). The obese wild-type group also had higher gastrocnemius oxidized-to-total glutathione, a more pro-inflammatory cytokine profile and lower phosphorylation of AKT^{S473} and GSK-$3\beta^{S9}$ (Figures 19 and 20). In Myh6/Ghrl mice, HFD induced moderately higher muscle oxidized-to-total glutathione and TNFα levels, but levels of these parameters remained however lower ($p<0.05$) than obese and comparable (p=NS) to lean wild-type animals (Figures 19B and 19E). In addition, UnAG overexpression prevented obesity-associated increase ($P<0.05$ vs HFD wild-type) in muscle pro-inflammatory cytokines IL-1α and IL-1β with lower IL-6, and normalized activating phosphorylation at AKT^{S473} and GSK-$3\beta^{S9}$ levels (P=NS vs lean Tg Myh6/Ghrl). Importantly, obese Tg Myh6/Ghrl were protected from obesity-induced hyperglycaemia and insulin resistance at whole body level (Figure 21A-C), with both parameters similar to lean wild-type animals. Mediators of the insulin signalling pathway upstream of AKT were not activated in Tg Myh6/Ghrl mice, and IRS-1 showed phosphorylation patterns in pIRS-1^{S312} and pIRS-1^{Y612} comparable to those observed in exogenously-treated animals (Figures 20A-B and 20G).

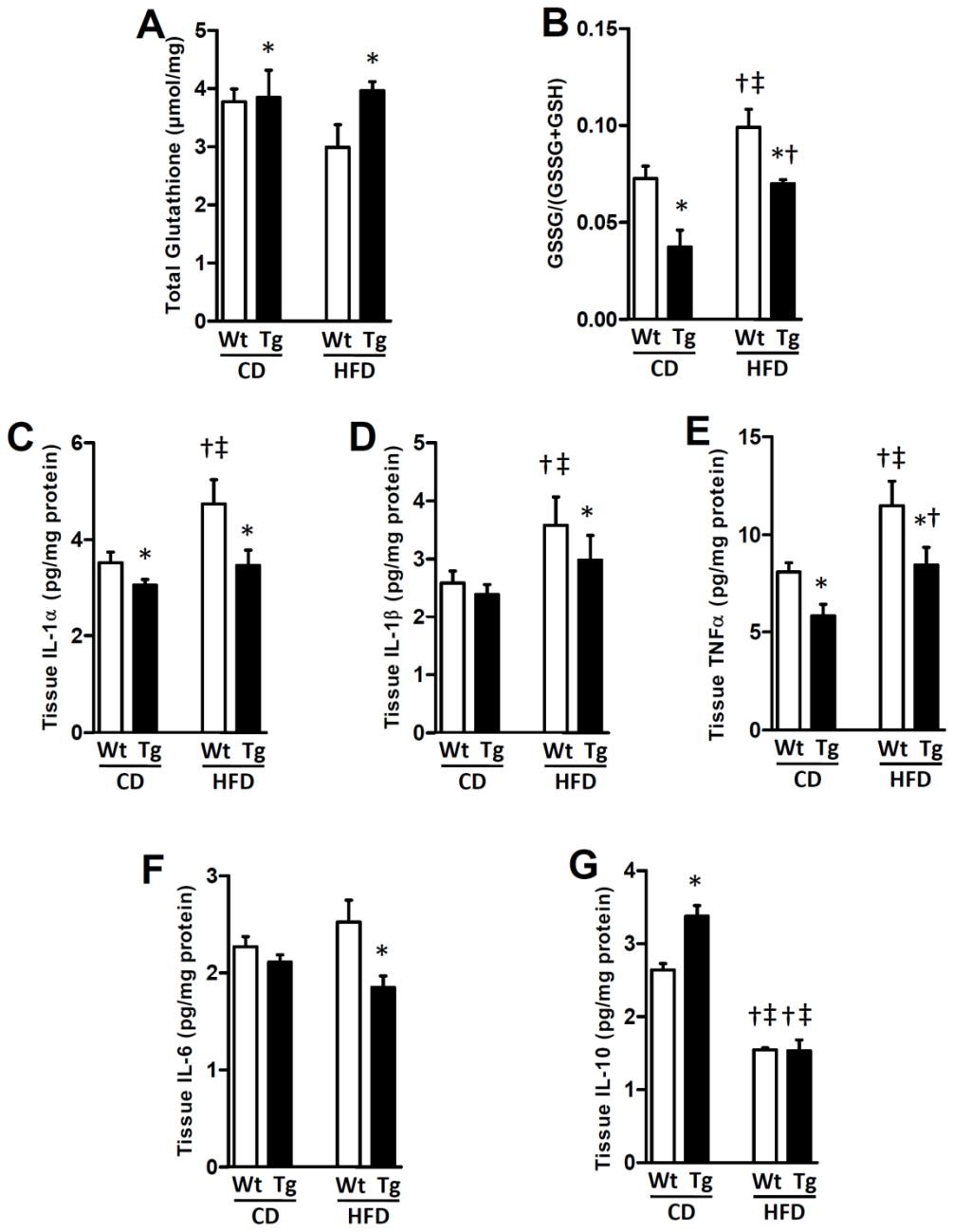

*Figure 19. Impact of systemic overexpression of UnAG on skeletal muscle redox state and inflammation in lean and obese mice. Effects of UnAG overexpression in transgenic Myh6/Ghrl (Tg) vs. wild type (Wt) mice fed 16 wks with Control- (CD) or High Fat- Diet (HFD) on total (A) and oxidized (GSSG) over total (B, GSH: reduced) glutathione and on gastrocnemius expression of IL-1α (C), IL-1β (D), TNFα (E), IL-6 (F) and IL-10 (G). *p<0.05 vs. Ct; †p<0.05 vs. same genotype-CD; ‡p<0.05 vs. other genotype-CD; mean±SEM, n=7/group.*

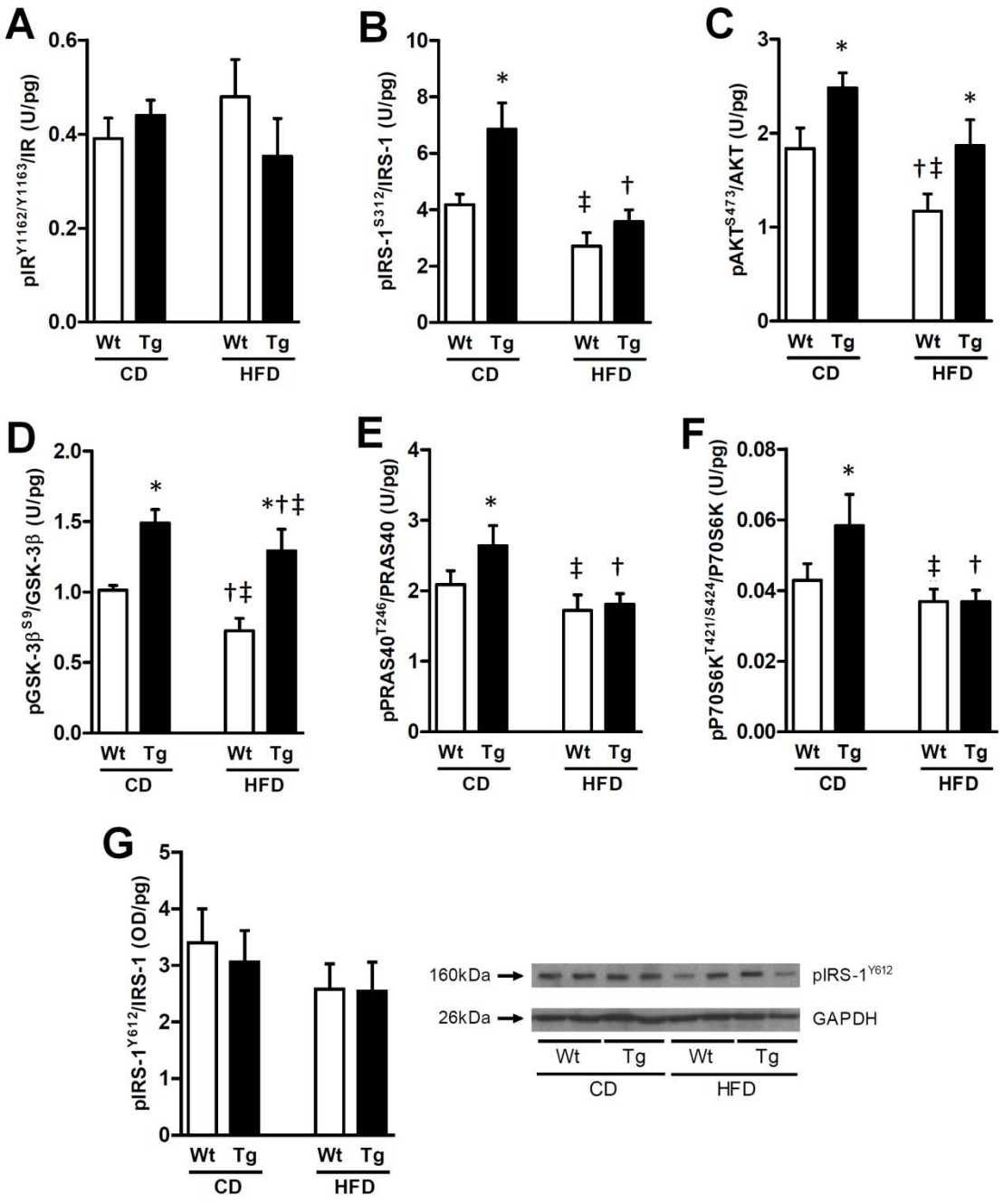

*Figure 20. Impact of UnAG systemic overexpression on skeletal muscle insulin signalling in lean and obese mice. Effects of UnAG overexpression in transgenic Myh6/Ghrl (Tg) vs. wild type (Wt) mice fed 16 wks with Control- (CD) or High Fat- Diet (HFD) on the phosphorylation of insulin receptor (IR$^{Y1162/Y1163}$, A), IRS-1^{S312} (B), AKT^{S473} (C), GSK-3β^{S9} (D), PRAS40^{T246} (E), P70S6K$^{T421/S424}$ (F) measured by xMAP technology in gastrocnemius muscle, effects on the phosphorylation of IRS-1^{Y612} (G) in gastrocnemius muscle with representative blots. *p<0.05 vs. Ct; †p<0.05 vs. same genotype-CD; ‡p<0.05 vs. other genotype-CD; OD: optical density; mean±SEM; n=7/group.*

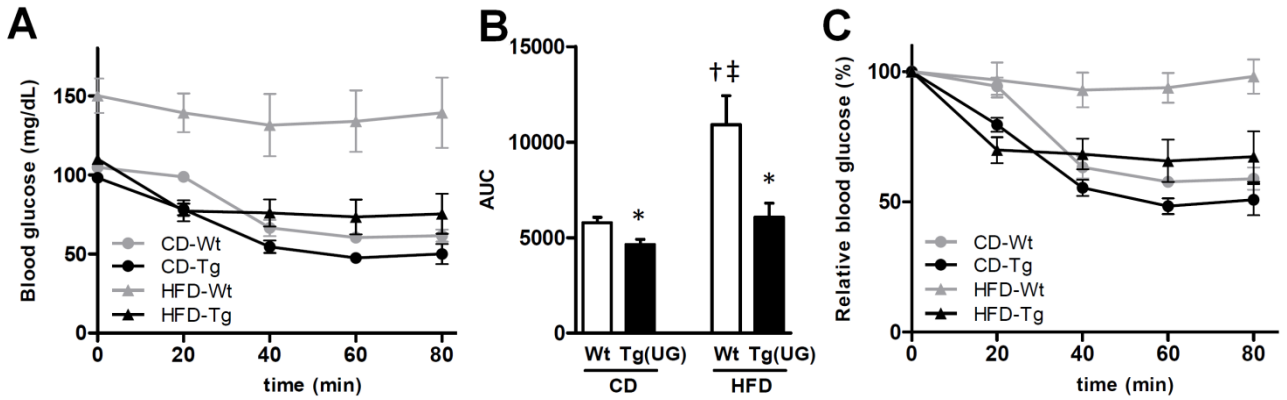

*Figure 21. Impact of systemic overexpression of UnAG on whole body insulin action in lean and obese mice. Effects of UnAG overexpression in transgenic Myh6/Ghrl (Tg) vs. wild type (Wt) mice fed 16 wks with Control- (CD) or High Fat- Diet (HFD) on absolute (A), with corresponding Area Under the Curve (AUC) analysis (B), and relative (C) blood glucose levels in Insulin Tolerance Test (ITT) experiments. *p<0.05 vs. Ct; †p<0.05 vs. same genotype-CD; ‡p<0.05 vs. other genotype-CD; mean±SEM, n=7/group.*

5.3.4 Effects of UnAG overexpression are not associated with enhanced skeletal muscle mitochondrial function

As in UnAG treated healthy rats, also lean mice with UnAG overexpression were characterized by lower ATP generation. High fat diet markedly increased skeletal muscle ATP production while maintaining lower ATP generation rates in obese Tg Myh6/Ghrl compared to obese wild-type (Figure 22).

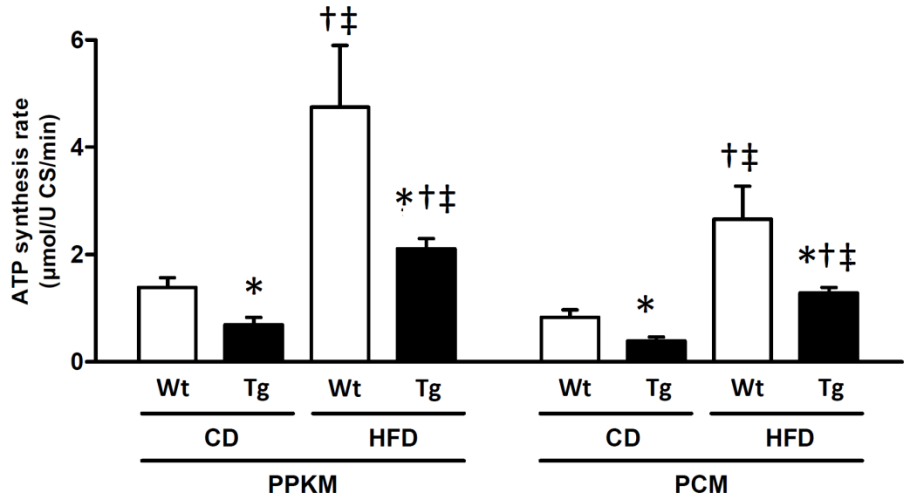

*Figure 22. Effects of UnAG overexpression on muscle ATP synthesis in obese mice. Effects on muscle ATP synthesis rate with different respiratory substrates (A, PPKM: Pyruvate+Palmitoyl-L-Carnintine+α-Ketoglutarate+Malate; PCM: Palmitoyl-L-Carnintine+Malate; GM: Glutamate+Malate; SR: Succinate+Rotenone) in isolated mitochondria from isolated mitochondria from gastrocnemius muscle of mice with UnAG up-regulation (Tg Myh6/Ghrl) vs. wild type (wt) fed 16 wks with Control- (CD) or High Fat- Diet (HFD) (B, n=7/group). *p<0.05 vs. Ct or Wt; †p<0.05 vs. same genotype-CD; ‡p<0.05 vs. other genotype-CD; mean±SEM.*

5.4 Effects of UnAG treatment in a rodent model of uraemia

5.4.1 Animal characteristics

5/6 nephrectomy increased plasma urea and creatinine levels at 40 days independently of ghrelin treatment. In agreement with other studies using the same model, blood glucose levels were not modified by surgery or ghrelin treatment. Conversely, insulin levels were markedly increased in uremic rats, indicating the development of systemic insulin resistance [298]. This derangement was not modified by AG treatment, while insulin levels in UnAG-treated rats were not statistically different from sham. Although average food intake and body length increase over time were equal among groups, in young-adult rats 5/6 nephrectomy markedly affected the physiological increase in body weight and abdominal circumpherence compared to sham (Table 9). Moreover, the expected parallel increase of body mass and obesity indexes was completely prevented by 5/6 nephrectomy, with no impact of either ghrelin form. However, weights of selected tissues as indicators of body

composition show that ghrelin forms differently impacted on nephrectomy-associated loss of muscle and fat mass. While AG treatment moderately increased retroperitoneal fat mass, UnAG lowered visceral adipose tissue but importantly completely recovered muscle mass compared to sham (Figure 23).

*Table 9. Animal characteristics. Animal characteristics in sham or 5/6 nephrectomized rats (Nx), without or with unacylated (UnAG) o acylated (AG) ghrelin 4-day treatment (200µg subcutaneous injection twice per day). BMI: body mass index. Mean±SEM; *p<0.05 vs. Sham.*

	Time	**Sham** (n=10)	**Nx** (n=10)	**Nx-AG** (n=10)	**Nx-UnAG** (n=10)
Body Weight (g)	**T0**	364±5	365±7	360±8	364±14
	T40	459±6	422±7 *	418±8 *	420±9 *
	Δ	94±4	61±4 *	58±7 *	61±4 *
Length (Nose-Anus)	**T0**	23.5±0.2	23.2±0.2	23.2±0.2	23.4±2
	T40	24.4±0.5	25.0±0.3	24.5±0.2	24.9±0.3
	Δ	1.3±0.3	1.7±0.2	1.3±0.2	1.5±0.3
Abdominal Circ. (cm)	**T0**	18.3±0.1	18.7±0.3	18.3±0.1	18.2±0.3
	T40	21.4±0.6 *	19.3±0.3 *	19.9±0.2 *	19.5±0.4 *
	Δ	3.1±0.6	1.0±0.2 *	1.5±0.2 *	1.3±1.2 *
BMI (g/cm^2)	**T0**	0.66±0.01	0.68±0.04	0.67	0.66±0.02
	T40	0.78±0.04	0.68±0.01 *	0.69±0.01 *	0.68±0.01 *
	Δ	0.12±0.05	0.01±0.02 *	0.02±0.01 *	0.01±0.01 *
Lee obesity index (g^3/cm)	**T0**	0.304±0.002	0.308±0.002	0.307±0.002	0.305±0.003
	T40	0.323±0.008	0.302±0.003 *	0.305±0.003 *	0.301±0.001 *
	Δ	0.020±0.010	-0.006±0.004 *	-0.002±0.003 *	-0.005±0.002 *
Average food intake (g/die)	**-**	19.7±0.4	20.2±0.6	20.6±0.3	19.8±0.5
Blood Glucose (mg/dL)	**T40**	105±4	103±4	107±2	103±7
INSULIN (µU/ml)	**T40**	12.4±0.6	17.6±1.3 *	17.8±1 *	15.0±1.5
NEFA (mmol/L)	**T40**	0.31±0.02	0.39±0.02 *	0.43±0.03 *	0.38±0.02 *
Plasma Urea (mg/dL)	**T40**	21.54±2.06	30.32±0.96 *	28.67±3.10 *	27.96±2.22 *
Plasma Creatinine (µmol/L)	**T40**	19.40±0.87	24.82±1.59 *	25.49±1.68 *	22.91±1.00 *

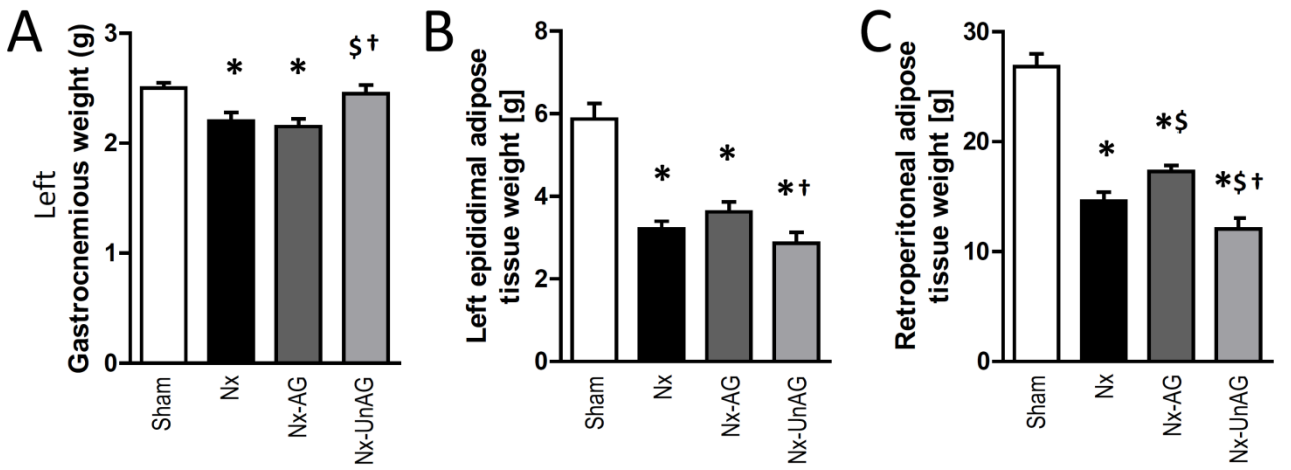

*Figure 23. Ghrelin forms treatment and selected body composition measurements in uremic rats. Effects of 4 day acylated (AG) and unacylated (UnAG) ghrelin treatment (200µg subcutaneous injection twice per day) on gastrocnemius muscle mass (A) and on epididimal (B) and retroperitoneal (C) adipose tissue weight (B) in young adults male rats 40 days after 5/6 nephrectomy (Nx). *p<0.05 vs. Sham; $ p<0.05 vs. Nx; †p<0.05 vs. Nx-AG; mean±SEM, n=10/group.*

5.4.2 UnAG but not AG treatment reverses 5/6 nephrectomy-associated increase in skeletal muscle ROS generation

Nephrectomy increased both mitochondrial H_2O_2 and superoxide anion production rate in the gastrocnemius muscle. UnAG but not AG treatment, as observed in physiological conditions, markedly reduced muscle ROS generation, completely normalizing mitochondrial respiration-dependent ROS production compared to sham (Figure 24A-B). Among non-mitochondrial sources, while AG, and partly UnAG selectively reduced xanthine oxidase-dependent superoxide production, only UnAG normalized NOS-dependent ROS generation, (Figure 24C). Consistently with data on ROS generation from mitochondria, a major cell ROS source, UnAG but not AG-treatment reversed increased nephrectomy-associated muscle oxidized-over-total glutathione ratio, thus restoring tissue redox state compared to sham (Figure 25A-B). Interestingly, levels of catalase but not of GPx antioxidant enzymes were also improved by UnAG treatment (Figure 25C-D).

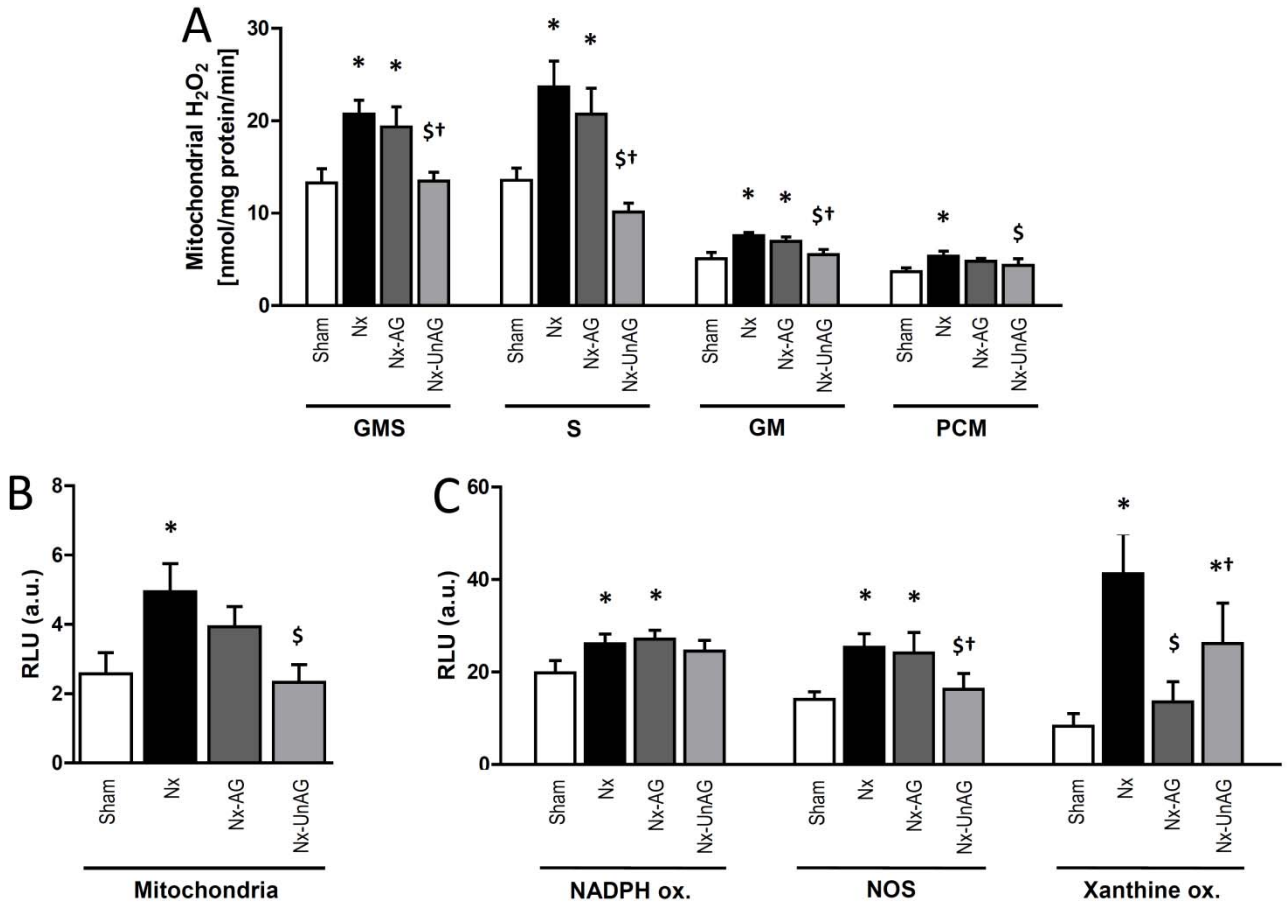

*Figure 24. Ghrelin forms and skeletal muscle reactive oxygen species generation in uremic rats. Effects of 4 day acylated (AG) and unacylated (UnAG) ghrelin treatment (200μg subcutaneous injection twice per day) in 5/6 nephrectomized rats (Nx) on gastrocnemius muscle H2O2 synthesis rate from intact mitochondria with different respiratory substrates (A, GMS: Glutamate+Succinate+Malate; S: Succinate; GM: Glutamate+Malate; PCM: Palmitoyl-L-Carnintine+Malate) and specific superoxide production from mitochondrial (B) and non mitochondrial (C) sources in whole tissue homogenate. RLU: relative light units; a.u.: arbitrary units. *p<0.05 vs. Sham; $ p<0.05 vs. Nx; †p<0.05 vs. Nx-AG; mean±SEM, n=10/group.*

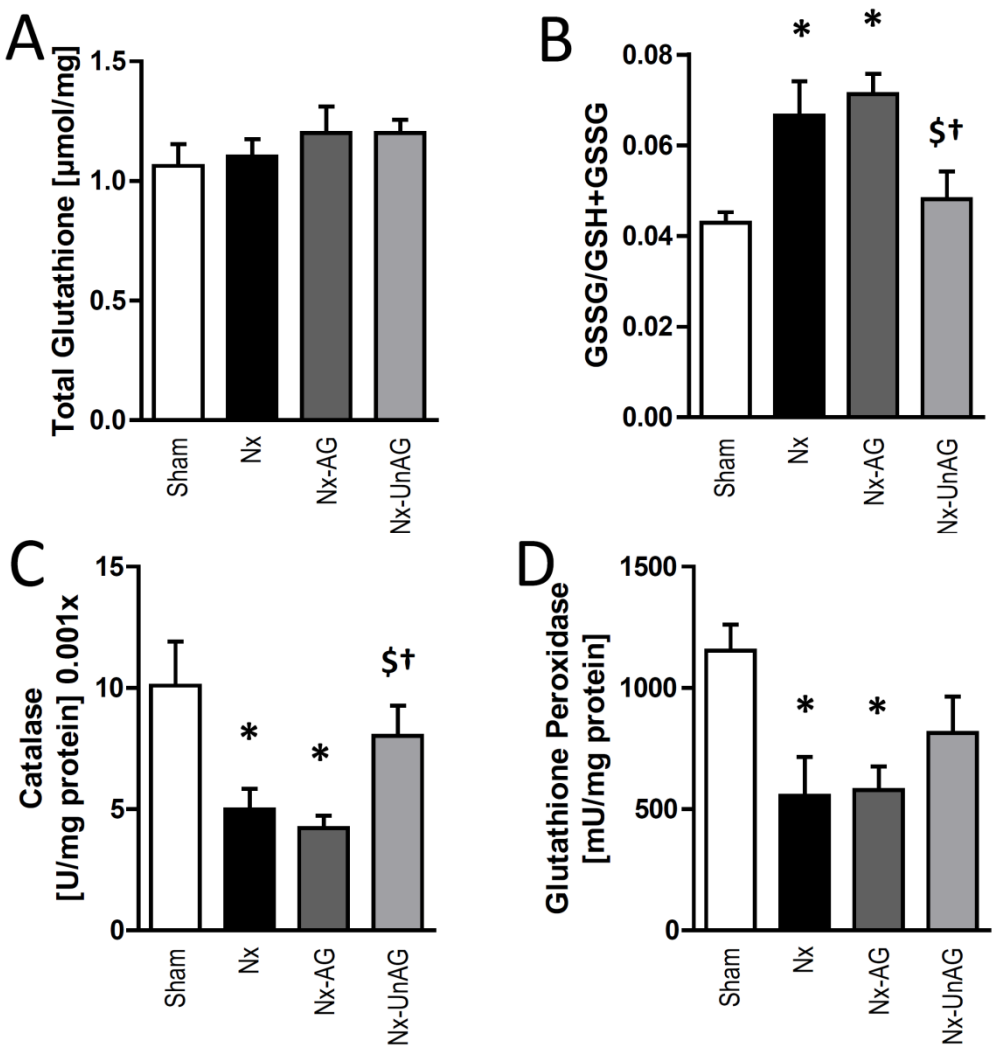

*Figure 25. Ghrelin forms and skeletal muscle redox state in uremic rats. Effects of 4 day acylated (AG) and unacylated (UnAG) ghrelin treatment (200µg subcutaneous injection twice per day) in 5/6 nephrectomized rats (Nx) on gastrocnemius muscle total (A) and oxidized (GSSG) over total (B, GSH: reduced) tissue glutathione and on enzyme activities of catalase (C) and glutathione peroxidase (GPx; D). *p<0.05 vs. Sham; $ p<0.05 vs. Nx; †p<0.05 vs. Nx-AG; mean±SEM, n=10/group.*

5.4.3 UnAG but not AG treatment reverses 5/6 nephrectomy-associated tissue pro-inflammatory cytokine pattern.

Compared to sham, 5/6 nephrectomy increased tissue pro-inflammatory cytokines IL-1α, IL-1β and TNFα levels while lowering anti-inflammatory IL-10. Consistently with the previously described UnAG anti-inflammatory effect in healthy rat skeletal muscle, in uremic rats UnAG completely reverted nephrectomy-associated pro-inflammatory cytokine pattern at IL-1α,

TNFα and IL-10 levels. In agreement with previous experiments in cultured myotubes, this effect was not observed in AG-treated animals (Figure 26).

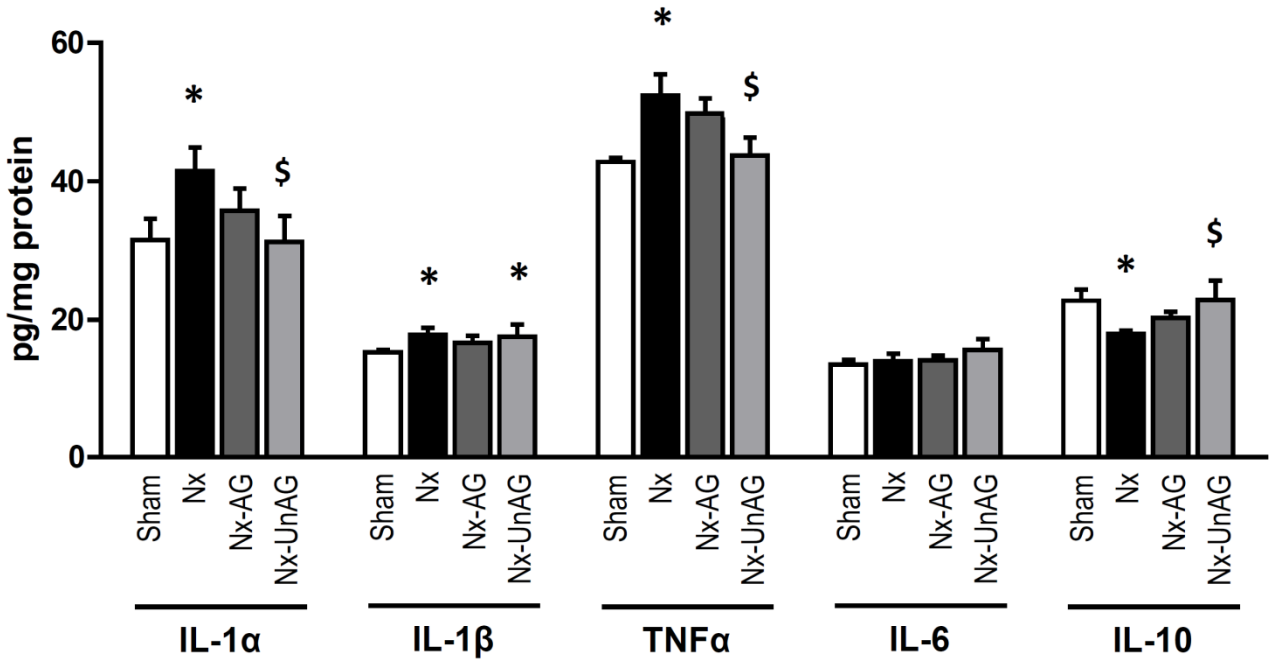

*Figure 26. UnAG and skeletal muscle cytokine expression in uremic rats. Effects of 4 day acylated (AG) and unacylated (UnAG) ghrelin treatment (200μg subcutaneous injection twice per day) in 5/6 nephrectomized rats (Nx) on gastrocnemius muscle expression of IL-1α, IL-1β, TNFα, IL-6 and IL-10 measured by xMAP technology. *p<0.05 vs. Sham; $ p<0.05 vs. Nx; mean±SEM, n=10/group.*

5.4.4 UnAG but not AG treatment recovers muscle insulin signalling and action after 5/6 nephrectomy

In skeletal muscle, 5/6 nephrectomy causes lower activating phosphorylation of insulin signalling mediators at $IR^{Y1162/Y1163}$, AKT^{S473}, GSK-$3\beta^{S9}$, $PRAS40^{T246}$ and $P70S6K^{T421/S424}$ levels (Figure 27). While AG treatment selectively improves activation at AKT level, UnAG more comprehensively enhances insulin signalling with increased phosphorylation of AKT^{S473}, GSK-$3\beta^{S9}$, $PRAS40^{T246}$ and $P70S6K^{T421/S424}$, consistently with results in healthy rats showing UnAG-induced activation of both mTORC complexes. Importantly, UnAG-induced improvement in signalling activation downstream of AKT, includes the protein-anabolic mediator P60S6K and results in a complete normalization to levels observed in

sham animals (Figure 27). Moreover, the decrease in tissue glucose uptake associated with uraemia is also recovered by UnAG (Figure 28).

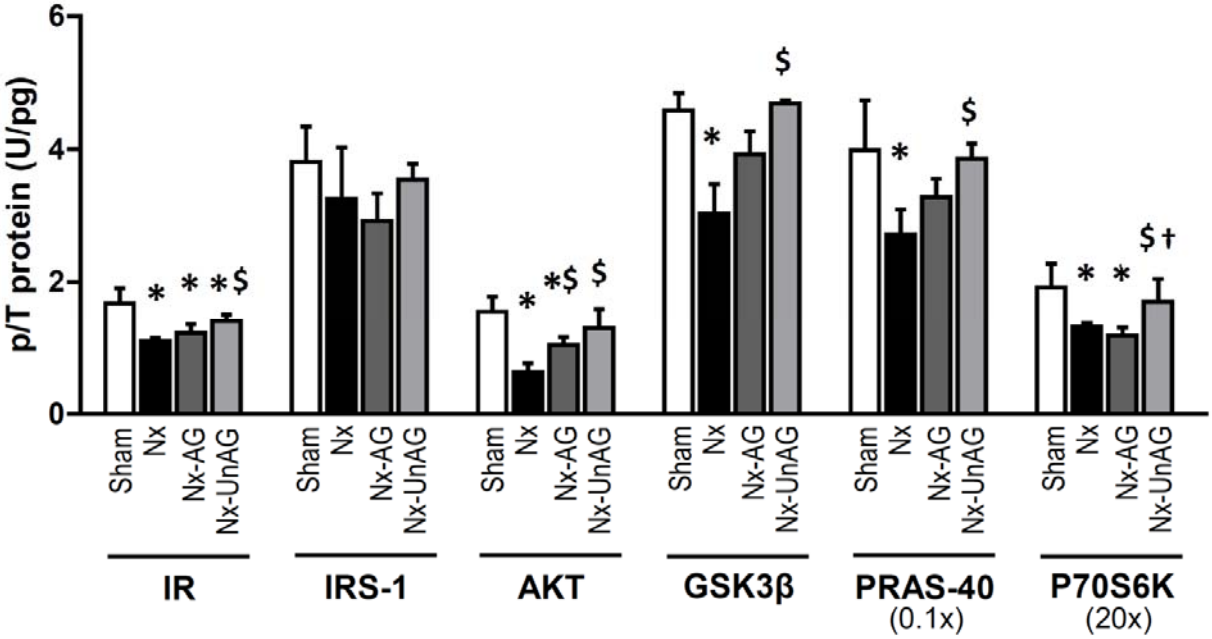

*Figure 27. UnAG and skeletal muscle insulin signalling in uremic rats. Effects of 4 day acylated (AG) and unacylated (UnAG) ghrelin treatment (200µg subcutaneous injection twice per day) in 5/6 nephrectomized rats (Nx) on gastrocnemius muscle relative phosphorylation of insulin receptor ($IR^{Y1162/Y1163}$), IRS-1^{S312}, AKT^{S473}, GSK-$3\beta^{S9}$, $PRAS40^{T246}$, $P70S6K^{T421/S424}$. p/T:phosphoprotein to total protein ratio *p<0.05 vs. Sham; $ p<0.05 vs. Nx; †p<0.05 vs. Nx-AG; mean±SEM, n=10/group.*

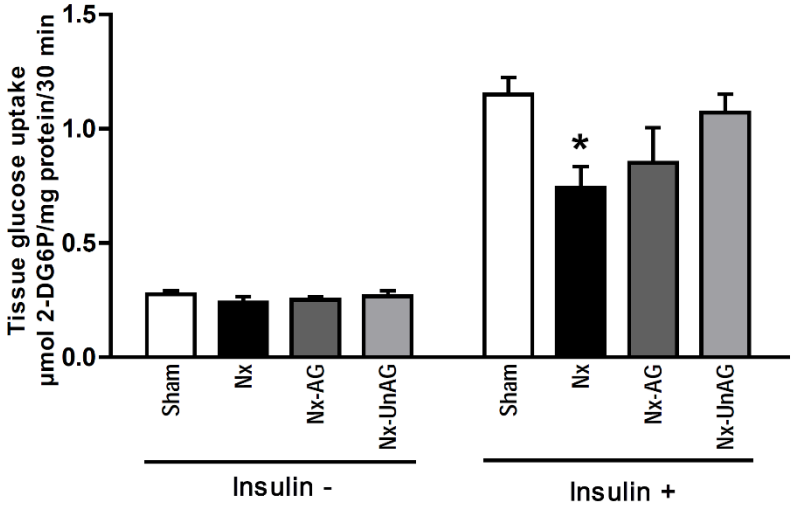

*Figure 28. UnAG and skeletal muscle glucose uptake in uremic rats. Effects of 4 day acylated (AG) and unacylated (UnAG) ghrelin treatment (200µg subcutaneous injection twice per day) in 5/6 nephrectomized rats (Nx) on EDL muscle glucose uptake in the presence or absence of insulin co-incubation. *p<0.05 vs. Sham and Nx-UnAG; mean±SEM, n=10/group.*

5.4.5 UnAG does not share mitochondrial function enhancing effects with AG in skeletal muscle of uremic rats

5/6 nephrectomy is associated with lower ATP synthesis rate in skeletal muscle. In agreement with previous reports [139,273], AG treatment markedly increased skeletal muscle mitochondrial function. This result, as shown in healthy animals, was not shared by UnAG (Figure 29).

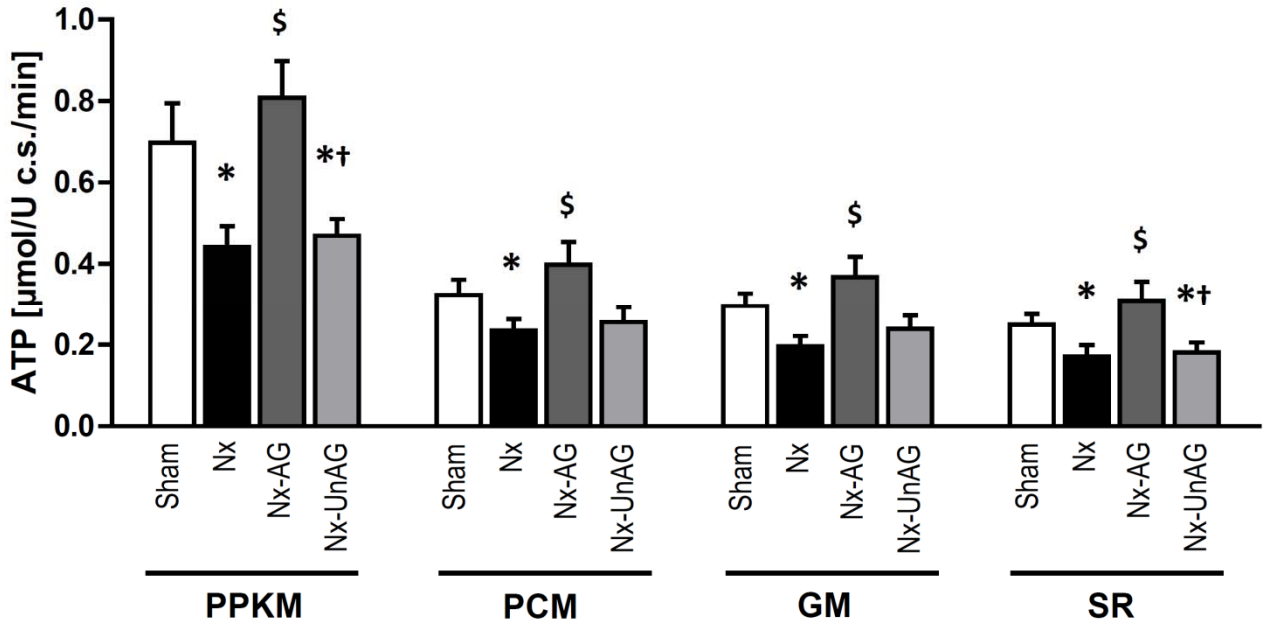

*Figure 29. UnAG and skeletal muscle ATP synthesis rate in uremic rats. Effects of 4 day acylated (AG) and unacylated (UnAG) ghrelin treatment (200µg subcutaneous injection twice per day) in 5/6 nephrectomized rats (Nx) on ATP synthesis rate with different respiratory substrates (A, PPKM: Pyruvate+Palmitoyl-L-Carnintine+α-Ketoglutarate+Malate; PCM: Palmitoyl-L-Carnintine+Malate; GM: Glutamate+Malate; SR: Succinate+Rotenone) in isolated mitochondria from rat gastrocnemius muscle. *p<0.05 vs. Sham; $ p<0.05 vs. Nx; †p<0.05 vs. Nx-AG; mean±SEM, n=10/group.*

5.5 Role of autophagy in UnAG-induced reduction of mitochondrial ROS generation

5.5.1 UnAG lowers mitochondrial ROS generation in association with increased removal of damaged mitochondria in cardiomyocytes vitro

In a study to identify novel biotherapeutics without a priori knowledge of their biological function, it was shown through a novel in vivo functional screening of secretome cDNA libraries, using adeno-associated virus (AAV) vectors (FunSel), that ghrelin peptide overexpression protects skeletal and heart muscle from ischemic damage [297]. In the context of that project, we showed that in neonatal rat ventricular myocytes this protective activity involves reduced mitochondrial ROS generation (Fig 30). Further experiments also showed that this result was associated with increased removal of damaged mitochondria by autophagy [297]. AG shared the effects on autophagy induction only in part and to a lesser extent, while it did not modify mitochondrial ROS generation (Figure 30).

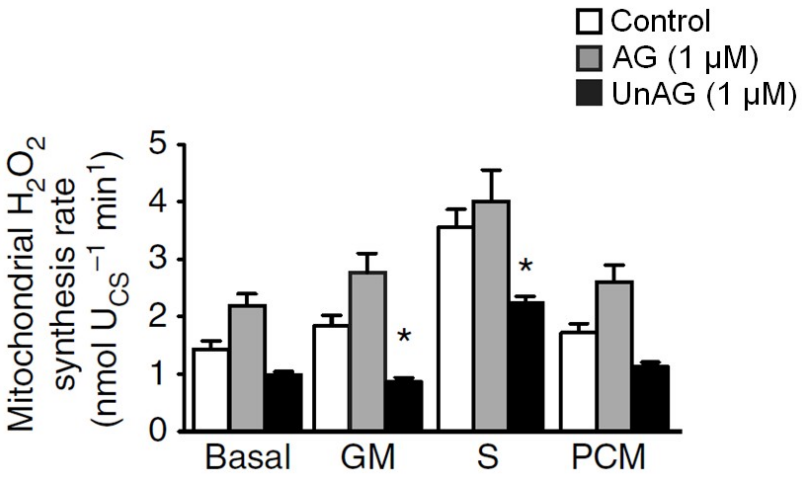

*Figure 30. Ghrelin modulation of mitochondrial ROS generation in neonatal ventricular cardiomyocytes. Reactive oxygen species (ROS) production in intact mitochondria isolated from neonatal rat cardiomyocytes after 48 h of starvation in the absence or presence of AG or UnAG for 48h (C, n=4). GM, glutamate/malate; S, succinate; PCM, palmitoyl-L-carnitine+malate). *p<0.05 vs. Control, †p<0.05 vs. AG.*

5.5.2 UnAG effects on ROS generation and insulin signalling are abolished by autophagy mediator ATG5 silencing in cultured myotubes

To further evaluate the potential role of autophagy in UnAG-induced effects, in additional experiments siRNA-mediated genomic silencing of the autophagy mediator ATG5 was induced before exposure of C2C12 myotubes to UnAG, and both UnAG-induced lower mitochondrial ROS production and enhanced insulin signalling were abolished by ATG5 silencing (Figure 31-32).

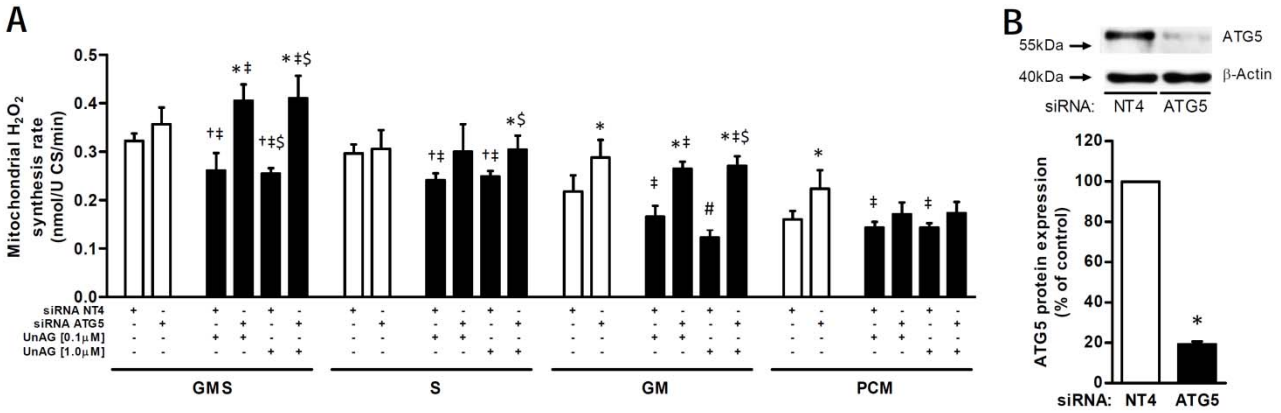

*Figure 31. Role of autophagy in UnAG effects on mitochondrial ROS generation. Effects of autophagy mediator ATG5 genomic silencing vs. non targeting NT4 siRNA transfection on C2C12 myotubes after 48 h incubation with increasing concentrations of acylated (AG) or unacylated ghrelin (UnAG) vs. control (Ct) on isolated mitochondria H2O2 synthesis rate with different respiratory substrates (A, GMS: Glutamate+Succinate+Malate; S: Succinate; GM: Glutamate+Malate; PCM: Palmitoyl-L-Carnintine+Malate) and cell protein expression of ATG5 after transfection with the two siRNA (B). U CS: units of citrate synthase. *p<0.05 vs. NT4, same UnAG concentration; †p<0.05 vs. same siRNA, no UnAG; ‡p<0.05 vs. other siRNA, no UnAG; § p<0.05 vs. same siRNA, UnAG 0.1µM; § p<0.05 vs. other siRNA, UnAG 0.1µM; #p<0.05 vs. all other groups; mean±SEM; n=3/group.*

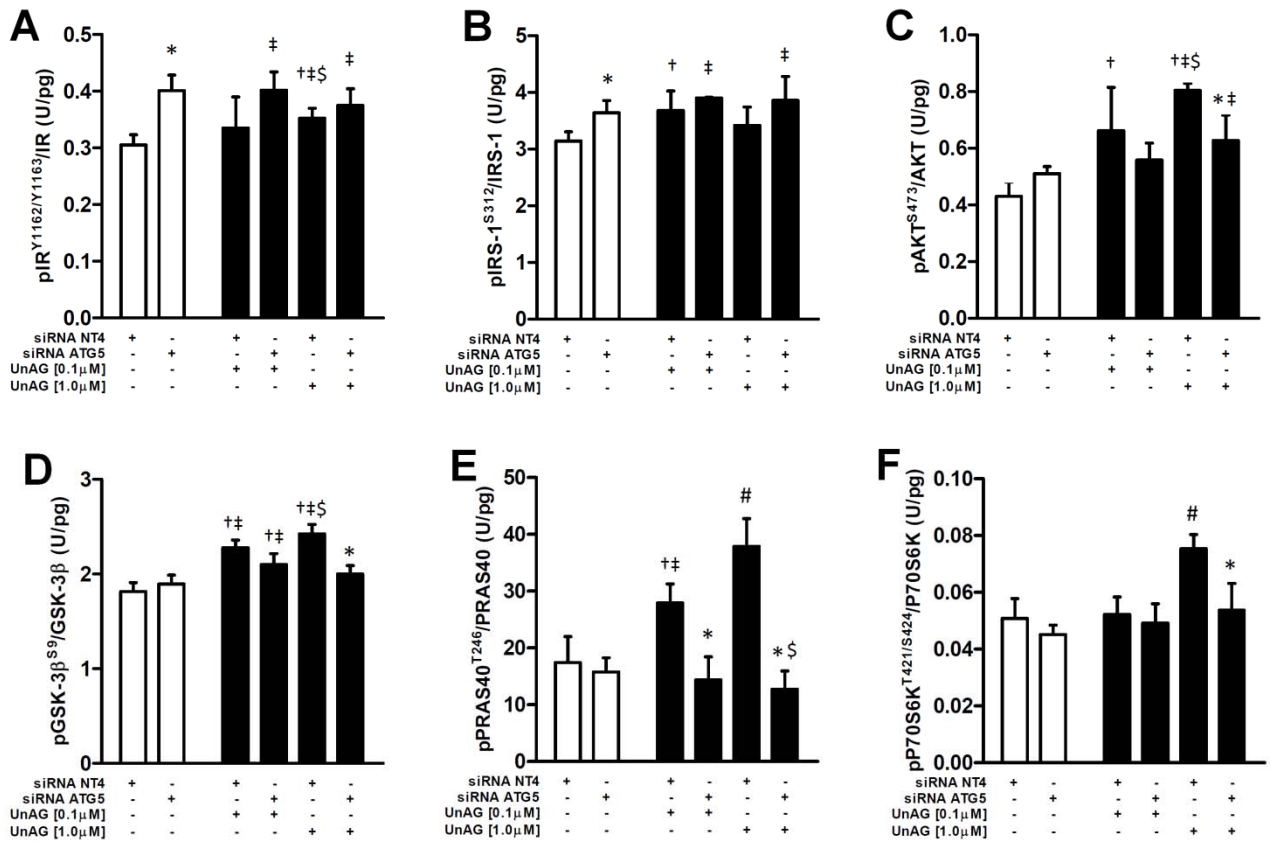

*Figure 32. Role of autophagy in UnAG effects on insulin signalling. Effects of autophagy mediator ATG5 genomic silencing vs. non targeting NT4 siRNA transfection on C2C12 myotubes after 48 h incubation with increasing concentrations of acylated (AG) or unacylated ghrelin (UnAG) vs. control (Ct) on the phosphorylation of insulin receptor (IR)$^{Y1162/Y1163}$ (A), IRS-1^{S312} (B), AKT^{S473} (C), GSK-3β^{S9} (D), PRAS40^{T246} (E), P70S6K$^{T421/S424}$ (F) measured by xMAP technology. *p<0.05 vs. NT4, same UnAG concentration; †p<0.05 vs. same siRNA, no UnAG; ‡p<0.05 vs. other siRNA, no UnAG; § p<0.05 vs. same siRNA, UnAG 0.1μM; § p<0.05 vs. other siRNA, UnAG 0.1μM; #p<0.05 vs. all other groups; mean±SEM; n=3/group.*

5.5.3 Overexpression of UnAG increases skeletal muscle autophagy activation in obese mice in vivo

Consistent with in vitro experiments HFD-obese Tg Myh6/Ghrl also had higher skeletal muscle levels of the autophagy activation marker LC3II/LC3I compared to wild-type mice (Figure 33).

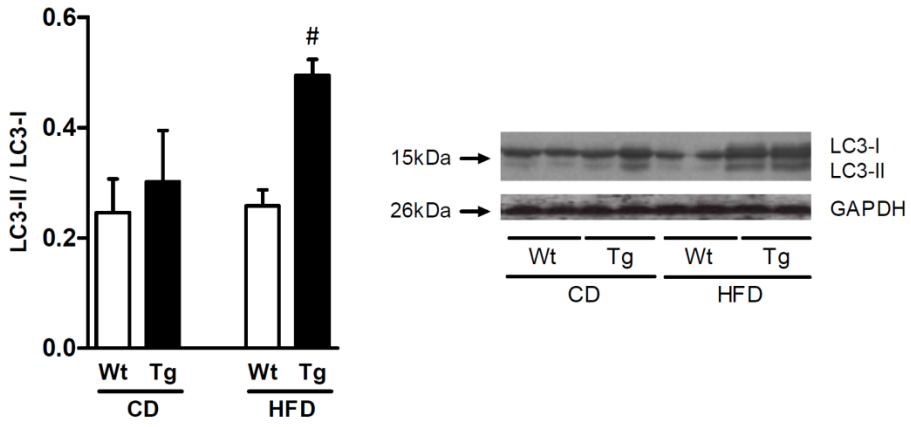

Figure 33. Effects of UnAG overexpression on gastrocnemius muscle autophagy activation in lean and obese mice. Autophagy activation marker LC3II/LC3I as measured by western blot in the gastrocnemius muscle of mice with UnAG up-regulation (Tg Myh6/Ghrl) vs. wild type (wt) fed 16 wks with Control- (CD) or High Fat-Diet (HFD) (n=7/group) with representative blot. #p<0.05 vs. all other groups; mean±SEM.

5.5.4 Autophagy inhibition by genomic silencing results in complete prevention of UnAG-mediated decrease in ROS generation in myotubes treated with uremic plasma

Treatment of cultured C2C12 myotubes with plasma from uremic patients, an established in vitro model of uraemia, causes increased mitochondrial ROS generation compared to control. Incubation with UnAG resulted in reduced ROS production both in control- and uremic-plasma treated cells. Importantly, siRNA-mediated genomic silencing of the autophagy inducer ATG5 completely prevents UnAG-induced decrease of mitochondrial ROS generation, strongly supporting that UnAG effects in uremic models may be at least in part dependent on increased autophagy activation (Figure 34).

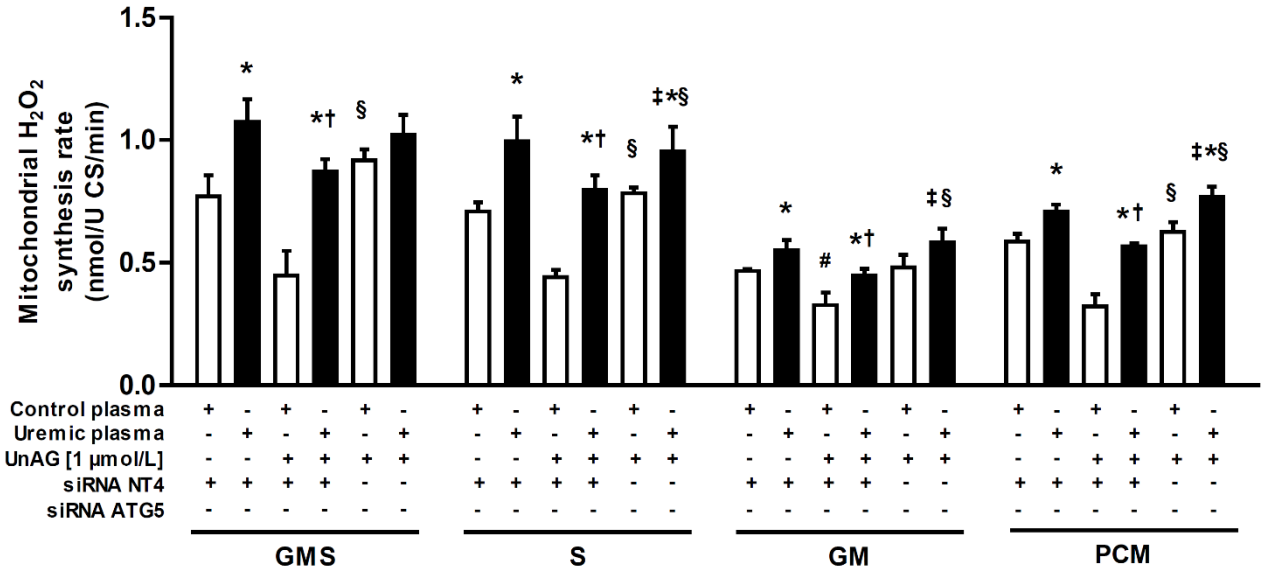

*Figure 34. Role of autophagy in UnAG effects on mitochondrial ROS generation. Effects on isolated mitochondria H_2O_2 synthesis rate with different respiratory substrates (GMS: Glutamate+Succinate+Malate; S: Succinate; GM: Glutamate+Malate; PCM: Palmitoyl-L-Carnintine+Malate)of UnAG and of autophagy mediator ATG5 genomic silencing vs. non targeting NT4 siRNA transfection after 48 h incubation with 10% (vol/vol) plasma from uremic or control subjects. U CS: units of citrate synthase. *p<0.05 vs. control plasma with same UnAG and siRNA, †p<0.05 vs. no UnAG, same plasma; ‡p<0.05 vs. UnAG, siRNA NT4, same plasma; § p<0.05 vs. no UnAG, other plasma; #p<0.05 vs. all other groups; mean±SEM; n=3/group.*

5.6 Ghrelin acylation and circulating free fatty acids level

5.6.1 Associations between plasma ghrelin forms and anthropometric and metabolic profile

Table 10 reports anthropometric and metabolic characteristics of the study population. Plasma TG levels were negatively associated with male gender, age, BMI, waist circumference, plasma triglycerides, glucose and insulin, HOMA index and arterial pressure. Prevalence of diabetes, hypertension and dyslipidaemia were also negatively associated with TG, while a positive association was observed between TG and plasma HDL-cholesterol. Weaker negative associations were also observed between AG and male gender, BMI, waist circumference and HOMA index. In contrast, AG/TG ratio was positively associated with age, BMI, waist circumference, plasma triglycerides, HOMA index, arterial pressure and presence of hypertension and dyslipidaemia.

Table 10. Study population. Gender, age (years), body mass index (BMI), waist circumference (WC), plasma triglycerides, total and HDL-cholesterol (Chol), free fatty acids (FFA), glucose and insulin levels, homeostasis model assessment of insulin resistance (HOMA), systolic (SBP) and diastolic (DBP) blood pressure, total (TG), acylated (AG) plasma ghrelin levels and AG/TG ratio; percent prevalence of diabetes mellitus, hypertension, hyperlipidaemia with percent pharmacological treatment (Tx) in the whole study cohort (n=850). Data are presented as Mean±SD (Range).

Gender	408/442
Age (years)	54±10 (18-73)
BMI (kg/m^2)	28.6±5.4 (17.8-51.1)
WC (cm)	98±13 (64-148)
Triglycerides (mmol/l)	1.64±0.98 (0.34-7.09)
Total-Chol (mmol/l)	5.56±1.08 (2.25-9.44)
HDL-Chol (mmol/l)	1.39±0.38 (0.55-3.11)
FFA (µmol/l)	0.41±0.21 (0.07-2.01)
Glucose (mmol/l)	5.6±1.1 (3.7-15.3)
Insulin (pmol/l)	83.3±59.2 (13.9-553.5)
HOMA	3.2±3.3 (0.4-26.2)
SBP (mmHg)	138±19 (95-215)
DBP (mmHg)	82±10 (53-121)
TG (pg/ml)	794±396 (67-3473)
AG (pg/ml)	75±68 (6-537)
AG/TG	0.11±0.98 (0.01-0.87)
Prevalence (%)	
Diabetes (Tx)	11.1 (7.3)
Hypertension (Tx)	67.5 (36.6)
Hyperlipidemia (Tx)	35.1 (10.2)

5.6.2 Associations between plasma free fatty acids (FFA), anthropometric and metabolic parameters and plasma ghrelin profile

Plasma FFA were positively associated with age, BMI, waist circumference, plasma triglycerides and total cholesterol, plasma glucose, insulin and HOMA index, arterial pressure and presence of diabetes, hypertension and dyslipidaemia (Table 11). Plasma FFA

were also associated negatively with TG (Figure 35A). In contrast, negative associations were observed between plasma FFA and both AG and AG/TG (Figure 35B-C).

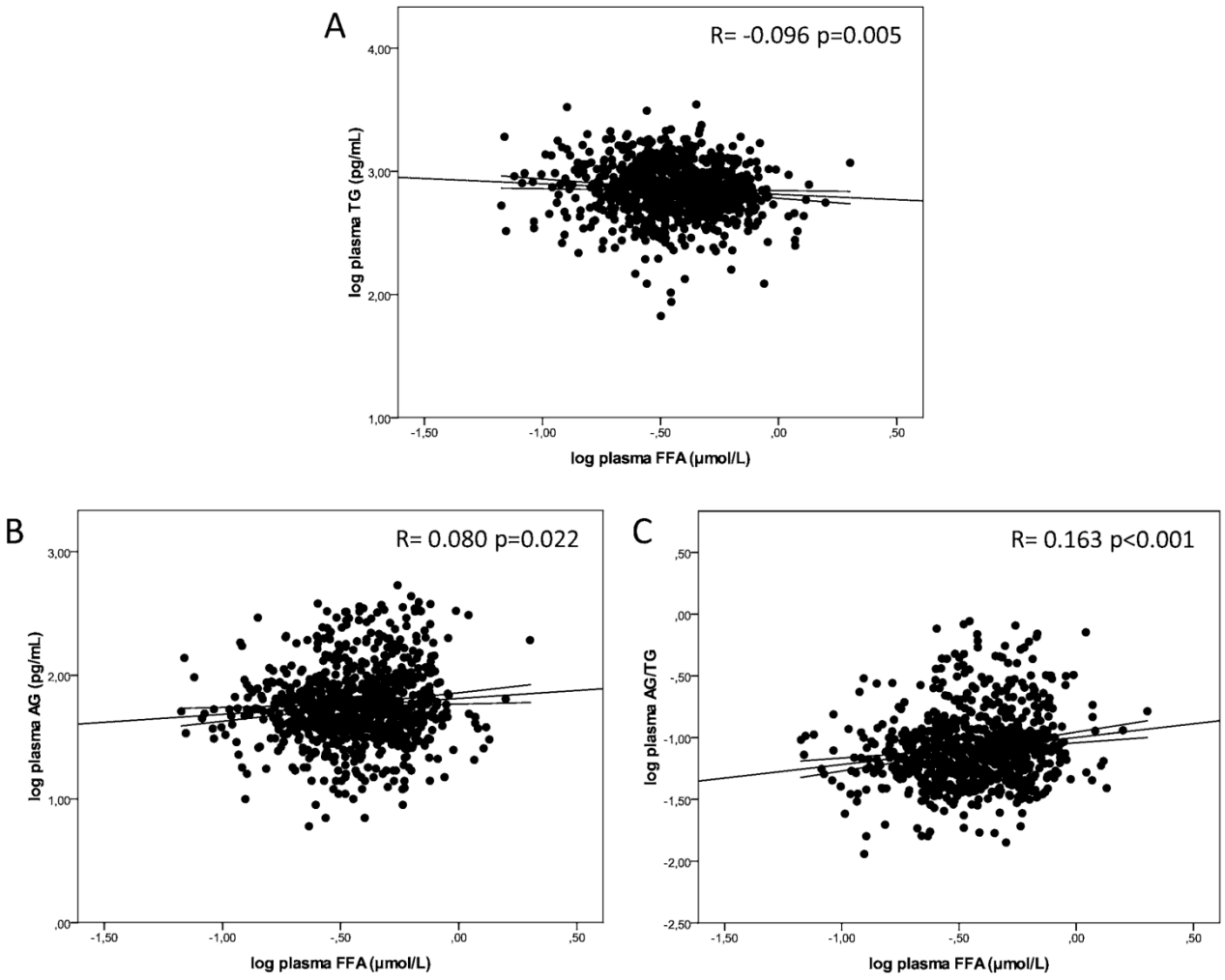

Figure 35. Associations between plasma free fatty acids and total (TG, A), acylated (AG, B), acylated-to-total (AG/TG, C) ghrelin in all study participants (n=850). Graph presents data with linear regression line and confidence interval for mean response.

To determine whether associations between plasma FFA and ghrelin forms were independent from confounding parameters, multiple regression analyses were performed with TG, AG or AG/TG as dependent variables.

Table 11: Correlation analysis between plasma total ghrelin (TG), acylated ghrelin (AG), acylated-to-total ghrelin ratio (AG/TG), plasma free fatty acids (FFA) and gender (M=male), age, body mass index (BMI), waist circumference (WC), plasma triglycerides, total and HDL-cholesterol (Chol), glucose, insulin, HOMA index, systolic (SBP) and diastolic blood pressure (DBP), diagnosis of diabetes, diagnosis of hypertension, diagnosis of dyslipidaemia.

	TG		**AG**		**AG/TG**		**FFA**	
	R	p	R	p	R	p	R	p
Gender (M)	-0.239	<0.001	-0.142	<0.001	0.037	0.286	-0.009	0.788
Age	-0.058	0.090	0.027	0.440	0.076	0.029	0.177	<0.001
BMI	-0.366	<0.001	-0.154	<0.001	0.121	<0.001	0.211	<0.001
WC	-0.343	<0.001	-0.139	0.002	0.109	0.002	0.186	<0.001
Triglycerides	-0.271	<0.001	-0.044	0.210	0.176	<0.001	0.313	<0.001
Total-Chol	0.020	0.567	0.060	0.082	0.063	0.070	0.075	0.028
HDL-Chol	0.295	<0.001	0.082	0.018	-0.144	<0.001	-0.115	0.001
Glucose	-0.183	<0.001	-0.053	0.130	0.090	0.010	0.279	<0.001
Insulin	-0.347	<0.001	-0.103	0.003	0.138	<0.001	0.241	<0.001
HOMA	-0.357	<0.001	-0.107	0.002	0.142	<0.001	0.284	<0.001
SBP	-0.186	<0.001	-0.054	0.122	0.097	0.005	0.199	<0.001
DBP	-0.202	<0.001	-0.035	0.316	0.119	0.001	0.161	<0.001
Diabetes	-0.141	<0.001	-0.071	0.042	0.021	0.542	0.164	<0.001
Hypertension	-0.231	<0.001	-0.063	0.069	0.129	<0.001	0.226	<0.001
Dyslipidemia	-0.202	<0.001	0.016	0.650	0.178	<0.001	0.288	<0.001

Table 12. Multiple regression analyses between plasma free fatty acids (FFA) and total (TG), acylated (AG) ghrelin or acylated-to-total ghrelin ratio (AG/TG) in the whole study cohort (n=850) with different adjustment models. Superimposable results were obtained when including waist circumference in model 1 instead of BMI.

		TG				AG				AG/TG			
	Model	B (95%C.I.)	F	R^2	p	B (95%C.I.)	F	R^2	p	B (95%C.I.)	F	R^2	p
FFA	1	-114.8 (-247.1-17.5)	34.5	0.138	0.089	42.5 (18.2-66.9)	5.29	0.025	0.001	0.062 (0.024-0.100)	4.79	0.018	0.002
	2	-82.3 (-216.1-51.4)	29.4	0.145	0.227	45.4 (20.7-70.1)	4.58	0.027	<0.001	0.060 (0.021-0.099)	3.88	0.017	0.002
	3	-1.3 (-143.6-141.0)	20.3	0.156	0.986	44.1 (17.5-70.7)	3.06	0.029	0.001	0.050 (0.009-0.092)	3.03	0.020	0.018
	4	8.4 (-134.0-150.8)	15.4	0.160	0.908	45.6 (19.0-72.3)	2.71	0.036	0.001	0.052 (0.010-0.094)	2.66	0.022	0.015

Data adjustments:
Model 1: gender, age, BMI
Model 2: Model 1 + HOMA-IR
Model 3: Model 2 + Triglycerides, HDL cholesterol, Mean Arterial Pressure
Model 4: Model 3 + Diabetes, Hypertension, Dyslipidemia

Associations between plasma FFA and AG or AG/TG remained statistically significant after multiple adjustments in different statistical models including gender, age, BMI or waist circumference, HOMA index, plasma triglycerides and HDL-cholesterol, arterial pressure and presence of diabetes, hypertension and dyslipidaemia (Table 12). Consistent with these observations, circulating AG and AG/TG increased with increasing quartiles of plasma FFA adjusted for the above potential confounders (Figure 36). In contrast, associations between plasma FFA and TG did not remain statistically significant after adjusting for gender, age and BMI or in any further adjustment models (Table 12).

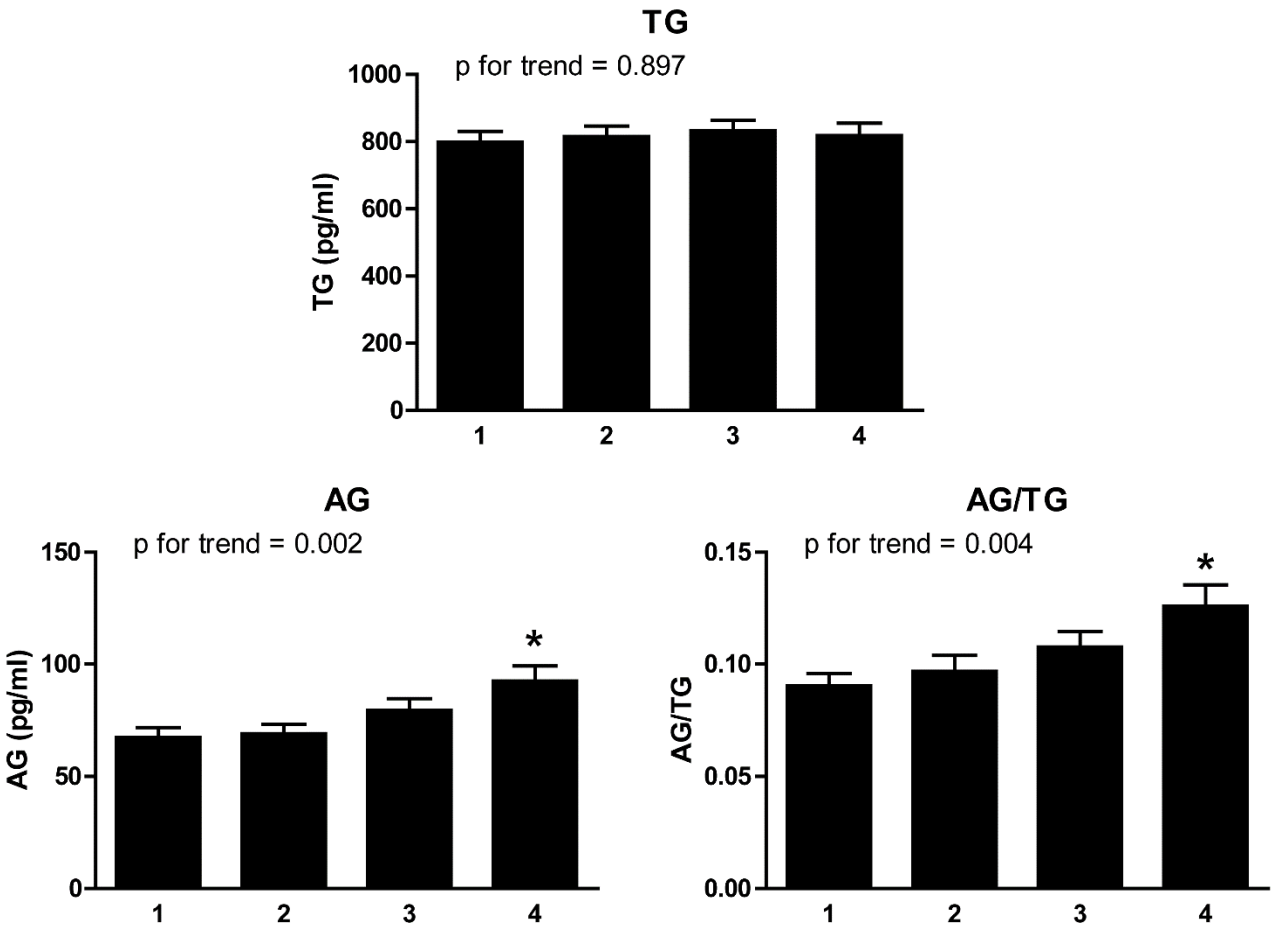

*Figure 36. Changes in plasma total (TG, A), acylated (AG, B) and acylated-to-total (AG/TG, C) ghrelin in plasma free fatty acid quartiles (FFA) adjusted for sex, age, BMI, HOMA, plasma triglycerides, mean arterial pressure, presence of diabetes, hypertension and dyslipidaemia. *p<0.05 vs quartiles 1 and 2.*

5.6.3 Effects of acute long chain fatty acids (LCFA) elevation on plasma TG, AG and AG/TG in rat

To further determine the potential causal role of enhanced plasma FFA availability to enhance plasma AG concentration, we measured plasma ghrelin profile following 150-minute intravenous lipid infusion in rats. Since circulating FFA are predominantly long-chain [299], we infused LCFA-based lipid emulsions with or without n-3 PUFA enrichment. Plasma FFA comparably increased to high-physiological concentrations following infusions of both lipid emulsions (Figure 37A). Under both conditions, plasma TG did not change but both plasma AG and AG/TG were acutely and comparably increased (Figure 37B-D).

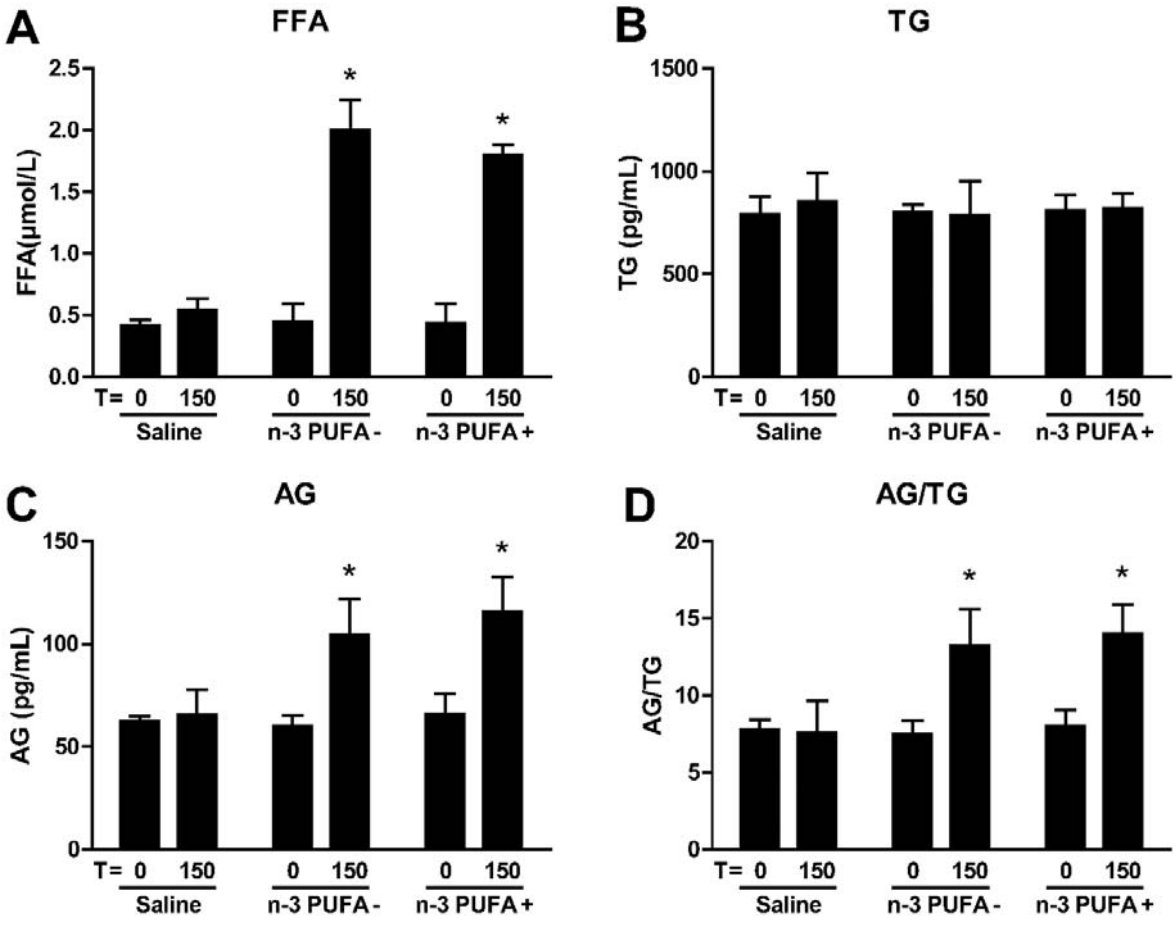

*Figure 37. Changes in plasma free fatty acids (FFA, A), total (TG,B), acylated (AG, C) and acylated-to-total (AG/TG, D) ghrelin after 150-minute infusions of long-chain fatty acid (LCFA)-based lipid emulsions with saturated and either mono- and n-6 polyunsaturated (n3-PUFA-) or n-3 polyunsaturated fatty acids (n3-PUFA+). *p<0.05 T150 vs. T0; n=8-10 rats/group.*

6 Discussion

6.1 UnAG and insulin resistance development in humans

The current study in a North-East Italy community-based population cohort demonstrated that circulating ghrelin forms AG and UnAG are differentially associated with insulin resistance as measured by the validated index HOMA index. In particular: 1) TG and calculated UnAG are negatively and independently associated with HOMA index in cross-sectional analyses; 2) TG and calculated UnAG also negatively predict 5-year HOMA index, and their changes are associated with changes in HOMA; 3) AG is not associated with HOMA index under any condition.

These findings identify TG and calculated UnAG as novel negative biomarkers of insulin resistance in both cross-sectional and prospective observations. Combined, independent cross-sectional and prospective associations further strongly support direct and potentially causal interactions between low TG, low calculated UnAG and insulin resistance. Interactions between these variables are indeed consistent with previous clinical and experimental reports that demonstrated favourable effects of UnAG on glucose metabolism [300]. In particular, UnAG prevented plasma glucose elevation induced by acute intravenous AG administration in GH-deficient humans [301] as well as glucogenic effects of AG in cultured hepatocytes [111]; in addition, UnAG was reported to directly enhance insulin signalling in rodent skeletal muscle in vivo [128]. The above observations collectively support insulin-sensitizing effects of the unacylated ghrelin form, which could mediate its role in predicting improved insulin sensitivity in the current study. Conversely, available knowledge is in excellent agreement with a less positive metabolic impact of AG at whole-body level, possibly resulting from differential tissue-specific effects in skeletal muscle, liver and adipose tissue [108,112,300]. Taken together, the current findings strengthen the rationale for therapeutic interventions aimed at inhibiting ghrelin acylation and preserving non-acylated plasma

ghrelin concentrations to reduce insulin resistance in vivo. To this regard, the acylating enzyme ghrelin O-acyl transferase (GOAT) [57] is an obvious potential therapeutic target, along with alternative strategies that could aim at enhancing ghrelin de-acylation at whole-body or target tissue levels. Although anthropometric parameters such as BMI and waist circumference remain the strongest and most clinically valuable predictors of insulin resistance, the current study also introduces a potential role for TG and calculated UnAG in the identification of individuals with higher risk of insulin resistance development in the general population.

The associations between TG, calculated UnAG, HOMA and their changes were independent of BMI as well as other potential confounders. However, the current data also demonstrated that TG and calculated UnAG are negatively associated with increasing BMI. At variance with AG, these associations were independent of gender and other relevant confounding variables. Associations between lower TG and increased BMI are in agreement with previous reports in humans and experimental models [55,153,300], and independent negative associations between BMI and UnAG are consistent with results from limited, smaller studies in metabolic syndrome patients [56]. Declining UnAG therefore appears to be the most relevant contributor to the BMI-associated decrease in total circulating hormone. The current findings also suggest that declining TG and its unacylated fraction could contribute to obesity-associated insulin resistance. It should also be pointed out that hyperinsulinaemia has been reported to acutely reduce total plasma ghrelin concentration in healthy humans [302], and to specifically suppress circulating non-acylated hormone [303]. Moderate hyperinsulinaemia could therefore inhibit ghrelin production and secretion, and in obese insulin resistant individuals a vicious cycle could therefore contribute to further worsen insulin resistance through progressive reduction of TG and UnAG.

In conclusion, circulating ghrelin forms are differentially associated with the validated insulin resistance marker HOMA in a North-East Italy community-based population cohort. In cross-sectional and prospective observations both TG and calculated UnAG hormone are negatively associated with insulin resistance, independently of gender, BMI and metabolic and pharmacological confounders. Conversely, no associations were observed between metabolic parameters and plasma AG. The current results strongly support a role of unacylated ghrelin in insulin resistance modulation in vivo. When available, plasma total and calculated unacylated ghrelin could also represent novel in vivo biomarkers of insulin resistance and of its longitudinal changes.

6.2 UnAG and skeletal muscle metabolism: mechanisms and impact on experimental models of disease

These studies showed that 1) sustained UnAG administration in vivo leads to a) reduced ROS generation and improved tissue redox state at muscle level; b) lower inflammation changes with reduced tissue NF-κB activation and a shift towards anti-inflammatory cytokine pattern; c) enhanced insulin signalling at AKT level and downstream, with increased insulin-stimulated muscle glucose uptake. 2) Muscle effects of UnAG are similarly observed in a) a model of HFD-induced obesity with systemic circulating UnAG up-regulation, resulting in prevention of obesity-associated hyperglycaemia and whole-body insulin resistance; b) a model of CKD-associated wasting, with UnAG sustained treatment resulting in muscle mass recovery. 3) UnAG effects are confirmed in myotubes with a dose dependent association in vitro, and are different from AG effects, thereby indicating that UnAG acts through mechanisms at least partly direct and independent of AG-related pathways. Finally, UnAG effects are prevented by autophagy inhibition in vitro, strongly supporting a mechanistic involvement of autophagy in UnAG activities.

The current results show that UnAG is a negative regulator of skeletal muscle ROS production and inflammation, and these effects are indirectly supported by previous in vitro observations in non-muscle cells [128,304,305]. While in recent studies in models of peripheral artery disease UnAG reduced endothelial oxidative stress by restoring SOD expression [131,304], in the current model skeletal muscle SOD expression and antioxidant enzyme activities were unchanged by UnAG. Therefore, these findings point toward lower mitochondrial ROS generation rather than enhanced antioxidant defences as a key mediator of UnAG-induced muscle antioxidant activity. Moreover, we identified UnAG as a potent inducer of autophagy in cardiomyocytes, and increased autophagy-mediated removal of dysfunctional mitochondria could have contributed to lower tissue redox state in the current experimental setting. Notably, this hypothesis was confirmed by siRNA-mediated autophagy inhibition experiments in myotubes. Among less quantitatively relevant ROS sources [306], UnAG selectively inhibited NOS-dependent superoxide production. This finding is intriguingly consistent with emerging co-localization and functional interactions between muscle mitochondria, nitric oxide synthase (NOS) and nitric oxide (NO) [307,308]. In particular, NO production may reportedly enhance mitochondrial ROS production [307] while in various settings UnAG was reported to reduce NO release induced by pro-inflammatory cytokines [104]. Taken together, these data strongly suggest that future studies should directly investigate the potential interactions between UnAG, NO and mitochondrial ROS generation.

Sustained UnAG administration enhanced skeletal muscle insulin signalling at AKT level and downstream, i.e. at mTORC complexes while not at IR-IRS-1 level, and these effects were paralleled by increased insulin-stimulated muscle glucose uptake. Importantly, these changes provide a molecular basis for the above reported the association of UnAG with preserved whole-body insulin sensitivity in humans, as well as being in agreement with

previously available data [56]. Interestingly, in vitro inhibition of autophagy abolished UnAG activities on both mitochondrial ROS production and insulin signalling, providing further strong support for a causal negative impact of mitochondrial ROS generation on AKT-dependent insulin signalling, in agreement with previous reports [132,134,135,201,252]. Intriguingly, UnAG effects were associated with increased inhibitory IRS-1^{S312} phosphorylation. Although this observation is seemingly paradoxical, it is consistent with recent reports indicating pIRS-1^{S312} as a physiological negative feedback modulation mediator after downstream signalling activation [175].

Effects of exogenous UnAG administration were also confirmed in Tg Myh6/Ghrl mice with chronic systemic UnAG over-exposure [128], and these results are in agreement with reported higher insulin sensitivity in a lean UnAG adipose transgenic model [127]. These findings also further confirm that UnAG effects are independent of changes in AG and its potential impact on GH-IGF1 through GHSR1a [128,309], as plasma AG and IGF-1 are unchanged in Tg Myh6/Ghrl [128]. Most importantly, circulating UnAG upregulation overall preserved muscle oxidative stress markers, inflammation and impaired insulin signalling at levels comparable with lean Tg Myh6/Ghrl or wild-type animals, in association with prevented HFD-induced hyperglycaemia and systemic insulin resistance. LC3II/LC3I ratio analysis also confirmed UnAG-dependent stimulation of muscle autophagy in vivo in HFD-obese Tg Myh6/Ghrl, suggesting a potential direct contribution of autophagy to the beneficial effects of UnAG overexpression [310]. Interestingly, pIRS-1^{S312} was not increased in obese Tg Myh6/Ghrl animals compared to wild-type counterparts, and this observation was paralleled with lack of insulin signalling activation at P70S6K levels. Combined, these observations are consistent with the hypothesis that IRS-1^{S312} phosphorylation is at least partly mediated by this feedback loop [175]. Potential mechanisms underlying differential regulation of PRAS40^{T246} and P70S6K$^{T421/S424}$ phosphorylation in obese vs. lean models in UnAG

exposure conditions should be investigated in future studies. Globally considered, results in the HFD-obesity model importantly demonstrate that the effects of UnAG observed in lean rats translate into beneficial metabolic changes in a clinically relevant model of diet-induced insulin resistance and hyperglycaemia, thereby providing a strong rationale for therapeutic strategies to increase UnAG availability in obese, insulin resistant and type 2 diabetic conditions.

The UnAG effects observed in the skeletal muscle of lean rats and HFD-obese mice were also consistently reproduced in a model of CKD-induced insulin resistance and muscle wasting [242,256]. Results from experiments in 5/6 nephrectomized rats largely confirmed UnAG related effects on tissue ROS generation, redox state, inflammation, insulin signalling stimulation and glucose uptake, with normalization of respective measurements compared to sham. Importantly, these effects were associated in vivo with a complete recovery in muscle mass loss by UnAG sustained treatment. Moreover, gene silencing experiments in an in vitro model of uraemia showed that autophagy inhibition completely abolished UnAG beneficial impact on mitochondrial ROS generation, suggesting that autophagy-mediated dysfunctional mitochondria removal may play a key role also in this setting.

At variance with results from experiments in healthy rats, in the CKD model UnAG was selectively associated with improved activity of the antioxidant enzyme catalase. This finding suggests that UnAG, while independently lowering ROS generation, in conditions of markedly increased ROS generation may also trigger the activation of this anti-oxidant enzyme. Intriguingly, catalase expression is known to be an important modulator of mitochondrial antioxidant systems and is increased by proliferator-activated receptor-coactivator-1 (PGC1 -α), a major positive regulator of mitochondrial biogenesis [311,312]. This finding, while further supporting a key role for mitochondria in UnAG modulation of CKD-

associated muscle metabolic derangements, also points out the need for further studies on the involved underlying mechanisms.

Parallel experiments with an equimolar non-orexigenic AG dose showed that the effects of ghrelin forms are largely differential also in CKD-induced wasting. In fact, AG did not modify oxidative stress and specific sources of ROS production, except for a full normalization of xanthine oxidase activity. While AG enhanced insulin signalling at AKT level, consistently with previous reports [139], downstream effects were limited to unacylated hormone. Thus, lack of recovery of skeletal muscle mass by AG was likely due to incomplete normalization of clustered metabolic alterations. Moreover, since AG failed to substantially reduce elevated ROS production, the above observations support a relevant role of redox state in uraemia-associated derangements in muscle metabolism and, ultimately, in the associated loss of muscle mass. Collectively these observations strongly support a potentially relevant positive clinical impact for UnAG treatment of cachectic or malnourished uremic patients.

Myotubes experiments were in excellent agreement with in vivo studies in showing superimposable effects of UnAG on ROS generation and insulin signalling. Importantly, these effects were not induced by equimolar AG concentrations. These observations strongly imply that UnAG directly stimulates insulin signalling in skeletal muscle and they are consistent with previously-reported UnAG anti-atrophic activities in skeletal muscle of both wild type and GHSR1a null mice [128]. Overall, these findings strongly support the hypothesis that UnAG effects in skeletal muscle are independent of GHSR1a and possibly mediated by alternative, yet-unidentified UnAG receptor(s). It should also be pointed out that both ghrelin forms induce C2C12 myoblasts differentiation [71], and that in C2C12 myotubes as well as in vivo in skeletal muscle of GHSR null mice, acute treatment with both AG and UnAG enhances mTORC2-mediated anti-atrophic signalling [112,128]. In the current studies with prolonged hormone incubation, highest AG doses selectively induced a moderate

increase of GSK-3β^{S9} phosphorylation but failed to reduce ROS production and to enhance downstream insulin signalling. Consistently, AG is a weaker autophagy inducer than UnAG and does not stimulate both mitophagy and skeletal muscle regeneration in a model of ischemic damage [131,313]. Based on available reports, differential muscle effects of ghrelin forms may depend on still uninvestigated acylation-selective and time-dependent AG activities. Overall, differential effects of ghrelin forms on muscle insulin signalling are fully consistent with both previous clinical observations and above reported data linking UnAG, but not AG to whole-body insulin sensitivity in humans [56].

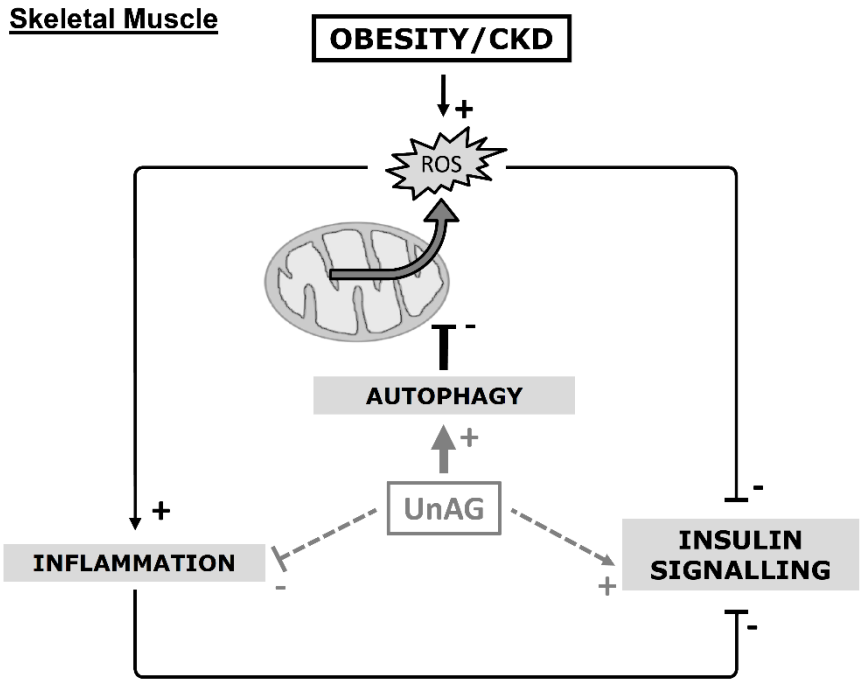

Figure 38: Proposed interactions between UnAG and clustered metabolic alterations in skeletal muscle of high-fat diet-induced obese or 5/6 nephrectomy insulin resistant rodents: higher mitochondrial production of reactive oxygen species (ROS), chronic UnAG over-exposure normalizes higher inflammation and lower insulin signalling activation. Our findings further indicate UnAG to directly lower mitochondrial ROS generation through autophagy stimulation, which may directly lead to lower inflammation and enhanced insulin signalling. Potential parallel UnAG activities to directly lower inflammation and enhance insulin signalling should be further investigated.

Finally, in all experimental models UnAG-induced lower ROS generation, lower inflammation and enhanced insulin signalling were associated with reduced or unchanged ATP synthesis. In agreement with previous studies, high-fat fed animals showed higher mitochondrial ATP

production despite higher tissue redox state and impaired insulin sensitivity, and this alteration could be related to enhanced substrate availability through feed-forward mechanisms [112]. Consistently, in CKD-induced uraemia ATP synthesis was markedly decreased compared to sham. Moreover, in this model ATP synthesis rate was markedly enhanced by AG but not UnAG treatment, confirming on one side differential effects for ghrelin forms, and on the other indicating that energy production does not play a primary role in maintenance of insulin signalling and muscle anabolism in uraemia.

Our results therefore provide further evidence against a role for low mitochondrial function as a primary cause of insulin resistance [314-318], conversely indicating UnAG as a novel modulator of muscle mitochondrial activity with negative impact on both ATP and ROS production in vivo. Unchanged mitochondrial ATP production in vitro however does not support a direct role of UnAG as a mitochondrial function inhibitor, while it further supports the hypothesis that reduced mitochondrial function is not necessary for reduced ROS generation. Interestingly, UnAG modified complex-related ATP generation by favouring complex I over complex II-related synthesis in vitro and in vivo, potentially reflecting preferential glucose over fat-derived substrate oxidation [319]. In turn, this mechanism could also contribute to inhibit ROS production, as glucose-related substrate oxidation may lower mitochondrial ROS generation [320,321]. These observations indicate the need for further studies on the mechanisms underlying the interactions between UnAG and muscle mitochondrial function.

In conclusion, these studies demonstrated that UnAG is a novel modulator of redox state, inflammation and insulin signalling in skeletal muscle. UnAG treatment induces lower mitochondrial ROS production, lower inflammation and enhanced insulin signalling and action in rat muscle. These effects are tissue-specific, they appear to be direct and independent of acylated hormone, and could be at least in part mediated by UnAG-induced

stimulation of autophagy. In experimental models of insulin resistance conditions, UnAG overexpression also prevents obesity-associated hyperglycaemia and systemic insulin resistance as well as muscle oxidative stress, inflammation activation and impaired insulin signalling. Moreover, similar results are induced by UnAG sustained treatment in CKD-associated insulin resistance and muscle wasting, with recovery of muscle mass loss (Figure 38). Collectively, the current findings indicate UnAG as a potential novel treatment for metabolic derangements in insulin resistance-prone clinical conditions, including obesity and wasting disorders.

6.3 Modulation of ghrelin acylation by FFA

The current study demonstrated that total plasma free fatty acid concentration is positively associated with plasma acylated ghrelin and its ratio to total hormone in a community-based general population cohort. In additional rodent experiments, plasma acylated ghrelin was also higher following sustained intravenous lipid infusion and high-physiological increments of circulating free fatty acids. These results therefore collectively support the novel concept that plasma total fatty acid availability positively modulates ghrelin acylation and-or acylated ghrelin secretion in vivo. This conclusion has relevant clinical and nutritional implications, since acylated ghrelin may negatively modulate metabolic and cardiovascular risk profiles both in experimental models [322] and in clinical studies [56]. Higher circulating fatty acids from excess dietary lipids or excess lipid stores are commonly observed and could lead to excess ghrelin acylation in obesity, metabolic syndrome and diabetes, and enhanced ghrelin acylation could independently contribute to the well-documented negative metabolic impact of fatty acids under these conditions [199,323]. Previous studies notably reported conflicting results with both higher and unchanged total ghrelin following acute elevation of total plasma fatty acids in humans [324-326]. Available studies are however limited in number and sample size, were performed in lean young volunteers and did not measure acylated hormone [324-

[326]. The current findings conversely demonstrate that fatty acids primarily modulate plasma acylated ghrelin levels, which should therefore be routinely measured when investigating the impact of lipid substrates on ghrelin profile.

The use of LCFA-based lipid emulsions in rat studies also demonstrated their independent effects to upregulate plasma acylated ghrelin. It should be pointed out that octanoate and medium-chain fatty acids (MCFA) are the only physiological substrates for GOAT-mediated ghrelin acylation [18,57], and MCFA supplementation was accordingly reported to enhance GOAT activity and acylated ghrelin in experimental models and in vivo [58]. MCFA however only represent a minor fraction of dietary lipids and total circulating fatty acids in humans and rodents [322,327], and recent evidence also indicates that octanoate does not account for physiological increments in ghrelin acylation under conditions characterized by higher total fatty acid availability such as fasting in humans [328]. Our combined findings are consistent with the above observations in strongly supporting the novel concept that LCFA may be alternative positive modulators of ghrelin acylation in vivo. A putative positive impact of LCFA availability on ghrelin acylation is importantly also in agreement with the emerging hypothesis that GOAT acylated ghrelin act as positive sensors to alert the central nervous system to available dietary energy, in order to enhance orexigenic responses aimed at optimizing energy intake and storage [57,329].

The current studies did not allow to identify molecular mechanisms of LCFA activities. LCFA receptors including GPR120 have been identified and recently described in ghrelin-secreting cells, and two available studies reported GRP120-dependent short-term inhibitory effects of high-dose palmitoleic and n-3 PUFA alpha-linolenic acid on total and octanoyl-ghrelin secretion in vitro [330,331]. In vivo administration of GRP120 agonists was however notably not able to reproduce in vitro inhibitory effects on ghrelin secretion [330]. Only transient inhibition with subsequent increase of total and acylated ghrelin was also reported in vivo following

intra-gastric fatty olive oil administration [331], and several studies did not confirm potential appetite-inhibiting effects of n-3 PUFA in vivo [276-278]. Also in agreement with stimulated ghrelin acylation following sustained exposure to fat substrates, one clinical study comparing meals with different macronutrient compositions showed bi-phasic responses with early reduction but later increments of both total and acylated plasma ghrelin following mixed fatty meal ingestion [332]. In the current experiments a physiological sustained administration of mixed LCFAs was also chosen by design, and it is possible that stimulatory effects of LCFA to enhance plasma acylated ghrelin resulted from differential activities of different fatty acids. Mediators of LCFA stimulatory activities could further include unidentified endocrine and metabolic pathways that should be investigated in future studies. Regardless of underlying mechanism(s), LCFA infusion experiments provide the first evidence and proof of principle that sustained elevation of LCFA availability causes acylated ghrelin elevation in vivo, and circulating LCFA are therefore likely contributors to the positive association between total circulating fatty acids and acylated ghrelin in humans. Finally and also importantly, the current results indicate no independent effects of n-3 PUFA enrichment per se to further modulate the increase in ghrelin acylation by mixed LCFA emulsions. Based on this observation, n-3 PUFA supplementation could directly contribute to enhance appetite through ghrelin acylation as recently reported in cachectic disease conditions [276] but it is conversely likely that n-3 PUFA-independent mechanisms mediate appetite inhibition as reported in selected studies in obese individuals [277].

In conclusion, we demonstrated that total plasma fatty acid concentration is directly associated with acylated ghrelin and the acylated-to-total ghrelin ratio in a community-based general population cohort. Acute fatty acid elevation with different LCFA-based lipid emulsions similarly increased circulating acylated and acylated-to-total ghrelin without affecting total plasma hormone. The current findings collectively provide novel evidence that

total fatty acid availability contributes to upregulate plasma acylated ghrelin in vivo. Positive interactions between circulating FFA availability and acylated ghrelin in humans could involve LCFA-mediated stimulation of ghrelin acylation.

7 Publications

- Results in Section 5.1 have been published in: Barazzoni, R., Gortan Cappellari, G., Semolic, A., Ius, M., Mamolo, L., Dore, F., ... & Guarnieri, G. (2015). Plasma total and unacylated ghrelin predict 5-year changes in insulin resistance. Clinical Nutrition, 2015 doi: 10.1016/j.clnu.2015.10.002. Elesevier License: 3815841503065.
- Results in Section 5.2 and 5.3 and part of 5.5 have been published in: Gortan Cappellari, G., Zanetti, M., Semolic, A., Vinci, P., Ruozi, G., Falcione, A., ... & Barazzoni, R. (2016). Unacylated Ghrelin Reduces Skeletal Muscle Reactive Oxygen Species Generation and Inflammation and Prevents High-Fat Diet Induced Hyperglycemia and Whole-Body Insulin Resistance in Rodents. Diabetes, db151019 doi: 10.2337/db15-1019. ADA License: 3832080471263.
- Part of results in Section 5.5 have been published in: Ruozi, G., Bortolotti, F., Falcione, A., Dal Ferro, M., Ukovich, L., Macedo, A., ... Gortan Cappellari, G. … Giacca, M. (2015). AAV-mediated in vivo functional selection of tissue-protective factors against ischaemia. Nature communications, 6, 2015 doi: 10.1038/ncomms8388. No license required as by publisher statement.

8 References

1. Kojima, M.*, et al.* Ghrelin is a growth-hormone-releasing acylated peptide from stomach. *Nature* **402**, 656-660 (1999).
2. Inui, A.*, et al.* Ghrelin, appetite, and gastric motility: the emerging role of the stomach as an endocrine organ. *FASEB journal : official publication of the Federation of American Societies for Experimental Biology* **18**, 439-456 (2004).
3. Bowers, C.Y.*, et al.* Structure-activity relationships of a synthetic pentapeptide that specifically releases growth hormone in vitro. *Endocrinology* **106**, 663-667 (1980).
4. Bowers, C.Y., Momany, F.A., Reynolds, G.A. & Hong, A. On the in vitro and in vivo activity of a new synthetic hexapeptide that acts on the pituitary to specifically release growth hormone. *Endocrinology* **114**, 1537-1545 (1984).
5. Howard, A.D.*, et al.* A receptor in pituitary and hypothalamus that functions in growth hormone release. *Science* **273**, 974-977 (1996).
6. Kojima, M. & Kangawa, K. Ghrelin: structure and function. *Physiological reviews* **85**, 495-522 (2005).
7. Tomasetto, C.*, et al.* Identification and characterization of a novel gastric peptide hormone: the motilin-related peptide. *Gastroenterology* **119**, 395-405 (2000).
8. Wajnrajch, M.P., Ten, I., Gertner, J.M. & Leibel, R.L. Genomic Organization of the Human GHRELIN Gene. *International Journal on Disability and Human Development* **1**, 231–234 (2000).
9. Seim, I., Collet, C., Herington, A.C. & Chopin, L.K. Revised genomic structure of the human ghrelin gene and identification of novel exons, alternative splice variants and natural antisense transcripts. *BMC genomics* **8**, 298 (2007).
10. Miraglia del Giudice, E.*, et al.* Molecular screening of the ghrelin gene in Italian obese children: the Leu72Met variant is associated with an earlier onset of obesity. *International journal of obesity and related metabolic disorders : journal of the International Association for the Study of Obesity* **28**, 447-450 (2004).
11. Poykko, S., Ukkola, O., Kauma, H., Savolainen, M.J. & Kesaniemi, Y.A. Ghrelin Arg51Gln mutation is a risk factor for Type 2 diabetes and hypertension in a random sample of middle-aged subjects. *Diabetologia* **46**, 455-458 (2003).
12. Ukkola, O.*, et al.* Mutations in the preproghrelin/ghrelin gene associated with obesity in humans. *The Journal of clinical endocrinology and metabolism* **86**, 3996-3999 (2001).
13. Ukkola, O.*, et al.* Role of ghrelin polymorphisms in obesity based on three different studies. *Obesity research* **10**, 782-791 (2002).

14. Hosoda, H., Kojima, M., Matsuo, H. & Kangawa, K. Ghrelin and des-acyl ghrelin: two major forms of rat ghrelin peptide in gastrointestinal tissue. *Biochemical and biophysical research communications* **279**, 909-913 (2000).

15. Sakata, I.*, et al.* Colocalization of ghrelin O-acyltransferase and ghrelin in gastric mucosal cells. *American journal of physiology. Endocrinology and metabolism* **297**, E134-141 (2009).

16. Yang, J., Zhao, T.J., Goldstein, J.L. & Brown, M.S. Inhibition of ghrelin O-acyltransferase (GOAT) by octanoylated pentapeptides. *Proceedings of the National Academy of Sciences of the United States of America* **105**, 10750-10755 (2008).

17. Lim, C.T., Kola, B., Grossman, A. & Korbonits, M. The expression of ghrelin O-acyltransferase (GOAT) in human tissues. *Endocrine journal* **58**, 707-710 (2011).

18. Gutierrez, J.A.*, et al.* Ghrelin octanoylation mediated by an orphan lipid transferase. *Proceedings of the National Academy of Sciences of the United States of America* **105**, 6320-6325 (2008).

19. Hosoda, H., Kojima, M., Mizushima, T., Shimizu, S. & Kangawa, K. Structural divergence of human ghrelin. Identification of multiple ghrelin-derived molecules produced by post-translational processing. *The Journal of biological chemistry* **278**, 64-70 (2003).

20. Yang, J., Brown, M.S., Liang, G., Grishin, N.V. & Goldstein, J.L. Identification of the acyltransferase that octanoylates ghrelin, an appetite-stimulating peptide hormone. *Cell* **132**, 387-396 (2008).

21. Dehlin, E.*, et al.* Regulation of ghrelin structure and membrane binding by phosphorylation. *Peptides* **29**, 904-911 (2008).

22. Sato, T.*, et al.* Structure, regulation and function of ghrelin. *Journal of biochemistry* **151**, 119-128 (2012).

23. Liu, B., Garcia, E.A. & Korbonits, M. Genetic studies on the ghrelin, growth hormone secretagogue receptor (GHSR) and ghrelin O-acyl transferase (GOAT) genes. *Peptides* **32**, 2191-2207 (2011).

24. Ariyasu, H.*, et al.* Stomach is a major source of circulating ghrelin, and feeding state determines plasma ghrelin-like immunoreactivity levels in humans. *The Journal of clinical endocrinology and metabolism* **86**, 4753-4758 (2001).

25. Sakata, I.*, et al.* Ghrelin-producing cells exist as two types of cells, closed- and opened-type cells, in the rat gastrointestinal tract. *Peptides* **23**, 531-536 (2002).

26. Knerr, I., Herzog, D., Rauh, M., Rascher, W. & Horbach, T. Leptin and ghrelin expression in adipose tissues and serum levels in gastric banding patients. *European journal of clinical investigation* **36**, 389-394 (2006).

27. Korbonits, M.*, et al.* The expression of the growth hormone secretagogue receptor ligand ghrelin in normal and abnormal human pituitary and other neuroendocrine tumors. *The Journal of clinical endocrinology and metabolism* **86**, 881-887 (2001).

28. Volante, M.*, et al.* Expression of ghrelin and of the GH secretagogue receptor by pancreatic islet cells and related endocrine tumors. *The Journal of clinical endocrinology and metabolism* **87**, 1300-1308 (2002).

29. Wierup, N., Svensson, H., Mulder, H. & Sundler, F. The ghrelin cell: a novel developmentally regulated islet cell in the human pancreas. *Regulatory peptides* **107**, 63-69 (2002).

30. Mori, K.*, et al.* Kidney produces a novel acylated peptide, ghrelin. *FEBS letters* **486**, 213-216 (2000).

31. Tena-Sempere, M.*, et al.* Novel expression and functional role of ghrelin in rat testis. *Endocrinology* **143**, 717-725 (2002).

32. Gualillo, O.*, et al.* Ghrelin, a novel placental-derived hormone. *Endocrinology* **142**, 788-794 (2001).

33. Date, Y.*, et al.* Ghrelin, a novel growth hormone-releasing acylated peptide, is synthesized in a distinct endocrine cell type in the gastrointestinal tracts of rats and humans. *Endocrinology* **141**, 4255-4261 (2000).

34. Date, Y.*, et al.* The role of the gastric afferent vagal nerve in ghrelin-induced feeding and growth hormone secretion in rats. *Gastroenterology* **123**, 1120-1128 (2002).

35. Kanamoto, N.*, et al.* Substantial production of ghrelin by a human medullary thyroid carcinoma cell line. *The Journal of clinical endocrinology and metabolism* **86**, 4984-4990 (2001).

36. Iglesias, M.J.*, et al.* Growth hormone releasing peptide (ghrelin) is synthesized and secreted by cardiomyocytes. *Cardiovascular research* **62**, 481-488 (2004).

37. Mundinger, T.O., Cummings, D.E. & Taborsky, G.J., Jr. Direct stimulation of ghrelin secretion by sympathetic nerves. *Endocrinology* **147**, 2893-2901 (2006).

38. Engelstoft, M.S.*, et al.* Seven transmembrane G protein-coupled receptor repertoire of gastric ghrelin cells. *Molecular metabolism* **2**, 376-392 (2013).

39. Tong, J.*, et al.* The pharmacokinetics of acyl, des-acyl, and total ghrelin in healthy human subjects. *European journal of endocrinology / European Federation of Endocrine Societies* **168**, 821-828 (2013).

40. Liu, J.*, et al.* Novel ghrelin assays provide evidence for independent regulation of ghrelin acylation and secretion in healthy young men. *The Journal of clinical endocrinology and metabolism* **93**, 1980-1987 (2008).

41. Akamizu, T.*, et al.* Separate measurement of plasma levels of acylated and desacyl ghrelin in healthy subjects using a new direct ELISA assay. *The Journal of clinical endocrinology and metabolism* **90**, 6-9 (2005).

42. Janssen, S.*, et al.* Bitter taste receptors and alpha-gustducin regulate the secretion of ghrelin with functional effects on food intake and gastric emptying. *Proceedings of the National Academy of Sciences of the United States of America* **108**, 2094-2099 (2011).

43. Mizutani, M.*, et al.* Localization of acyl ghrelin- and des-acyl ghrelin-immunoreactive cells in the rat stomach and their responses to intragastric pH. *American journal of physiology. Gastrointestinal and liver physiology* **297**, G974-980 (2009).

44. De Vriese, C.*, et al.* Ghrelin degradation by serum and tissue homogenates: identification of the cleavage sites. *Endocrinology* **145**, 4997-5005 (2004).

45. Banks, W.A., Tschop, M., Robinson, S.M. & Heiman, M.L. Extent and direction of ghrelin transport across the blood-brain barrier is determined by its unique primary

structure. *The Journal of pharmacology and experimental therapeutics* **302**, 822-827 (2002).

46. Banks, W.A., Burney, B.O. & Robinson, S.M. Effects of triglycerides, obesity, and starvation on ghrelin transport across the blood-brain barrier. *Peptides* **29**, 2061-2065 (2008).
47. Barazzoni, R.*, et al.* Hyperleptinemia prevents increased plasma ghrelin concentration during short-term moderate caloric restriction in rats. *Gastroenterology* **124**, 1188-1192 (2003).
48. Gualillo, O.*, et al.* Effect of food restriction on ghrelin in normal-cycling female rats and in pregnancy. *Obesity research* **10**, 682-687 (2002).
49. Cummings, D.E. & Overduin, J. Gastrointestinal regulation of food intake. *The Journal of clinical investigation* **117**, 13-23 (2007).
50. Cummings, D.E.*, et al.* A preprandial rise in plasma ghrelin levels suggests a role in meal initiation in humans. *Diabetes* **50**, 1714-1719 (2001).
51. Tschop, M.*, et al.* Post-prandial decrease of circulating human ghrelin levels. *Journal of endocrinological investigation* **24**, RC19-21 (2001).
52. Cummings, D.E., Foster-Schubert, K.E. & Overduin, J. Ghrelin and energy balance: focus on current controversies. *Current drug targets* **6**, 153-169 (2005).
53. Sanchez, J., Oliver, P., Palou, A. & Pico, C. The inhibition of gastric ghrelin production by food intake in rats is dependent on the type of macronutrient. *Endocrinology* **145**, 5049-5055 (2004).
54. Otto, B.*, et al.* Weight gain decreases elevated plasma ghrelin concentrations of patients with anorexia nervosa. *European journal of endocrinology / European Federation of Endocrine Societies* **145**, 669-673 (2001).
55. Tschop, M.*, et al.* Circulating ghrelin levels are decreased in human obesity. *Diabetes* **50**, 707-709 (2001).
56. Barazzoni, R.*, et al.* Relationships between desacylated and acylated ghrelin and insulin sensitivity in the metabolic syndrome. *The Journal of clinical endocrinology and metabolism* **92**, 3935-3940 (2007).
57. Kirchner, H.*, et al.* GOAT links dietary lipids with the endocrine control of energy balance. *Nature medicine* **15**, 741-745 (2009).
58. Nishi, Y.*, et al.* Ingested medium-chain fatty acids are directly utilized for the acyl modification of ghrelin. *Endocrinology* **146**, 2255-2264 (2005).
59. Muller, T.D.*, et al.* Ghrelin. *Molecular metabolism* **4**, 437-460 (2015).
60. Mary, S.*, et al.* Heterodimerization with Its splice variant blocks the ghrelin receptor 1a in a non-signaling conformation: a study with a purified heterodimer assembled into lipid discs. *The Journal of biological chemistry* **288**, 24656-24665 (2013).
61. Bednarek, M.A.*, et al.* Structure-function studies on the new growth hormone-releasing peptide, ghrelin: minimal sequence of ghrelin necessary for activation of growth hormone secretagogue receptor 1a. *Journal of medicinal chemistry* **43**, 4370-4376 (2000).

62. Gnanapavan, S.*, et al.* The tissue distribution of the mRNA of ghrelin and subtypes of its receptor, GHS-R, in humans. *The Journal of clinical endocrinology and metabolism* **87**, 2988 (2002).

63. Hattori, N.*, et al.* GH, GH receptor, GH secretagogue receptor, and ghrelin expression in human T cells, B cells, and neutrophils. *The Journal of clinical endocrinology and metabolism* **86**, 4284-4291 (2001).

64. Shuto, Y.*, et al.* Generation of polyclonal antiserum against the growth hormone secretagogue receptor (GHS-R): evidence that the GHS-R exists in the hypothalamus, pituitary and stomach of rats. *Life sciences* **68**, 991-996 (2001).

65. Papotti, M.*, et al.* Growth hormone secretagogue binding sites in peripheral human tissues. *The Journal of clinical endocrinology and metabolism* **85**, 3803-3807 (2000).

66. Guan, X.M.*, et al.* Distribution of mRNA encoding the growth hormone secretagogue receptor in brain and peripheral tissues. *Brain research. Molecular brain research* **48**, 23-29 (1997).

67. Gershon, E. & Vale, W.W. CRF type 2 receptors mediate the metabolic effects of ghrelin in C2C12 cells. *Obesity* **22**, 380-389 (2014).

68. McGirr, R., McFarland, M.S., McTavish, J., Luyt, L.G. & Dhanvantari, S. Design and characterization of a fluorescent ghrelin analog for imaging the growth hormone secretagogue receptor 1a. *Regulatory peptides* **172**, 69-76 (2011).

69. Moreno, M.*, et al.* Ghrelin attenuates hepatocellular injury and liver fibrogenesis in rodents and influences fibrosis progression in humans. *Hepatology* **51**, 974-985 (2010).

70. Ueberberg, B., Unger, N., Saeger, W., Mann, K. & Petersenn, S. Expression of ghrelin and its receptor in human tissues. *Hormone and metabolic research = Hormon- und Stoffwechselforschung = Hormones et metabolisme* **41**, 814-821 (2009).

71. Filigheddu, N.*, et al.* Ghrelin and des-acyl ghrelin promote differentiation and fusion of C2C12 skeletal muscle cells. *Molecular biology of the cell* **18**, 986-994 (2007).

72. Sun, Y., Garcia, J.M. & Smith, R.G. Ghrelin and growth hormone secretagogue receptor expression in mice during aging. *Endocrinology* **148**, 1323-1329 (2007).

73. Cassoni, P.*, et al.* Expression of ghrelin and biological activity of specific receptors for ghrelin and des-acyl ghrelin in human prostate neoplasms and related cell lines. *European journal of endocrinology / European Federation of Endocrine Societies* **150**, 173-184 (2004).

74. Baldanzi, G.*, et al.* Ghrelin and des-acyl ghrelin inhibit cell death in cardiomyocytes and endothelial cells through ERK1/2 and PI 3-kinase/AKT. *The Journal of cell biology* **159**, 1029-1037 (2002).

75. Dardzinska, J.A.*, et al.* Fasting and postprandial acyl and desacyl ghrelin levels in obese and non-obese subjects. *Endokrynologia Polska* **65**, 377-381 (2014).

76. Gil-Campos, M., Aguilera, C.M., Canete, R. & Gil, A. Ghrelin: a hormone regulating food intake and energy homeostasis. *The British journal of nutrition* **96**, 201-226 (2006).

77. Nakazato, M.*, et al.* A role for ghrelin in the central regulation of feeding. *Nature* **409**, 194-198 (2001).

78. Wren, A.M.*, et al.* Ghrelin causes hyperphagia and obesity in rats. *Diabetes* **50**, 2540-2547 (2001).

79. Tschop, M., Smiley, D.L. & Heiman, M.L. Ghrelin induces adiposity in rodents. *Nature* **407**, 908-913 (2000).

80. Dornonville de la Cour, C.*, et al.* Ghrelin treatment reverses the reduction in weight gain and body fat in gastrectomised mice. *Gut* **54**, 907-913 (2005).

81. Adachi, S.*, et al.* Effects of ghrelin administration after total gastrectomy: a prospective, randomized, placebo-controlled phase II study. *Gastroenterology* **138**, 1312-1320 (2010).

82. Arnold, M., Mura, A., Langhans, W. & Geary, N. Gut vagal afferents are not necessary for the eating-stimulatory effect of intraperitoneally injected ghrelin in the rat. *The Journal of neuroscience : the official journal of the Society for Neuroscience* **26**, 11052-11060 (2006).

83. Kola, B.*, et al.* The orexigenic effect of ghrelin is mediated through central activation of the endogenous cannabinoid system. *PloS one* **3**, e1797 (2008).

84. Bagnasco, M., Dube, M.G., Kalra, P.S. & Kalra, S.P. Evidence for the existence of distinct central appetite, energy expenditure, and ghrelin stimulation pathways as revealed by hypothalamic site-specific leptin gene therapy. *Endocrinology* **143**, 4409-4421 (2002).

85. Wang, L., Saint-Pierre, D.H. & Tache, Y. Peripheral ghrelin selectively increases Fos expression in neuropeptide Y - synthesizing neurons in mouse hypothalamic arcuate nucleus. *Neuroscience letters* **325**, 47-51 (2002).

86. Willesen, M.G., Kristensen, P. & Romer, J. Co-localization of growth hormone secretagogue receptor and NPY mRNA in the arcuate nucleus of the rat. *Neuroendocrinology* **70**, 306-316 (1999).

87. Andrews, Z.B.*, et al.* UCP2 mediates ghrelin's action on NPY/AgRP neurons by lowering free radicals. *Nature* **454**, 846-851 (2008).

88. Zigman, J.M., Jones, J.E., Lee, C.E., Saper, C.B. & Elmquist, J.K. Expression of ghrelin receptor mRNA in the rat and the mouse brain. *The Journal of comparative neurology* **494**, 528-548 (2006).

89. Malik, S., McGlone, F., Bedrossian, D. & Dagher, A. Ghrelin modulates brain activity in areas that control appetitive behavior. *Cell metabolism* **7**, 400-409 (2008).

90. Asakawa, A.*, et al.* Stomach regulates energy balance via acylated ghrelin and desacyl ghrelin. *Gut* **54**, 18-24 (2005).

91. Inhoff, T.*, et al.* Desacyl ghrelin inhibits the orexigenic effect of peripherally injected ghrelin in rats. *Peptides* **29**, 2159-2168 (2008).

92. Toshinai, K.*, et al.* Des-acyl ghrelin induces food intake by a mechanism independent of the growth hormone secretagogue receptor. *Endocrinology* **147**, 2306-2314 (2006).

93. Broglio, F.*, et al.* Ghrelin, a natural GH secretagogue produced by the stomach, induces hyperglycemia and reduces insulin secretion in humans. *The Journal of clinical endocrinology and metabolism* **86**, 5083-5086 (2001).

94. Tong, J.*, et al.* Ghrelin suppresses glucose-stimulated insulin secretion and deteriorates glucose tolerance in healthy humans. *Diabetes* **59**, 2145-2151 (2010).

95. Sun, Y., Butte, N.F., Garcia, J.M. & Smith, R.G. Characterization of adult ghrelin and ghrelin receptor knockout mice under positive and negative energy balance. *Endocrinology* **149**, 843-850 (2008).

96. Dezaki, K., Kakei, M. & Yada, T. Ghrelin uses Galphai2 and activates voltage-dependent K+ channels to attenuate glucose-induced Ca2+ signaling and insulin release in islet beta-cells: novel signal transduction of ghrelin. *Diabetes* **56**, 2319-2327 (2007).

97. Park, S., Jiang, H., Zhang, H. & Smith, R.G. Modification of ghrelin receptor signaling by somatostatin receptor-5 regulates insulin release. *Proceedings of the National Academy of Sciences of the United States of America* **109**, 19003-19008 (2012).

98. Scott, M.M.*, et al.* Hindbrain ghrelin receptor signaling is sufficient to maintain fasting glucose. *PloS one* **7**, e44089 (2012).

99. Poykko, S.M.*, et al.* Low plasma ghrelin is associated with insulin resistance, hypertension, and the prevalence of type 2 diabetes. *Diabetes* **52**, 2546-2553 (2003).

100. Barazzoni, R.*, et al.* Higher total ghrelin levels are associated with higher insulin-mediated glucose disposal in non-diabetic maintenance hemodialysis patients. *Clinical nutrition* **27**, 142-149 (2008).

101. McLaughlin, T., Abbasi, F., Lamendola, C., Frayo, R.S. & Cummings, D.E. Plasma ghrelin concentrations are decreased in insulin-resistant obese adults relative to equally obese insulin-sensitive controls. *The Journal of clinical endocrinology and metabolism* **89**, 1630-1635 (2004).

102. Broglio, F.*, et al.* Non-acylated ghrelin counteracts the metabolic but not the neuroendocrine response to acylated ghrelin in humans. *The Journal of clinical endocrinology and metabolism* **89**, 3062-3065 (2004).

103. Gauna, C.*, et al.* Unacylated ghrelin acts as a potent insulin secretagogue in glucose-stimulated conditions. *American journal of physiology. Endocrinology and metabolism* **293**, E697-704 (2007).

104. Granata, R.*, et al.* Acylated and unacylated ghrelin promote proliferation and inhibit apoptosis of pancreatic beta-cells and human islets: involvement of 3',5'-cyclic adenosine monophosphate/protein kinase A, extracellular signal-regulated kinase 1/2, and phosphatidyl inositol 3-Kinase/Akt signaling. *Endocrinology* **148**, 512-529 (2007).

105. Gauna, C.*, et al.* Unacylated ghrelin is active on the INS-1E rat insulinoma cell line independently of the growth hormone secretagogue receptor type 1a and the corticotropin releasing factor 2 receptor. *Molecular and cellular endocrinology* **251**, 103-111 (2006).

106. Tong, J.*, et al.* Acute administration of unacylated ghrelin has no effect on Basal or stimulated insulin secretion in healthy humans. *Diabetes* **63**, 2309-2319 (2014).

107. Heijboer, A.C.*, et al.* Ghrelin differentially affects hepatic and peripheral insulin sensitivity in mice. *Diabetologia* **49**, 732-738 (2006).

108. Barazzoni, R.*, et al.* Ghrelin regulates mitochondrial-lipid metabolism gene expression and tissue fat distribution in liver and skeletal muscle. *American journal of physiology. Endocrinology and metabolism* **288**, E228-235 (2005).

109. Pardo, M.*, et al.* Peripheral leptin and ghrelin receptors are regulated in a tissue-specific manner in activity-based anorexia. *Peptides* **31**, 1912-1919 (2010).

110. van Thuijl, H., Kola, B. & Korbonits, M. Appetite and metabolic effects of ghrelin and cannabinoids: involvement of AMP-activated protein kinase. *Vitamins and hormones* **77**, 121-148 (2008).

111. Gauna, C.*, et al.* Ghrelin stimulates, whereas des-octanoyl ghrelin inhibits, glucose output by primary hepatocytes. *The Journal of clinical endocrinology and metabolism* **90**, 1055-1060 (2005).

112. Barazzoni, R.*, et al.* Ghrelin enhances in vivo skeletal muscle but not liver AKT signaling in rats. *Obesity* **15**, 2614-2623 (2007).

113. Obay, B.D., Tasdemir, E., Tumer, C., Bilgin, H. & Atmaca, M. Dose dependent effects of ghrelin on pentylenetetrazole-induced oxidative stress in a rat seizure model. *Peptides* **29**, 448-455 (2008).

114. Li, Y.*, et al.* Administration of ghrelin improves inflammation, oxidative stress, and apoptosis during and after non-alcoholic fatty liver disease development. *Endocrine* **43**, 376-386 (2013).

115. Barazzoni, R., Semolic, A., Cattin, M.R., Zanetti, M. & Guarnieri, G. Acylated ghrelin limits fat accumulation and improves redox state and inflammation markers in the liver of high-fat-fed rats. *Obesity* **22**, 170-177 (2014).

116. Murata, M.*, et al.* Ghrelin modulates the downstream molecules of insulin signaling in hepatoma cells. *The Journal of biological chemistry* **277**, 5667-5674 (2002).

117. Liu, H.Y.*, et al.* Increased basal level of Akt-dependent insulin signaling may be responsible for the development of insulin resistance. *American journal of physiology. Endocrinology and metabolism* **297**, E898-906 (2009).

118. Davies, J.S.*, et al.* Ghrelin induces abdominal obesity via GHS-R-dependent lipid retention. *Molecular endocrinology* **23**, 914-924 (2009).

119. Muccioli, G.*, et al.* Ghrelin and des-acyl ghrelin both inhibit isoproterenol-induced lipolysis in rat adipocytes via a non-type 1a growth hormone secretagogue receptor. *European journal of pharmacology* **498**, 27-35 (2004).

120. Perez-Tilve, D.*, et al.* Ghrelin-induced adiposity is independent of orexigenic effects. *FASEB journal : official publication of the Federation of American Societies for Experimental Biology* **25**, 2814-2822 (2011).

121. Wortley, K.E.*, et al.* Absence of ghrelin protects against early-onset obesity. *The Journal of clinical investigation* **115**, 3573-3578 (2005).

122. Zigman, J.M.*, et al.* Mice lacking ghrelin receptors resist the development of diet-induced obesity. *The Journal of clinical investigation* **115**, 3564-3572 (2005).

123. Kim, M.S.*, et al.* The mitogenic and antiapoptotic actions of ghrelin in 3T3-L1 adipocytes. *Molecular endocrinology* **18**, 2291-2301 (2004).

124. Choi, K.*, et al.* The role of ghrelin and growth hormone secretagogues receptor on rat adipogenesis. *Endocrinology* **144**, 754-759 (2003).

125. Andrews, Z.B.*, et al.* Uncoupling protein-2 decreases the lipogenic actions of ghrelin. *Endocrinology* **151**, 2078-2086 (2010).

126. Miegueu, P., St Pierre, D., Broglio, F. & Cianflone, K. Effect of desacyl ghrelin, obestatin and related peptides on triglyceride storage, metabolism and GHSR signaling in 3T3-L1 adipocytes. *Journal of cellular biochemistry* **112**, 704-714 (2011).

127. Zhang, W., Chai, B., Li, J.Y., Wang, H. & Mulholland, M.W. Effect of des-acyl ghrelin on adiposity and glucose metabolism. *Endocrinology* **149**, 4710-4716 (2008).

128. Porporato, P.E.*, et al.* Acylated and unacylated ghrelin impair skeletal muscle atrophy in mice. *The Journal of clinical investigation* **123**, 611-622 (2013).

129. Yu, A.P.*, et al.* Acylated and unacylated ghrelin inhibit doxorubicin-induced apoptosis in skeletal muscle. *Acta physiologica* **211**, 201-213 (2014).

130. Reano, S., Graziani, A. & Filigheddu, N. Acylated and unacylated ghrelin administration to blunt muscle wasting. *Current opinion in clinical nutrition and metabolic care* **17**, 236-240 (2014).

131. Togliatto, G.*, et al.* Unacylated ghrelin promotes skeletal muscle regeneration following hindlimb ischemia via SOD-2-mediated miR-221/222 expression. *Journal of the American Heart Association* **2**, e000376 (2013).

132. Wei, Y.*, et al.* Angiotensin II-induced skeletal muscle insulin resistance mediated by NF-kappaB activation via NADPH oxidase. *American journal of physiology. Endocrinology and metabolism* **294**, E345-351 (2008).

133. Cai, D.*, et al.* IKKbeta/NF-kappaB activation causes severe muscle wasting in mice. *Cell* **119**, 285-298 (2004).

134. Schenk, S., Saberi, M. & Olefsky, J.M. Insulin sensitivity: modulation by nutrients and inflammation. *The Journal of clinical investigation* **118**, 2992-3002 (2008).

135. Morino, K., Petersen, K.F. & Shulman, G.I. Molecular mechanisms of insulin resistance in humans and their potential links with mitochondrial dysfunction. *Diabetes* **55 Suppl 2**, S9-S15 (2006).

136. Saleh, M.C., Wheeler, M.B. & Chan, C.B. Uncoupling protein-2: evidence for its function as a metabolic regulator. *Diabetologia* **45**, 174-187 (2002).

137. Echtay, K.S.*, et al.* Superoxide activates mitochondrial uncoupling proteins. *Nature* **415**, 96-99 (2002).

138. Lopez, N.E.*, et al.* Early ghrelin treatment attenuates disruption of the blood brain barrier and apoptosis after traumatic brain injury through a UCP-2 mechanism. *Brain research* **1489**, 140-148 (2012).

139. Barazzoni, R.*, et al.* Combined effects of ghrelin and higher food intake enhance skeletal muscle mitochondrial oxidative capacity and AKT phosphorylation in rats with chronic kidney disease. *Kidney international* **77**, 23-28 (2010).

140. Suematsu, M.*, et al.* Decreased circulating levels of active ghrelin are associated with increased oxidative stress in obese subjects. *European journal of endocrinology / European Federation of Endocrine Societies* **153**, 403-407 (2005).

141. Omrani, H., Alipour, M.R. & Mohaddes, G. Ghrelin Improves Antioxidant Defense in Blood and Brain in Normobaric Hypoxia in Adult Male Rats. *Advanced pharmaceutical bulletin* **5**, 283-288 (2015).

142. El Eter, E., Al Tuwaijiri, A., Hagar, H. & Arafa, M. In vivo and in vitro antioxidant activity of ghrelin: Attenuation of gastric ischemic injury in the rat. *Journal of gastroenterology and hepatology* **22**, 1791-1799 (2007).

143. Iseri, S.O.*, et al.* Ghrelin against alendronate-induced gastric damage in rats. *The Journal of endocrinology* **187**, 399-406 (2005).

144. Chang, L.*, et al.* Protective effects of ghrelin on ischemia/reperfusion injury in the isolated rat heart. *Journal of cardiovascular pharmacology* **43**, 165-170 (2004).

145. Kawczynska-Drozdz, A.*, et al.* Ghrelin inhibits vascular superoxide production in spontaneously hypertensive rats. *American journal of hypertension* **19**, 764-767 (2006).

146. Togliatto, G.*, et al.* Unacylated ghrelin rescues endothelial progenitor cell function in individuals with type 2 diabetes. *Diabetes* **59**, 1016-1025 (2010).

147. Kheradmand, A., Alirezaei, M. & Birjandi, M. Ghrelin promotes antioxidant enzyme activity and reduces lipid peroxidation in the rat ovary. *Regulatory peptides* **162**, 84-89 (2010).

148. Zwirska-Korczala, K.*, et al.* Role of leptin, ghrelin, angiotensin II and orexins in 3T3 L1 preadipocyte cells proliferation and oxidative metabolism. *Journal of physiology and pharmacology : an official journal of the Polish Physiological Society* **58 Suppl 1**, 53-64 (2007).

149. Neamati, S., Alirezaei, M. & Kheradmand, A. Ghrelin Acts as an Antioxidant Agent in the Rat Kidney. *International Journal of Peptide Research and Therapeutics* **17**, 239-245 (2011).

150. Iantorno, M.*, et al.* Ghrelin has novel vascular actions that mimic PI 3-kinase-dependent actions of insulin to stimulate production of NO from endothelial cells. *American journal of physiology. Endocrinology and metabolism* **292**, E756-764 (2007).

151. Guzik, T.J., West, N.E., Pillai, R., Taggart, D.P. & Channon, K.M. Nitric oxide modulates superoxide release and peroxynitrite formation in human blood vessels. *Hypertension* **39**, 1088-1094 (2002).

152. Shimada, T.*, et al.* Des-acyl ghrelin protects microvascular endothelial cells from oxidative stress-induced apoptosis through sirtuin 1 signaling pathway. *Metabolism: clinical and experimental* **63**, 469-474 (2014).

153. Barazzoni, R.*, et al.* High-fat diet with acyl-ghrelin treatment leads to weight gain with low inflammation, high oxidative capacity and normal triglycerides in rat muscle. *PloS one* **6**, e26224 (2011).

154. Baatar, D., Patel, K. & Taub, D.D. The effects of ghrelin on inflammation and the immune system. *Molecular and cellular endocrinology* **340**, 44-58 (2011).

155. Dixit, V.D.*, et al.* Ghrelin inhibits leptin- and activation-induced proinflammatory cytokine expression by human monocytes and T cells. *The Journal of clinical investigation* **114**, 57-66 (2004).

156. Soriano, R.N., Nicoli, L.G., Carnio, E.C. & Branco, L.G. Exogenous ghrelin attenuates endotoxin fever in rats. *Peptides* **32**, 2372-2376 (2011).

157. Vila, G.*, et al.* Bacterial endotoxin induces biphasic changes in plasma ghrelin in healthy humans. *The Journal of clinical endocrinology and metabolism* **92**, 3930-3934 (2007).

158. Li, W.G.*, et al.* Ghrelin inhibits proinflammatory responses and nuclear factor-kappaB activation in human endothelial cells. *Circulation* **109**, 2221-2226 (2004).

159. Yilmaz, Z., Ilcol, Y.O. & Ulus, I.H. Endotoxin increases plasma leptin and ghrelin levels in dogs. *Critical care medicine* **36**, 828-833 (2008).

160. Waseem, T., Duxbury, M., Ito, H., Ashley, S.W. & Robinson, M.K. Exogenous ghrelin modulates release of pro-inflammatory and anti-inflammatory cytokines in LPS-stimulated macrophages through distinct signaling pathways. *Surgery* **143**, 334-342 (2008).

161. Gonzalez-Rey, E., Chorny, A. & Delgado, M. Therapeutic action of ghrelin in a mouse model of colitis. *Gastroenterology* **130**, 1707-1720 (2006).

162. Kodama, T., Ashitani, J., Matsumoto, N., Kangawa, K. & Nakazato, M. Ghrelin treatment suppresses neutrophil-dominant inflammation in airways of patients with chronic respiratory infection. *Pulmonary pharmacology & therapeutics* **21**, 774-779 (2008).

163. Takata, A.*, et al.* Randomized Phase II Study of the Anti-inflammatory Effect of Ghrelin During the Postoperative Period of Esophagectomy. *Annals of surgery* **262**, 230-236 (2015).

164. Valerio, A.*, et al.* TNF-alpha downregulates eNOS expression and mitochondrial biogenesis in fat and muscle of obese rodents. *The Journal of clinical investigation* **116**, 2791-2798 (2006).

165. Han, D.*, et al.* Ghrelin improves functional survival of engrafted adipose-derived mesenchymal stem cells in ischemic heart through PI3K/Akt signaling pathway. *BioMed research international* **2015**, 858349 (2015).

166. Hao, X.K.*, et al.* Ghrelin alleviates early brain injury after subarachnoid hemorrhage via the PI3K/Akt signaling pathway. *Brain research* **1587**, 15-22 (2014).

167. Waseem, T., Duxbury, M., Ashley, S.W. & Robinson, M.K. Ghrelin promotes intestinal epithelial cell proliferation through PI3K/Akt pathway and EGFR trans-activation both converging to ERK 1/2 phosphorylation. *Peptides* **52**, 113-121 (2014).

168. Yang, D., Liu, Z., Zhang, H. & Luo, Q. Ghrelin protects human pulmonary artery endothelial cells against hypoxia-induced injury via PI3-kinase/Akt. *Peptides* **42**, 112-117 (2013).

169. Chen, X., Chen, Q., Wang, L. & Li, G. Ghrelin induces cell migration through GHSR1a-mediated PI3K/Akt/eNOS/NO signaling pathway in endothelial progenitor cells. *Metabolism: clinical and experimental* **62**, 743-752 (2013).

170. Lear, P.V.*, et al.* Des-acyl ghrelin has specific binding sites and different metabolic effects from ghrelin in cardiomyocytes. *Endocrinology* **151**, 3286-3298 (2010).

171. Vestergaard, E.T.*, et al.* Acute effects of ghrelin administration on glucose and lipid metabolism. *The Journal of clinical endocrinology and metabolism* **93**, 438-444 (2008).

172. Vestergaard, E.T.*, et al.* Acute peripheral metabolic effects of intraarterial ghrelin infusion in healthy young men. *The Journal of clinical endocrinology and metabolism* **96**, 468-477 (2011).

173. Cross, D.A., Alessi, D.R., Cohen, P., Andjelkovich, M. & Hemmings, B.A. Inhibition of glycogen synthase kinase-3 by insulin mediated by protein kinase B. *Nature* **378**, 785-789 (1995).

174. Cheng, Z., Tseng, Y. & White, M.F. Insulin signaling meets mitochondria in metabolism. *Trends in endocrinology and metabolism: TEM* **21**, 589-598 (2010).

175. Hancer, N.J.*, et al.* Insulin and metabolic stress stimulate multisite serine/threonine phosphorylation of insulin receptor substrate 1 and inhibit tyrosine phosphorylation. *The Journal of biological chemistry* **289**, 12467-12484 (2014).

176. Ashford, T.P. & Porter, K.R. Cytoplasmic components in hepatic cell lysosomes. *The Journal of cell biology* **12**, 198-202 (1962).

177. Glick, D., Barth, S. & Macleod, K.F. Autophagy: cellular and molecular mechanisms. *The Journal of pathology* **221**, 3-12 (2010).

178. Kim, I., Rodriguez-Enriquez, S. & Lemasters, J.J. Selective degradation of mitochondria by mitophagy. *Archives of biochemistry and biophysics* **462**, 245-253 (2007).

179. Klionsky, D.J. & Emr, S.D. Autophagy as a regulated pathway of cellular degradation. *Science* **290**, 1717-1721 (2000).

180. Pattingre, S.*, et al.* Bcl-2 antiapoptotic proteins inhibit Beclin 1-dependent autophagy. *Cell* **122**, 927-939 (2005).

181. Slupecka, M., Wolinski, J. & Pierzynowski, S.G. The effects of enteral ghrelin administration on the remodeling of the small intestinal mucosa in neonatal piglets. *Regulatory peptides* **174**, 38-45 (2012).

182. Fleming, A., Noda, T., Yoshimori, T. & Rubinsztein, D.C. Chemical modulators of autophagy as biological probes and potential therapeutics. *Nature chemical biology* **7**, 9-17 (2011).

183. Xu, Y., Pang, X., Dong, M., Wen, F. & Zhang, Y. Ghrelin inhibits ovarian epithelial carcinoma cell proliferation in vitro. *Oncology reports* **30**, 2063-2070 (2013).

184. Bonfili, L.*, et al.* Ghrelin induces apoptosis in colon adenocarcinoma cells via proteasome inhibition and autophagy induction. *Apoptosis : an international journal on programmed cell death* **18**, 1188-1200 (2013).

185. Rodriguez, A.*, et al.* The ghrelin O-acyltransferase-ghrelin system reduces TNF-alpha-induced apoptosis and autophagy in human visceral adipocytes. *Diabetologia* **55**, 3038-3050 (2012).

186. Mao, Y.*, et al.* Ghrelin Attenuated Lipotoxicity via Autophagy Induction and Nuclear Factor-kappaB Inhibition. *Cellular physiology and biochemistry : international journal of experimental cellular physiology, biochemistry, and pharmacology* **37**, 563-576 (2015).

187. Zhang, Y., Fang, F., Goldstein, J.L., Brown, M.S. & Zhao, T.J. Reduced autophagy in livers of fasted, fat-depleted, ghrelin-deficient mice: reversal by growth hormone. *Proceedings of the National Academy of Sciences of the United States of America* **112**, 1226-1231 (2015).

188. Mao, Y.*, et al.* Ghrelin reduces liver impairment in a model of concanavalin A-induced acute hepatitis in mice. *Drug design, development and therapy* **9**, 5385-5396 (2015).

189. Mao, Y.*, et al.* Ghrelin Attenuates Liver Fibrosis through Regulation of TGF-beta1 Expression and Autophagy. *International journal of molecular sciences* **16**, 21911-21930 (2015).

190. Wang, X.*, et al.* Ghrelin inhibits doxorubicin cardiotoxicity by inhibiting excessive autophagy through AMPK and p38-MAPK. *Biochemical pharmacology* **88**, 334-350 (2014).

191. Tong, X.X., *et al.* Ghrelin protects against cobalt chloride-induced hypoxic injury in cardiac H9c2 cells by inhibiting oxidative stress and inducing autophagy. *Peptides* **38**, 217-227 (2012).

192. Tam, B.T., *et al.* Unacylated ghrelin restores insulin and autophagic signaling in skeletal muscle of diabetic mice. *Pflugers Archiv : European journal of physiology* **467**, 2555-2569 (2015).

193. Corcelles, R., Daigle, C.R. & Schauer, P.R. MANAGEMENT OF ENDOCRINE DISEASE: Metabolic effects of bariatric surgery. *European journal of endocrinology / European Federation of Endocrine Societies* **174**, R19-28 (2016).

194. Haslam, D.W. & James, W.P. Obesity. *Lancet* **366**, 1197-1209 (2005).

195. Fontaine, K.R., Redden, D.T., Wang, C., Westfall, A.O. & Allison, D.B. Years of life lost due to obesity. *Jama* **289**, 187-193 (2003).

196. Peeters, A., *et al.* Obesity in adulthood and its consequences for life expectancy: a life-table analysis. *Annals of internal medicine* **138**, 24-32 (2003).

197. Jung, U.J. & Choi, M.S. Obesity and its metabolic complications: the role of adipokines and the relationship between obesity, inflammation, insulin resistance, dyslipidemia and nonalcoholic fatty liver disease. *International journal of molecular sciences* **15**, 6184-6223 (2014).

198. Abate, N., Chandalia, M., Snell, P.G. & Grundy, S.M. Adipose tissue metabolites and insulin resistance in nondiabetic Asian Indian men. *The Journal of clinical endocrinology and metabolism* **89**, 2750-2755 (2004).

199. Barazzoni, R., *et al.* Fatty acids acutely enhance insulin-induced oxidative stress and cause insulin resistance by increasing mitochondrial reactive oxygen species (ROS) generation and nuclear factor-kappaB inhibitor (IkappaB)-nuclear factor-kappaB (NFkappaB) activation in rat muscle, in the absence of mitochondrial dysfunction. *Diabetologia* **55**, 773-782 (2012).

200. Anderson, E.J., *et al.* Mitochondrial H2O2 emission and cellular redox state link excess fat intake to insulin resistance in both rodents and humans. *The Journal of clinical investigation* **119**, 573-581 (2009).

201. Bonnard, C., *et al.* Mitochondrial dysfunction results from oxidative stress in the skeletal muscle of diet-induced insulin-resistant mice. *The Journal of clinical investigation* **118**, 789-800 (2008).

202. Shoelson, S.E., Lee, J. & Goldfine, A.B. Inflammation and insulin resistance. *The Journal of clinical investigation* **116**, 1793-1801 (2006).

203. Williams, K.J. & Wu, X. Imbalanced insulin action in chronic over nutrition: Clinical harm, molecular mechanisms, and a way forward. *Atherosclerosis* **247**, 225-282 (2016).

204. JAMA. From the NIH: Successful diet and exercise therapy is conducted in Vermont for "diabesity". *Jama* **243**, 519-520 (1980).

205. Sims, E.A., *et al.* Endocrine and metabolic effects of experimental obesity in man. *Recent progress in hormone research* **29**, 457-496 (1973).

206. Stevens, J., *et al.* The effect of age on the association between body-mass index and mortality. *The New England journal of medicine* **338**, 1-7 (1998).

207. Robbins, S.L., Kumar, V. & Cotran, R.S. *Robbins and Cotran pathologic basis of disease*, (Saunders/Elsevier, Philadelphia, PA, 2010).

208. Kahn, B.B. Type 2 diabetes: when insulin secretion fails to compensate for insulin resistance. *Cell* **92**, 593-596 (1998).

209. American Diabetes, A. (2) Classification and diagnosis of diabetes. *Diabetes care* **38 Suppl**, S8-S16 (2015).

210. DeFronzo, R.A., Tobin, J.D. & Andres, R. Glucose clamp technique: a method for quantifying insulin secretion and resistance. *The American journal of physiology* **237**, E214-223 (1979).

211. Fraser, R., Albright, F. & Smith, P.H. Carbohydrate metabolism. The value of the glucose tolerance test, the insulin tolerance test and the glucose-insulin tolerance test in the diagnosis of endocrinologic disorders of glucose metabolism. *JCEM* **1**, 297-306 (1941).

212. Matthews, D.R.*, et al.* Homeostasis model assessment: insulin resistance and beta-cell function from fasting plasma glucose and insulin concentrations in man. *Diabetologia* **28**, 412-419 (1985).

213. DeFronzo, R.A. & Ferrannini, E. Insulin resistance. A multifaceted syndrome responsible for NIDDM, obesity, hypertension, dyslipidemia, and atherosclerotic cardiovascular disease. *Diabetes care* **14**, 173-194 (1991).

214. Eriksson, J.*, et al.* Early metabolic defects in persons at increased risk for non-insulin-dependent diabetes mellitus. *The New England journal of medicine* **321**, 337-343 (1989).

215. Joslin, E.P. The prevention of diabetes mellitus. *Jama* **76**, 79-84 (1921).

216. Kaur, J. A comprehensive review on metabolic syndrome. *Cardiology research and practice* **2014**, 943162 (2014).

217. Okafor, C.I. The metabolic syndrome in Africa: Current trends. *Indian journal of endocrinology and metabolism* **16**, 56-66 (2012).

218. Haffner, S.M.*, et al.* Prospective analysis of the insulin-resistance syndrome (syndrome X). *Diabetes* **41**, 715-722 (1992).

219. Kaplan, N.M. The deadly quartet. Upper-body obesity, glucose intolerance, hypertriglyceridemia, and hypertension. *Archives of internal medicine* **149**, 1514-1520 (1989).

220. Phillips, G.B. Relationship between serum sex hormones and glucose, insulin and lipid abnormalities in men with myocardial infarction. *Proceedings of the National Academy of Sciences of the United States of America* **74**, 1729-1733 (1977).

221. Ford, E.S. Prevalence of the metabolic syndrome defined by the International Diabetes Federation among adults in the U.S. *Diabetes care* **28**, 2745-2749 (2005).

222. Vanuzzo, D.*, et al.* [Cardiovascular epidemiology: trends of risk factors in Italy]. *Italian heart journal : official journal of the Italian Federation of Cardiology* **5 Suppl 8**, 19S-27S; discussion 33S-34, 116S-121S (2004).

223. Kuppens, R.J., Delhanty, P.J., Huisman, T.M., van der Lely, A.J. & Hokken-Koelega, A.C. Acylated and unacylated ghrelin during OGTT in Prader-Willi syndrome: Support for normal response to food intake. *Clinical endocrinology* (2016).

224. Choe, Y.H., *et al.* Increased density of ghrelin-expressing cells in the gastric fundus and body in Prader-Willi syndrome. *The Journal of clinical endocrinology and metabolism* **90**, 5441-5445 (2005).

225. Cummings, D.E., *et al.* Elevated plasma ghrelin levels in Prader Willi syndrome. *Nature medicine* **8**, 643-644 (2002).

226. Nicholls, R.D. & Knepper, J.L. Genome organization, function, and imprinting in Prader-Willi and Angelman syndromes. *Annual review of genomics and human genetics* **2**, 153-175 (2001).

227. Gagnon, J., Zhu, L., Anini, Y. & Wang, Q. Neutralizing circulating ghrelin by expressing a growth hormone secretagogue receptor-based protein protects against high-fat diet-induced obesity in mice. *Gene therapy* **22**, 750-757 (2015).

228. Wiedmer, P., Nogueiras, R., Broglio, F., D'Alessio, D. & Tschop, M.H. Ghrelin, obesity and diabetes. *Nature clinical practice. Endocrinology & metabolism* **3**, 705-712 (2007).

229. Wortley, K.E., *et al.* Genetic deletion of ghrelin does not decrease food intake but influences metabolic fuel preference. *Proceedings of the National Academy of Sciences of the United States of America* **101**, 8227-8232 (2004).

230. McFarlane, M.R., Brown, M.S., Goldstein, J.L. & Zhao, T.J. Induced ablation of ghrelin cells in adult mice does not decrease food intake, body weight, or response to high-fat diet. *Cell metabolism* **20**, 54-60 (2014).

231. Gual, P., Le Marchand-Brustel, Y. & Tanti, J.F. Positive and negative regulation of insulin signaling through IRS-1 phosphorylation. *Biochimie* **87**, 99-109 (2005).

232. Delhanty, P.J., *et al.* Des-acyl ghrelin analogs prevent high-fat-diet-induced dysregulation of glucose homeostasis. *FASEB journal : official publication of the Federation of American Societies for Experimental Biology* **27**, 1690-1700 (2013).

233. Levey, A.S. & Coresh, J. Chronic kidney disease. *Lancet* **379**, 165-180 (2012).

234. Levey, A.S., *et al.* National Kidney Foundation practice guidelines for chronic kidney disease: evaluation, classification, and stratification. *Annals of internal medicine* **139**, 137-147 (2003).

235. Gava, A.L., Freitas, F.P., Balarini, C.M., Vasquez, E.C. & Meyrelles, S.S. Effects of 5/6 nephrectomy on renal function and blood pressure in mice. *International journal of physiology, pathophysiology and pharmacology* **4**, 167-173 (2012).

236. Fouque, D., *et al.* A proposed nomenclature and diagnostic criteria for protein-energy wasting in acute and chronic kidney disease. *Kidney international* **73**, 391-398 (2008).

237. Mak, R.H., *et al.* Wasting in chronic kidney disease. *Journal of cachexia, sarcopenia and muscle* **2**, 9-25 (2011).

238. Mak, R.H. & Cheung, W.W. Is ghrelin a biomarker for mortality in end-stage renal disease? *Kidney international* **79**, 697-699 (2011).

239. Lorenzo, C., Nath, S.D., Hanley, A.J., Abboud, H.E. & Haffner, S.M. Relation of low glomerular filtration rate to metabolic disorders in individuals without diabetes and with normoalbuminuria. *Clinical journal of the American Society of Nephrology : CJASN* **3**, 783-789 (2008).

240. Cheung, W.W.*, et al.* Peripheral administration of the melanocortin-4 receptor antagonist NBI-12i ameliorates uremia-associated cachexia in mice. *Journal of the American Society of Nephrology : JASN* **18**, 2517-2524 (2007).

241. Holecek, M. Muscle wasting in animal models of severe illness. *International journal of experimental pathology* **93**, 157-171 (2012).

242. Evans, W.J. Skeletal muscle loss: cachexia, sarcopenia, and inactivity. *The American journal of clinical nutrition* **91**, 1123S-1127S (2010).

243. Muscaritoli, M.*, et al.* Consensus definition of sarcopenia, cachexia and pre-cachexia: joint document elaborated by Special Interest Groups (SIG) "cachexia-anorexia in chronic wasting diseases" and "nutrition in geriatrics". *Clinical nutrition* **29**, 154-159 (2010).

244. Evans, W.J.*, et al.* Cachexia: a new definition. *Clinical nutrition* **27**, 793-799 (2008).

245. Laviano, A.*, et al.* Chronic renal failure, cachexia, and ghrelin. *International journal of peptides* **2010**(2010).

246. Kalantar-Zadeh, K.*, et al.* Kidney insufficiency and nutrient-based modulation of inflammation. *Current opinion in clinical nutrition and metabolic care* **8**, 388-396 (2005).

247. Li, Y.P. & Reid, M.B. NF-kappaB mediates the protein loss induced by TNF-alpha in differentiated skeletal muscle myotubes. *American journal of physiology. Regulatory, integrative and comparative physiology* **279**, R1165-1170 (2000).

248. Locatelli, F.*, et al.* Oxidative stress in end-stage renal disease: an emerging threat to patient outcome. *Nephrology, dialysis, transplantation : official publication of the European Dialysis and Transplant Association - European Renal Association* **18**, 1272-1280 (2003).

249. Himmelfarb, J., Stenvinkel, P., Ikizler, T.A. & Hakim, R.M. The elephant in uremia: oxidant stress as a unifying concept of cardiovascular disease in uremia. *Kidney international* **62**, 1524-1538 (2002).

250. Witko-Sarsat, V.*, et al.* Advanced oxidation protein products as novel mediators of inflammation and monocyte activation in chronic renal failure. *Journal of immunology* **161**, 2524-2532 (1998).

251. Supinski, G.S. & Callahan, L.A. Free radical-mediated skeletal muscle dysfunction in inflammatory conditions. *Journal of applied physiology* **102**, 2056-2063 (2007).

252. Victor, V.M., Espulgues, J.V., Hernandez-Mijares, A. & Rocha, M. Oxidative stress and mitochondrial dysfunction in sepsis: a potential therapy with mitochondria-targeted antioxidants. *Infectious disorders drug targets* **9**, 376-389 (2009).

253. Sandri, M.*, et al.* PGC-1alpha protects skeletal muscle from atrophy by suppressing FoxO3 action and atrophy-specific gene transcription. *Proceedings of the National Academy of Sciences of the United States of America* **103**, 16260-16265 (2006).

254. Adey, D., Kumar, R., McCarthy, J.T. & Nair, K.S. Reduced synthesis of muscle proteins in chronic renal failure. *American journal of physiology. Endocrinology and metabolism* **278**, E219-225 (2000).

255. Ramos, L.F., Shintani, A., Ikizler, T.A. & Himmelfarb, J. Oxidative stress and inflammation are associated with adiposity in moderate to severe CKD. *Journal of the American Society of Nephrology : JASN* **19**, 593-599 (2008).

256. Siew, E.D. & Ikizler, T.A. Determinants of insulin resistance and its effects on protein metabolism in patients with advanced chronic kidney disease. *Contributions to nephrology* **161**, 138-144 (2008).

257. Fiaschi, E.*, et al.* Muscle glucose content and hexokinase activity in patients with chronic uremia. *Kidney international. Supplement*, 341-344 (1975).

258. Siew, E.D.*, et al.* Insulin resistance is associated with skeletal muscle protein breakdown in non-diabetic chronic hemodialysis patients. *Kidney international* **71**, 146-152 (2007).

259. Bailey, J.L., Zheng, B., Hu, Z., Price, S.R. & Mitch, W.E. Chronic kidney disease causes defects in signaling through the insulin receptor substrate/phosphatidylinositol 3-kinase/Akt pathway: implications for muscle atrophy. *Journal of the American Society of Nephrology : JASN* **17**, 1388-1394 (2006).

260. Stump, C.S., Short, K.R., Bigelow, M.L., Schimke, J.M. & Nair, K.S. Effect of insulin on human skeletal muscle mitochondrial ATP production, protein synthesis, and mRNA transcripts. *Proceedings of the National Academy of Sciences of the United States of America* **100**, 7996-8001 (2003).

261. Perez-Fontan, M.*, et al.* Plasma ghrelin levels in patients undergoing haemodialysis and peritoneal dialysis. *Nephrology, dialysis, transplantation : official publication of the European Dialysis and Transplant Association - European Renal Association* **19**, 2095-2100 (2004).

262. Rodriguez Ayala, E.*, et al.* Associations between plasma ghrelin levels and body composition in end-stage renal disease: a longitudinal study. *Nephrology, dialysis, transplantation : official publication of the European Dialysis and Transplant Association - European Renal Association* **19**, 421-426 (2004).

263. Yoshimoto, A.*, et al.* Plasma ghrelin and desacyl ghrelin concentrations in renal failure. *Journal of the American Society of Nephrology : JASN* **13**, 2748-2752 (2002).

264. Mak, R.H., Cheung, W. & Purnell, J. Ghrelin in chronic kidney disease: too much or too little? *Peritoneal dialysis international : journal of the International Society for Peritoneal Dialysis* **27**, 51-55 (2007).

265. Jarkovska, Z.*, et al.* Plasma levels of active and total ghrelin in renal failure: a relationship with GH/IGF-I axis. *Growth hormone & IGF research : official journal of the Growth Hormone Research Society and the International IGF Research Society* **15**, 369-376 (2005).

266. Bossola, M.*, et al.* Anorexia and plasma levels of free tryptophan, branched chain amino acids, and ghrelin in hemodialysis patients. *Journal of renal nutrition : the official journal of the Council on Renal Nutrition of the National Kidney Foundation* **19**, 248-255 (2009).

267. Muscaritoli, M.*, et al.* Anorexia in hemodialysis patients: the possible role of des-acyl ghrelin. *American journal of nephrology* **27**, 360-365 (2007).

268. Ashitani, J., Matsumoto, N. & Nakazato, M. Ghrelin and its therapeutic potential for cachectic patients. *Peptides* **30**, 1951-1956 (2009).

269. DeBoer, M.D.*, et al.* Ghrelin treatment causes increased food intake and retention of lean body mass in a rat model of cancer cachexia. *Endocrinology* **148**, 3004-3012 (2007).

270. Ashby, D.R.*, et al.* Sustained appetite improvement in malnourished dialysis patients by daily ghrelin treatment. *Kidney international* **76**, 199-206 (2009).

271. Deboer, M.D.*, et al.* Ghrelin treatment of chronic kidney disease: improvements in lean body mass and cytokine profile. *Endocrinology* **149**, 827-835 (2008).

272. Wang, W., Bansal, S., Falk, S., Ljubanovic, D. & Schrier, R. Ghrelin protects mice against endotoxemia-induced acute kidney injury. *American journal of physiology. Renal physiology* **297**, F1032-1037 (2009).

273. Tamaki, M.*, et al.* Improvement of Physical Decline Through Combined Effects of Muscle Enhancement and Mitochondrial Activation by a Gastric Hormone Ghrelin in Male 5/6Nx CKD Model Mice. *Endocrinology* **156**, 3638-3648 (2015).

274. Barazzoni, R.*, et al.* The association between hematological parameters and insulin resistance is modified by body mass index - results from the North-East Italy MoMa population study. *PloS one* **9**, e101590 (2014).

275. Deboer, M.D. Animal models of anorexia and cachexia. *Expert opinion on drug discovery* **4**, 1145-1155 (2009).

276. Sanchez-Lara, K.*, et al.* Effects of an oral nutritional supplement containing eicosapentaenoic acid on nutritional and clinical outcomes in patients with advanced non-small cell lung cancer: randomised trial. *Clinical nutrition* **33**, 1017-1023 (2014).

277. Harden, C.J.*, et al.* Long-chain polyunsaturated fatty acid supplementation had no effect on body weight but reduced energy intake in overweight and obese women. *Nutrition research* **34**, 17-24 (2014).

278. Kratz, M., Callahan, H.S., Yang, P.Y., Matthys, C.C. & Weigle, D.S. Dietary n-3-polyunsaturated fatty acids and energy balance in overweight or moderately obese men and women: a randomized controlled trial. *Nutrition & metabolism* **6**, 24 (2009).

279. Collesi, C., Zentilin, L., Sinagra, G. & Giacca, M. Notch1 signaling stimulates proliferation of immature cardiomyocytes. *The Journal of cell biology* **183**, 117-128 (2008).

280. Deng, X.F., Rokosh, D.G. & Simpson, P.C. Autonomous and growth factor-induced hypertrophy in cultured neonatal mouse cardiac myocytes. Comparison with rat. *Circulation research* **87**, 781-788 (2000).

281. Lovric, J.*, et al.* Terminal differentiation of cardiac and skeletal myocytes induces permissivity to AAV transduction by relieving inhibition imposed by DNA damage response proteins. *Molecular therapy : the journal of the American Society of Gene Therapy* **20**, 2087-2097 (2012).

282. Ryter, S.W., Koo, J.K. & Choi, A.M. Molecular regulation of autophagy and its implications for metabolic diseases. *Current opinion in clinical nutrition and metabolic care* **17**, 329-337 (2014).

283. Martinez Cantarin, M.P., Keith, S.W., Waldman, S.A. & Falkner, B. Adiponectin receptor and adiponectin signaling in human tissue among patients with end-stage renal disease. *Nephrology, dialysis, transplantation : official publication of the European Dialysis and Transplant Association - European Renal Association* **29**, 2268-2277 (2014).

284. Folli, F., Sinha, M.K., Brancaccio, D. & Caro, J.F. Insulin resistance in uremia: in vitro model in the rat liver using human serum to study mechanisms. *Metabolism: clinical and experimental* **35**, 989-998 (1986).

285. Barazzoni, R.*, et al.* High plasma retinol binding protein 4 (RBP4) is associated with systemic inflammation independently of low RBP4 adipose expression and is normalized by transplantation in nonobese, nondiabetic patients with chronic kidney disease. *Clinical endocrinology* **75**, 56-63 (2011).

286. Gortan Cappellari, G.*, et al.* Treatment with n-3 polyunsaturated fatty acids reverses endothelial dysfunction and oxidative stress in experimental menopause. *The Journal of nutritional biochemistry* **24**, 371-379 (2013).

287. Barazzoni, R.*, et al.* Moderate caloric restriction, but not physiological hyperleptinemia per se, enhances mitochondrial oxidative capacity in rat liver and skeletal muscle--tissue-specific impact on tissue triglyceride content and AKT activation. *Endocrinology* **146**, 2098-2106 (2005).

288. Rahman, I., Kode, A. & Biswas, S.K. Assay for quantitative determination of glutathione and glutathione disulfide levels using enzymatic recycling method. *Nature protocols* **1**, 3159-3165 (2006).

289. Fulton, R.J., McDade, R.L., Smith, P.L., Kienker, L.J. & Kettman, J.R., Jr. Advanced multiplexed analysis with the FlowMetrix system. *Clinical chemistry* **43**, 1749-1756 (1997).

290. Yamamoto, N., Kawasaki, K., Kawabata, K. & Ashida, H. An enzymatic fluorimetric assay to quantitate 2-deoxyglucose and 2-deoxyglucose-6-phosphate for in vitro and in vivo use. *Analytical biochemistry* **404**, 238-240 (2010).

291. Clerk, L.H., Rattigan, S. & Clark, M.G. Lipid infusion impairs physiologic insulin-mediated capillary recruitment and muscle glucose uptake in vivo. *Diabetes* **51**, 1138-1145 (2002).

292. Bonen, A., Tan, M.H. & Watson-Wright, W.M. Insulin binding and glucose uptake differences in rodent skeletal muscles. *Diabetes* **30**, 702-704 (1981).

293. McCurdy, C.E. & Cartee, G.D. Akt2 is essential for the full effect of calorie restriction on insulin-stimulated glucose uptake in skeletal muscle. *Diabetes* **54**, 1349-1356 (2005).

294. Lanza, I.R. & Nair, K.S. Functional assessment of isolated mitochondria in vitro. *Methods in enzymology* **457**, 349-372 (2009).

295. Cao, S., Zhang, X., Edwards, J.P. & Mosser, D.M. NF-kappaB1 (p50) homodimers differentially regulate pro- and anti-inflammatory cytokines in macrophages. *The Journal of biological chemistry* **281**, 26041-26050 (2006).

296. Gortan Cappellari, G.*, et al.* Unacylated ghrelin does not alter mitochondrial function, redox state and triglyceride content in rat liver in vivo. *Clinical Nutrition Experimental* **4**, 1-7 (2015).

297. Ruozi, G.*, et al.* AAV-mediated in vivo functional selection of tissue-protective factors against ischaemia. *Nature communications* **6**(2015).

298. D'Apolito, M.*, et al.* Urea-induced ROS generation causes insulin resistance in mice with chronic renal failure. *The Journal of clinical investigation* **120**, 203-213 (2010).

299. Hodson, L., Skeaff, C.M. & Fielding, B.A. Fatty acid composition of adipose tissue and blood in humans and its use as a biomarker of dietary intake. *Progress in lipid research* **47**, 348-380 (2008).

300. Delhanty, P.J., Neggers, S.J. & van der Lely, A.J. Mechanisms in endocrinology: Ghrelin: the differences between acyl- and des-acyl ghrelin. *European journal of endocrinology / European Federation of Endocrine Societies* **167**, 601-608 (2012).

301. Gauna, C.*, et al.* Administration of acylated ghrelin reduces insulin sensitivity, whereas the combination of acylated plus unacylated ghrelin strongly improves insulin sensitivity. *The Journal of clinical endocrinology and metabolism* **89**, 5035-5042 (2004).

302. Anderwald, C.*, et al.* Insulin-dependent modulation of plasma ghrelin and leptin concentrations is less pronounced in type 2 diabetic patients. *Diabetes* **52**, 1792-1798 (2003).

303. Blijdorp, K.*, et al.* Desacyl ghrelin is influenced by changes in insulin concentration during an insulin tolerance test. *Growth hormone & IGF research : official journal of the Growth Hormone Research Society and the International IGF Research Society* **23**, 193-195 (2013).

304. Togliatto, G.*, et al.* Unacylated ghrelin induces oxidative stress resistance in a glucose intolerance and peripheral artery disease mouse model by restoring endothelial cell miR-126 expression. *Diabetes* **64**, 1370-1382 (2015).

305. Dieci, E., Casati, L., Pagani, F., Celotti, F. & Sibilia, V. Acylated and unacylated ghrelin protect MC3T3-E1 cells against tert-butyl hydroperoxide-induced oxidative injury: pharmacological characterization of ghrelin receptor and possible epigenetic involvement. *Amino acids* **46**, 1715-1725 (2014).

306. Barbieri, E. & Sestili, P. Reactive oxygen species in skeletal muscle signaling. *Journal of signal transduction* **2012**, 982794 (2012).

307. Soraru, G.*, et al.* Activities of mitochondrial complexes correlate with nNOS amount in muscle from ALS patients. *Neuropathology and applied neurobiology* **33**, 204-211 (2007).

308. Brookes, P.S., Levonen, A.L., Shiva, S., Sarti, P. & Darley-Usmar, V.M. Mitochondria: regulators of signal transduction by reactive oxygen and nitrogen species. *Free radical biology & medicine* **33**, 755-764 (2002).

309. Chen, C.Y., Asakawa, A., Fujimiya, M., Lee, S.D. & Inui, A. Ghrelin gene products and the regulation of food intake and gut motility. *Pharmacological reviews* **61**, 430-481 (2009).

310. Liu, Y.*, et al.* Adiponectin stimulates autophagy and reduces oxidative stress to enhance insulin sensitivity during high-fat diet feeding in mice. *Diabetes* **64**, 36-48 (2015).

311. St-Pierre, J.*, et al.* Suppression of reactive oxygen species and neurodegeneration by the PGC-1 transcriptional coactivators. *Cell* **127**, 397-408 (2006).

312. Murphy, M.P. How mitochondria produce reactive oxygen species. *The Biochemical journal* **417**, 1-13 (2009).

313. Ruozi, G.*, et al.* AAV-mediated in vivo functional selection of tissue-protective factors against ischaemia. *Nat Commun* **6**, 7388 (2015).

314. Fisher-Wellman, K.H.*, et al.* Mitochondrial respiratory capacity and content are normal in young insulin-resistant obese humans. *Diabetes* **63**, 132-141 (2014).

315. Holloszy, J.O. "Deficiency" of mitochondria in muscle does not cause insulin resistance. *Diabetes* **62**, 1036-1040 (2013).

316. Nair, K.S.*, et al.* Asian Indians have enhanced skeletal muscle mitochondrial capacity to produce ATP in association with severe insulin resistance. *Diabetes* **57**, 1166-1175 (2008).

317. Barazzoni, R. Skeletal muscle mitochondrial protein metabolism and function in ageing and type 2 diabetes. *Current opinion in clinical nutrition and metabolic care* **7**, 97-102 (2004).

318. Sreekumar, R.*, et al.* Impact of high-fat diet and antioxidant supplement on mitochondrial functions and gene transcripts in rat muscle. *American journal of physiology. Endocrinology and metabolism* **282**, E1055-1061 (2002).

319. Fink, B.D.*, et al.* Mitochondrial targeted coenzyme Q, superoxide, and fuel selectivity in endothelial cells. *PloS one* **4**, e4250 (2009).

320. Anderson, E.J., Yamazaki, H. & Neufer, P.D. Induction of endogenous uncoupling protein 3 suppresses mitochondrial oxidant emission during fatty acid-supported respiration. *The Journal of biological chemistry* **282**, 31257-31266 (2007).

321. St-Pierre, J., Buckingham, J.A., Roebuck, S.J. & Brand, M.D. Topology of superoxide production from different sites in the mitochondrial electron transport chain. *The Journal of biological chemistry* **277**, 44784-44790 (2002).

322. Barnett, B.P.*, et al.* Glucose and weight control in mice with a designed ghrelin O-acyltransferase inhibitor. *Science* **330**, 1689-1692 (2010).

323. Boden, G. & Shulman, G.I. Free fatty acids in obesity and type 2 diabetes: defining their role in the development of insulin resistance and beta-cell dysfunction. *European journal of clinical investigation* **32 Suppl 3**, 14-23 (2002).

324. Gormsen, L.C.*, et al.* Effects of free fatty acids, growth hormone and growth hormone receptor blockade on serum ghrelin levels in humans. *Clinical endocrinology* **66**, 641-645 (2007).

325. Gormsen, L.C.*, et al.* Free fatty acids decrease circulating ghrelin concentrations in humans. *European journal of endocrinology / European Federation of Endocrine Societies* **154**, 667-673 (2006).

326. Mohlig, M.*, et al.* Euglycemic hyperinsulinemia, but not lipid infusion, decreases circulating ghrelin levels in humans. *Journal of endocrinological investigation* **25**, RC36-38 (2002).

327. Marten, B., Pfeuffer, M. & Schrezenmeir, J. Medium-chain triglycerides. *International Dairy Journal* **16**, 1374-1382 (2006).

328. Nass, R.*, et al.* The level of circulating octanoate does not predict ghrelin O-acyl transferase (GOAT)-mediated acylation of ghrelin during fasting. *The Journal of clinical endocrinology and metabolism* **100**, E110-113 (2015).

329. Heppner, K.M., Tong, J., Kirchner, H., Nass, R. & Tschop, M.H. The ghrelin O-acyltransferase-ghrelin system: a novel regulator of glucose metabolism. *Current opinion in endocrinology, diabetes, and obesity* **18**, 50-55 (2011).

330. Janssen, S., Laermans, J., Iwakura, H., Tack, J. & Depoortere, I. Sensing of fatty acids for octanoylation of ghrelin involves a gustatory G-protein. *PloS one* **7**, e40168 (2012).

331. Lu, X.*, et al.* Postprandial inhibition of gastric ghrelin secretion by long-chain fatty acid through GPR120 in isolated gastric ghrelin cells and mice. *American journal of physiology. Gastrointestinal and liver physiology* **303**, G367-376 (2012).

332. Foster-Schubert, K.E.*, et al.* Acyl and total ghrelin are suppressed strongly by ingested proteins, weakly by lipids, and biphasically by carbohydrates. *The Journal of clinical endocrinology and metabolism* **93**, 1971-1979 (2008).